SOIL LOSS RISK ASSESSMENT UNDER CLIMATE CHANGE AND MANAGEMENT PRACTICES: A CASE OF NERI WATERSHED, OMO-GIBE BASIN, SOUTHWESTERN ETHIOPIA

MSc THESIS

BY: ABEBE HEGANO HEMACHO

HAWASSA UNIVERSITY, INTITUTE OF TECHNOLOGY, FACULTY OF BIOSYSTEM AND WATER RESOURCES ENGINEERING

HAWASSA, ETHIOPIA

JULY, 2019

SOIL LOSS RISK ASSESSMENT UNDER CLIMATE CHANGE AND MANAGEMENT PRACTICES: A CASE OF NERI WATERSHED, OMO-GIBE BASIN, SOUTHWESTERN ETHIOPIA

ABEBE HEGANO HEMACHO

MAJOR ADVISOR: Dr. AWDENEGEST MOGES (PhD)

CO-ADVISOR: Dr. NIGATU WONDERADE (PhD)

A THESIS SUBMITTED TO FACULTY OF BIOSYSTEM AND WATER RESOURCES ENGINEERING, INTITUTE OF TECHNOLOGY,

HAWASSA UNIVERSITY

HAWASSA, ETHIOPIA

IN PARTIAL FULFILLMENT OF THE

REQUIREMENTS FOR THE

DEGREE OF

MASTER OF SCIENCE IN SOIL AND WATER CONSERVATION ENGINEERING

JULY, 2019

APPROVAL SHEET

This is to certify that the thesis entitled "Soil loss risk assessment under climate change and anticipated management practices:- A case of Neri watershed, Omo-Gibe basin, Ethiopia" submitted in partial Fulfillment of the Requirements for the degree of master of science in Soil and water conservation engineering of the graduate program of the Department of Bio system and Water Resource Engineering, and is a record of original research carried out by Abebe Hegano ID No SWCE R/01/09, under my supervision, no part of the thesis has been submitted for any other degree or diploma. The assistance and help received during the course of this investigation have been duly acknowledged. Therefore I recommend that it be accepted as fulfilling the thesis requirements.

Dr. Awdenegest Moges	_____	_____
Name of major advisor	Signature	Date
Dr. Nigatu Wonderade	_____	_____
Name of co-advisor	Signature	Date

DEDICATION

I dedicate this thesis to my Family.

STATEMENT OF THE AUTHOUR

I, Abebe Hegano, declare that this thesis is my original work and all sources of materials used for this thesis have been duly acknowledged. This thesis has been submitted in partial fulfillment of the requirements for M.Sc. degree in Soil and Water Conservation Engineering at the Hawassa University and is deposited at the University Library to be made available to borrowers under rules of the Library. I solemnly declare that this thesis is not submitted to any other institution anywhere for the award of any academic degree, diploma or certificate.

Name: Abebe Hegano Signature----------

Date of Submission: July, 2019

E-mail address: - abehegeno@gmail.com

Place: - Hawassa University, Hawassa

SKETCH OF BIOGRAPHY

The author was born on 5 April 1990 in SNNPR, Wolaita Zone, Boditi. He attended his elementary school education in Aro Wogera Primary and Elementary school from the year 1996 to 2003 and secondary school education in Boditi Academic technical and vocational school from 2004 to 2008. After the completion of his high school education he joined Wollega University of college of Agriculture and Natural resources to study his B.Sc. degree in Natural Resource Management and graduated in 2011.

After graduation, the author get job opportunity in Damot Gale woreda agricultural office in the position of vice head of the office and Natural resources protection and development work process coordinator from November 2011 to June 2013. The author changed organization in June 2013 to Southern Agricultural Research Institute (SARI), Jinka Agricultural Research Center (JARC) as soil science assistance researcher. During his service year, the author had executed research activities in soil fertility, soil and water conservation and irrigation based research trials at various agro ecological zones of South Omo zone. In addition, the author served as the team coordinator of natural resources research work process during his stay.

Totally after 5 years of service in the above listed organizations, he joined the School of Graduate Studies at the Hawassa University in September 2016 to pursue his studies for M.Sc. degree in Soil and Water Conservation Engineering

AKNOWLEDGEMENTS

Numerous individuals and organizations have assisted me in various ways to accomplish my study indeed. But firstly, I would like to thank the almighty God for extending my life through this study. Then, I would like to continue expressing my sincere gratitude to my major advisor Dr. Awdenegest Moges who first opened the way to pursue my study. His treatment and stimulating comments right from proposal preparation up to thesis write up is very much appreciated. I thank him whole heartedly for his continuous guidance, mentorship and outstanding contributions during this work. Similarly, I am highly indebted to express my gratefulness to my co-advisor Dr. Nigatu Wonderade who supported me throughout this thesis work. I lack words to express his help of Mihretu Bergene, who supported me both technically in overall GIS software application and morally as well. It is an overwhelming excitement to come to this final point to express my deepest gratitude to all organizations and individuals who contributed in one way or another to my study in general and this thesis in particular.

I am pleased with Southern Agricultural research institute (SARI) for sponsoring me this Masters study. Hawassa University also deserves acknowledgement for accepting me as MSc student. I'll not pass without expressing my thanks to National Meteorological Agency (NMA), Hawassa branch for sharing me all necessary meteorological data without charge. My deepest and heartfelt thanks go to my beloved wife Firehiwot Tesfaye who encouraged me to pursue the MSc study and shouldered the responsibility of caring for the family alone during my class course study period; I also owe to thank my close friends Mesfin Belay, Asmamaw Abera and Getahun Berhanu supported me in various ways. God bless you all for the support.

Finally, I appreciate my beloved wife Firehiwot Tesfaye and my daughter, Nardos Abebe, for their patience during our several months of separation.

ABBREVIATIONS

ANSWERS	Areal Nonpoint Source Watershed Environment Response Simulation
ASTER	Advanced Space borne Thermal Emission and Reflection Radiometer
CORDEX	Coordinated Downscaling Experiment
DEM	Digital Elevation Model
EMA	Ethiopian Mapping Agency
ENSO	El Nino-Southern Oscillation
Esri	Environmental systems research institute
EUROSEM	European Soil Erosion Model
FAO	Food and Agricultural Organization
GCM	Global Circulation Model
GCP	Ground Control Point
GIS	Geographical Information System
GPS	Global Positioning System
IPCC	Inter Governmental Panel for Climate Change
LULC	Land Use Land Cover
MMF	Morgan, Morgan and Finney
MNP	Mago National Park
MoWR	Ministry of Water Resources
NASA	National Aeronautics and Space Administration
NDVI	Normalized Difference Vegetation Index
OLI	Operational Land Imager
RCM	Regional Climate Model
RCP	Representative Concentration Pathways
RUSLE	Revised Universal Soil Loss Equation
SCRP	Soil Conservation Research Program
SLEMSA	Soil loss Estimation Model for South Africa

SLT	Soil Loss Tolerance
SOZDWID	South Omo Zone Department of Water and Irrigation development
SOZDARN	South Omo Zone Department of Agriculture and Natural Resources
SST	Sea Surface Temperature
SW	Sub Watershed
SWC	Soil and Water Conservation
SWCS	Soil and Water Conservation Service
TIRS	Thermal Infrared Sensor
UNDP	United Nations Development Program
UNEP	United Nations Environment Program
USA	United States of America
USDA	United States Department of Agriculture
USGS	United States Geological Survey
USLE	Universal Soil Loss Equation
UTM	Universal Transverse Mercator
WEPP	Water Erosion Prediction Project
WCRP	World Climate Research Project
WGS 37	World Geographic System, Zone 37

TABLE OF CONTENTS

List of tables

List of figures

ABSTRACT

Soil erosion is one of the biggest global environmental problems resulting in both on-site and off-site effects. Climate change is expected to affect soil erosion based on a variety of factors, including a direct impact on soil loss by increasing precipitation amounts and erosive power. Neri watershed was chosen for this study. The objective of study is to assess soil loss risk under climate change and anticipated management practices. Revised Universal Soil Loss Equation model was applied by integrating bio physical and remote sensing data. Model parameters were computed from available data. Three Representative concentration Pathway scenarios ($RCP_{2.6}$, $RCP_{4.5}$ and $RCP_{8.5}$) and management practices considered for estimation of annual soil loss rates. The resultant annual soil loss map under baseline condition shows the mean and total of 9.955t/ha/yr^{-1} and 0.46m t/yr respectively. Estimates suggest that out of the total (46546 ha), about 32.7% % of the total area exceeded the tolerable limit and 67.3%% of the total area were below tolerable rate. The future soil loss rates are higher than the baseline period if no management actions are taken. Under no- management action scenario, the predicted the incremental rate of soil loss from (21.95%) for $RCP_{8.5}$ (2051-2080) followed by 4.57% $RCP_{4.5}$ (2021-2050) to insignificant decline (-0.75%) for $RCP_{2.6}$ (2021-2050) compared to baseline period whereas, the other two predicted reduction. Moreover, inclusion of comprehensive management may result much higher reduction in soil loss over baseline and future condition of no action. The maximum reduction by 41.2% of its soil loss due to climate change is predicted $RCP_{8.5}$ (2051-2080). The resultant soil loss map of baseline period was used in prioritization of intervention areas based on soil loss tolerance. Among eleven (11) sub-watersheds, eight and ten administrative kebeles out of nineteen are above the tolerable limit. However, watershed as planning unit, taking the proportion of soil loss to area, seven sub watersheds were identified as areas of intervention. To ensure sustainable resource use, management practice like contour cropping system complimented with terraces in agricultural fields and with giving special attention through strong policy measures to climate change, erosion minimization in non-agricultural land use classes were needed. Finaly, the study indicates a need for further study to understand the land suitability that consider the climate change.

Key words: - Soil loss, RUSLE, Ethiopia, Climate Change, RCP scenarios, Management practices

1. INTRODUCTION

1.1. Background

Soil erosion is clearing away of land surface by water and/ or wind as well as decline in soil productivity due to loss of top soil itself, which makes plant root depth shallow, removes plant nutrients and losses water (Mahmud et al., 2005). It is the process of detachment, transportation, and accumulation of surface soil particles from area of its formation to the area of deposition. There are varieties of soil erosion and, rill and inter-rill erosion are the recurrent types of water erosion, involving detachment, transport, and accumulation of soil particles to a new depositional area, deteriorating soil quality as well as diminishing the productivity of vulnerable lands (Arnold et al., 1998).

Despite the fact that soil loss can occur due to geological erosion, soil loss by surface runoff is a severe ecological problem occupying 56% (1,100 million hectares) of the world wide area as accelerated by human-induced soil degradation as (Bai et al., 2008). The extent and distribution is widespread in Africa and Asia, due to high population pressure, land shortage and critical lack of resources for conservation by subsistence small holder farmers (Blanco and lal, 2008).

About 43% (537,000 km2) of the total highland areas of Ethiopia are highly affected by soil erosion (Hurni, 1990). There are several causes reported for it. For instance, human activities resulted from rapid population**,** deforestation, unsuitable land cultivation, uncontrolled and overgrazing (Reusing et al., 2000; Tamene & Vlek, 2006; Zemenu & Minale, 2014). In Ethiopian high lands non-fallow farming has been aggravating it (Aster, 2004; Zemenu & Minale, 2014). Moreover, the reports by (Bationo *et al*., 2006 and Tilahun *et al*., 2001) has pointed out poor soil and land management issues such as, nutrient mining with interaction of factors such as slope length and steepness.

Among threats to the sustainability of environment and productive capacity of agriculture, soil erosion is the major one (Yang et al., 2003; Feng et al., 2010). It is the prime contributor to temporary or permanent decline of the productivity of land (Oldeman et al., 1991; Young, 1998). It also results in serious food insecurity in many developing countries as it depletes productive soils (Blanco and Lal, 2008). This can possibly be attributed to the fact that the impact of soil erosion is more damaging on bare land and cultivated land than any other types of land use/land cover. A 17% productivity reduction in the global scale since the end of world war second (Angima

et al., 2003). The severe situation in Ethiopia is quantified by loss of 1 billion USD per year (Sonneveld, 2002) and is still affecting 50% of the agricultural area. Still also the decline in soil fertility associated with removal of top soil by erosion, the crop productivity of land in Ethiopia is very low. Its effects are also recognized to be severe threats to the national economy of Ethiopia (Tamene, 2005).

Quantitative understanding of the removal of valuable soil resource has get attention of scientific community in different parts of Ethiopia. For instance, in the Ethiopian highlands only, an annual soil loss reaches 200-300 tons $ha^{-1}yr^{-1}$ (FAO, 1984; Hurni, 1993) and soil loss due to erosion in Ethiopia amounts to 1493 million tons per year, of which about 42t ha^{-1} yr^{-1} was estimated from cultivated fields of Ethiopia (Hurni, 2008). Specific studies indicate that, average annual soil loss of 24.95 t/ha/yr. from Zingin watershed, northwestern Ethiopia (Gizachew, 2015) and estimated soil loss of 93 t ha^{-1} yr^{-1} in case of Chemoga watershed (Woldeamlak & Teferi, 2009).

Climate change is now taking place globally. The global average air surface temperature increased between 0.3^0C and 0.6^0C since 1990 (IPCC, 1995). The global average surface temperature increased by 0.85^oC over the period 1880 to 2012 (IPCC, 2013). The spatial and temporal variability of precipitation is high thus large-scale trends do not necessarily reflect local conditions due to inherent uncertainty of climate models and processes (Brohan et al.,2006; Schnieder et al., 2008; IPCC, 2007).

In Africa, a 0.7°C rise in mean continental surface temperatures over the 20th century and a further warming of 0.2–0.5°C per decade is predicted for 2070–2100 (Hulme *et al*., 2001). Ethiopia's mean annual temperature has increased by 1.3°C between 1960 and 2006, an average rate of 0.28°C per decade (McSweeney et al., 2010).

Climate change is getting an exacerbating cause of soil erosion. Its impacts on soil erosion is associated with various forms of climatic elements. Research works affirmed that an increase in frequency and intensity of extreme weather events as a consequence of global warming, will inevitably intensify erosion (Nunes and Seixas, 2003; Nearing et al., 2005). The global average soil erosion is projected to increase approximately 9% by 2090 due to climate changes (Yang et al., 2003). The work at southern Arizona of Mexico to evaluate the potential impacts of precipitation changes on runoff and soil erosion on rangelands for three future climate emission scenarios (A2, A1B, and B1) from seven GCMs suggested that, future runoff and soil erosion

might increase significantly even if there is no change in total annual amount (Zhang et al., 2012). Also impacts on soil moisture and plant growth due to precipitation amount and intensity, and direct fertilization effects on plants due to of greater CO_2 concentrations among others (Zhang and Nearing, 2005), alteration of precipitation patterns, snow cover change and seasonal snow melting (Beniston, 2006), by climate change displace vegetation cover, decrease infiltration capacity (Zuazo and Pleguezuelo, 2008).

The most direct impact of climate change on soil erosion is the change in the erosive power of rainfall (Mortlock and Boardman, 1995; Mullan, D. et al., 2012; Pruski, F.F. and Nearing, 2002) changes in the magnitude and frequency of extreme events with potential consequent effects on erosion and sediment yield (Fowler and Hennessey, 1995).

1.2. Statement of the problem

Past research reports on the assessment of soil erosion, threats and drivers were addressed and identified at global, continental and national level. Additionally, climate change projections call for the future erosion might be aggravated due to changing climate.

Specially, in tropical continents (the northern and mid-latitudes), recent models projections have been predicted El-Nino Oscillation Southern (ENSO) events and sea surface temperature (SSTs) variability stimulates continue with increased CO_2 - associated with the mean temperature increment. There could be enhanced precipitation variability (Cubasch *et al.,* 1995). Small changes in the mean climate or its variability can produce relatively large changes in the frequency of extreme events (IPCC, 1995). With this regard, Ethiopia lies in the path of the seasonal migration of the Inter-tropical convergence zone (ITCZ), the atmospheric boundary between north easterly continental trade winds and on shore south easterly trade winds (Raymond, 2017). Also in Ethiopia, a more than 2°C rise in temperature was projected at the Upper Blue Nile Basin under two scenarios, ($RCP_{4.5}$ and $RCP_{8.5}$) in the 2050s and 2090s and it was pointed out a consistent both extreme wet and dry events indicating the possible occurrence of flooding and drought (Geremew and Agizew, 2015).

Ethiopia, as a country's ambitious plan to achieve middle-income status by 2025 based on the growth and transformation plan (FDRE, 2011) might be hindered by vulnerability to accelerated soil erosion because of existing pressures and climate change.

The study area, Neri watershed, part of Omo Gibe basin, is acknowledged as the main agricultural production area for rain fed and irrigated agriculture in South Ari woreda, South Omo zone. According to (SOZDWID, 2017), to boost the agricultural production, the modernized irrigation schemes with a command area of totally 124 hectare (83 hectare by constructed furrows by means of gravity and 41 by pressurized motor pumps) has been implemented and some are on the way. Besides, the agro-ecology was conducive for cereal crop production since earlier period and the expectation is high to deserve a high crop yield to fulfil the food security demand of the dwellers with in the watershed. Moreover, enormous mega development projects like development construction activities such as, airport, road and university have made this watershed their destiny.

Despite such a considerable potential this watershed obviously shares the above mentioned hazards and threats of soil erosion due to human activities and the aggravating impact of climate change. In turn this, decline in productivity of agricultural crops and growth of the rangeland grasses within in this watershed is being retarded (SOZDANR, 2017). The situation might had net effect of restricted crop choice for food production and a substantial decline in land value (Stocking, 1986). Through all this no attention was given to curb this problem and sustained resource use on today and future.

Consequently, information on spatial and temporal soil loss is needed within this watershed for decision makers in policy and strategy formulation and, for natural resource managers in providing a necessary tool to design the right intervention strategy for the specific climate, soil type, and topography and land use situation. In the meantime, the farmers in the study area are unable to curb the pace of global climate change and its impact on soil erosion. However, they may be able to adapt to climate change and devise management practices that are more resilient to climate impacts. Moreover, knowledge of potential risks of soil erosion in a changing climate may help inform farmers' agricultural management decisions. So this is why it is timely agenda to seek the insight for the alternative state of management practices due lack of previous information specific to Neri watershed.

Revised Universal Soil Loss Equation (RUSLE) model (Renard et al., 1997), is capable to quantify the annual rate of sol loss from the watershed based on the established data base. It's broad applicability and fit for various land use types, and better approximation of the topographic effect makes preferable (McCool et al., 1996; Renard et al. 1995). Due to RUSLE's conceptualization

which permits soil loss to be estimated, It is one of the most commonly applied models to estimate soil erosion (Woldeamlak and Teferi, 2009; López and Navas, 2010), and enables prediction of an average annual rate of soil erosion for a site of interest for any number of scenarios involving cropping systems, management techniques, and erosion control practices by using knowledge of the catchment characteristics and local hydro-climatic conditions (Garde and Kathyari, 1990).

1.3. Objective of the study

The main objective of this study is to assess soil loss risk under current conditions for priority intervention and to predict the outcome under future climate change conditions, should erosion management practices come to pass in Neri watershed, Omo-Gibe basin, Ethiopia.

1.3.1. Specific objectives

- To estimate the average annual soil loss rate under baseline condition (1988-2017) using RUSLE model
- To predict near and mid future soil loss as response in climate change and under management practices.
- To identify priority area for intervention.

2. LITERATURE REVIEW

2.1. Overview of Soil Erosion, processes and mechanisms

Soil erosion washes away the soil particles from sloping and bare lands while, wind blows away loose and detached soil particles from flat and unprotected lands due to two agents, water and wind that degrade soils (Oldeman, 1994). Water erosion is the process in which soil is detached and transported from the land by the action of rainfall, runoff, seepage and/or ice. Types of water erosion include splash, sheet, rill, gully, stream bank and tunnel erosion (Houghton and Charman, 1986; Rosewell, et al., 2007). Wind erosion is an erosion process in which soil is detached and transported from the land surface by the action of wind. Transport of windblown particles occurs by suspension, saltation or surface creep (McTainsh, 1995; Rosewell *et al.*, 2007).

Soil erosion is a two-phase process that consists the detachment of individual soil particles from the soil mass and their transport by erosive agents such as running water and wind. When sufficient energy is no longer available to transport the particles, a third phase, deposition occurs (Morgan, 2005).

2.2. Soil erosion in the world and Ethiopian context

Worldwide, land degradation has affected about 1.9 billion hectares of land. The loss of potential productivity due to soil erosion is estimated at 20 million tons of grains per year (UNEP, 1999). Soil erosion increased throughout the 20th century. About 85% of land degradation in the world is associated with soil erosion, most of which occurred since the end of World War II, causing a 17% reduction in crop productivity (Oldeman et al., 1990). Soil erosion by water affects nearly 1,100 million hectares worldwide, representing about 56% of the total degraded land while wind erosion affects about 28% of the total degraded land area (Oldeman, 1994).

Particularly, in developing countries the competition on limited resources and poverty exacerbated the degradation of natural resources. The estimated national level study indicate, the average soil removal over the Ethiopia is about 2 billion (FAO,1986) the highest rate of soil loss 42 $tha^{-1}yr^{-1}$ on average occurs on cultivated fields (Hurni, 1993). In the Ethiopian highlands only, an annual soil loss reaches 200-300 tons $ha^{-1}yr^{-1}$ (FAO, 1984; Hurni, 1993).

2.3.Soil erosion measurement and Models

Research on soil erosion and its effect on agricultural productivity started in USA in 1930s. During 1940 and 1956, research scientists began to develop a quantitative procedure for estimating soil

loss. The measurement of soil loss is done either by field measurement or by using models. Soil erosion measurements allow rates of erosion to be determined at different positions in the landscape over various spatial and temporal scales. But, it is challenging to take unbiased measurements to study how erosion rates respond to changes in land use and climate at every point in the landscape through extreme event or a few years of abnormally high rainfall. To achieve this, it is time and finance consuming. Unlike measurements, models can be used to predict erosion under a wide range of conditions (Morgan, 2005). Models also simplify those problems of direct measurement as a model is a representation of processes and their interactions with the aim of extracting, evaluating and simulating the relevant processes (Renschler, 1996). Model results are thought to be a better tools than absolute predictions of soil loss rate as it is clearly stated in the study by (Nearing et al., 2005). .

2.3.1. Types of Soil erosion models

Physically based models

This model is based on mathematical equations to describe the processes involved in the model taking account of the laws of conservation of mass and energy. Physically based models are based on knowledge of the fundamental erosion processes and incorporate the laws of conservation of mass and energy (Petter, 1992). Some of the examples include ANSWERS (Beasley, *et al.,* 1980) WEPP (Flanagan D.C. & Nearing M.A.), EUROSEM (Morgan *et al.,* 1991, 1992) and AGNPS. The main limitation of these models is that they are data hungry.

Stochastic models

Based on generating synthetic sequences of data from the statistical characteristics of existing sample data; useful for generating input sequences to physically based and empirical models where data are only available for short periods of observation.

Empirical models

These models are statistical or metric. By strict sense, these are models primarily based on an observation (not on theory) and are usually statistical in nature. Empirical models are based on inductive logic, and generally are applicable only to those conditions for which the parameters have been calibrated (Nearing, *et al.,* 1984). Empirical models are generally the simplest of all three model types and they are frequently used in preference to complex physically based models as they can be implemented in situations with limited data and parameter inputs, particularly as a first step in identifying sources and rate of soil loss (Merritt *et al.,* 2003).

Empirical Based on identifying statistically significant relationships between assumed important variables where a reasonable data base exists. Three types of analysis are recognized are black-box (only main inputs and outputs are studied), grey-box, where some detail of how the system works is known and white-box, where all details of how the system operates are known.

There are widely applied empirical models such as USLE, RUSLE and SLEMSA the detail of some of them is as follows.

2.3.1.1. Universal Soil Loss Equation (USLE)

USLE model is the most widely and universally used model for erosion hazard assessment. The first attempt to develop a soil loss equation for areas such as hill slopes and fields was that of (Ziang, 1940), who related erosion to slope steepness and slope length. Further developments led to the addition of a climatic factor based on the maximum 30-minute rainfall total with a two-year return period (Musgrave, 1947), a crop factor, to take account of the protection effectiveness of different crops, a conservation factor and a soil erodibility factor. Changing the climatic factor to the rainfall erosivity index (R) ultimately yielded the Universal Soil Loss Equation (USLE; Wischmeier & Smith 1978). The equation

$$A=R* K* L* S* C*P \quad \text{..... Equation (1)}$$

Where, A is the mean annual soil loss, R is the rainfall erosivity factor, K is the soil erodibility factor, L is the slope length factor, S is the slope steepness factor, C is the crop management factor and P is the erosion-control practice factor. Since K represents mean annual soil loss per unit of R, A has the same units as K. Thus, if K is in t ha^{-1} for one unit of metric R, multiplication by the metric R value will give the value of E in t ha^{-1}. If K is in US tons per acre per unit of American R, multiplication by the American R value yields a value of E in US tons per acre. In both cases, the A value is then adjusted by multiplying by the values of L, S, C and P, which are dimensionless coefficients. The individual factors in the equation are derived as follows.

Rainfall erosivity factor (R-factor)

R factor: The R factor is an expression of the erosivity of rainfall and runoff at a particular location. The value of "R" increases as the amount and intensity of rainfall increase. The R factor represents the erosivity of the climate at a particular location. An average annual value of R is determined from historical weather records using erosivity values determined for individual storms. The

erosivity of an individual storm is computed as the product of the storm's total energy, which is closely related to storm amount, and the storm's maximum 30-minute intensity (USDA, 2003). Rills and sediment deposits observed after an unusually intense storm have sometimes led to the conclusion that significant erosion is associated with only a few severe storms. The significant erosion is solely a function of peak intensities though it is not always true (Wischmeier, 1978). The numerical value used for R in USLE must quantify the effect of raindrop impact and must also reflect the amount and rate of runoff likely to be associated with the rain. The erosion index (R) derived by Wischmeier appears to meet these requirements better than any of the many other rainfall parameters and groups of parameters tested against the plot data. It is the product of total storm energy (E) and maximum 30 minutes rainfall intensity (I30) (Wischmeier and Smith, 1958). The EI is computed as the product of total storm energy (E) times the maximum 30-min intensity (I_{30}) of the rain.

$$EI = E \times I30 \quad \text{.....Equation 2}$$

The USLE uses the annual *EI* which is computed by adding *EI* values from individual storms that occurred during the year. According to Wischmeier and Smith (1978), the EI corresponds closely with the amount of soil loss from a field.

***Soil Erodibility Factor* (*K*)**

Soil erodibility index defined as mean annual soil loss per unit of *R* for a standard condition of bare soil, recently tilled up-and-down slope with no conservation practice and on a slope of 5° and 22 m length. *K* can be defined for a unit of both American and metric *R*. Wherever possible, *K* should be based on measured values. If the value is obtained from the nomograph, it should be remembered that this is an estimated value and will be subject to error.

The soil erodibility nomograph (Wischmeier et al., 1971) is a popular tool for estimating K values, but it does not apply to some soils. Updating the K-factor for RUSLE involved developing guides so the user could identify soils where the nomograph does not apply and estimate K using alternative methods. Erodibility data from around the world have been reviewed, and an equation has been developed that gives a useful estimate of K as a function of an "average" diameter of the soil particles. Only soils with less than 10% of rock fragments were considered. The equation in SI units (Foster, 1981) can be expressed as:

$$K = \frac{0.00021\times M1.14\times 12-a) + 3.25\times(b-2)+3.3\times 10-3(c-3)}{100} \quad \text{.....(3)}$$

M = (% *silt* + % *very fine sand*) × (100 - % clay)

Where, M is particle-size parameter, a is % of soil organic matter content, b is soil structure code (1 = very fine granular; 2 = fine granular; 3 = medium or coarse granular; 4 = blocky, platy, or massive), and c profile permeability (saturated hydraulic conductivity) class [1 = rapid (150 mm h^{-1}); 2 = moderate to rapid (50–150 mm h^{-1}); 3 = moderate (12–50 mm h^{-1}); 4 = slow to moderate (5–15 mm h^{-1}); 5 = slow (1–5 mm h^{-1}); 6 = very slow (<1 mm h^{-1})]. The size of soil particles for very fine sand fraction ranges between 0.05 and 0.10 mm, for silt content between 0.002 and 0.05, and clay <0.002 mm. The soil organic matter content is computed as the product of percent organic carbon and 1.72.

Topographic Factor (LS-Factor)

The factors of slope length (*L*) and slope steepness (*S*) can be combined in a single index, which expresses the ratio of soil loss under a given slope steepness and slope length to the soil loss from the standard condition of a 5° slope, 22 m long, for which *LS* = 1.0. The appropriate value can be obtained from nomographs (Wischmeier & Smith 1978) or from the equation

$$LS = \left(\frac{x}{22.13}\right)^{n} * 0.065+0.45s+0.0065s^{2} \quad \text{..... (4)}$$

Where, x is the slope length (m) and s is the slope gradient in per cent and the value of *n* should be varied according to the slope steepness.

***Cover-Management Factor* (*C*-factor)**

Cover-management is based on the concept that soil loss changes in response to the vegetative crop cover during the five crop stage periods: rough fallow, seedling, establishment, growing, and maturing crop, and residue or stubble. The crop management factor represents the ratio of soil loss under a given crop to that from bare soil. Since soil loss varies with the erosivity and the morphology of the plant cover. It is computed as the soil loss ratio from a field under a given crop stage period compared to the loss from a field under continuous and bare fallow conditions with up- and down-slope tillage (Wischmeier and Smith, 1978)

Support Practice Factor (P)

The P-factor refers to the practices that are used to control erosion. It is defined as the ratio of soil lost from a field with support practices to that lost from a field under up-and down-

slope tillage without these practices. The P-values vary from 0 to 1 where the highest values correspond to a bare without any support practices.

2.3.1.2. RUSLE Model Description

A RUSLE model is an erosion model predicting longtime average annual soil loss (A) resulting from raindrop splash and runoff from specified slopes in specified in specified cropping and management system and from rangeland. It is also applicable to nonagricultural conditions such as construction sites (Renald et al., 1997). RUSLE takes into account average soil loss over field slopes different greatly from one another.

A=R*K*L*S*C*P..... (5)

Where, A is the computed soil loss ($t \cdot ha^{-1} year^{-1}$), R is the rainfall-runoff erosivity factor ($MJ \cdot mm \cdot ha^{-1} \cdot hr^{-1} yr^{-1}$, K is the soil erodibility factor ($t*ha*hr^{-1}*ha^{-1}*MJ^{-1}*mm^{-1}$), L is the slope length factor, S is the slope steepness factor, C is the cover-management factor, and P is the supporting practices factor. **L, S, C** and **P** are dimensionless. This empirically based equation, derived from a large mass of field data, computes combined inter rill and rill erosion using values.

Rainfall erosivity factor (R-factor)

The latent capacity of rain drop to cause soil erosion is termed as erosivity (R) factor (Renard et al., 1991). Although the methods used to calculate the R-factor and EI_{30} are described by Wischmeier and Smith (1978) and in the RUSLE user guide (Renard et al., 1994). The R-factor is the sum of individual storm EI-values for a year averaged over long time periods (> 20 years) to accommodate apparent cyclical rainfall patterns.

Rainfall erosivity concept refers to the ability of any rainfall event to erode soil. The rainfall erosivity is defined as the average annual value of the rainfall erosion index (Wischmeier and Smith, 1958). The monthly rainfall erosivity value was computed by summing up EI_{30} values of storms that occurred during the month (Foster et al., 1991). The RUSLE model uses (Brown and Foster, 1987) approach for calculating the average annual rainfall erosivity, *R* ($MJ\ mmha^{-1}\ h^{-1}y^{-1}$).

$$\mathbf{R = 1/n \sum_{j=0}^{n} [\sum_{k=0}^{m} (E) k\ (I30)\ k]} \quad \text{..... (6)}$$

Where, *E is* the total storm kinetic energy ($MJ\ ha^{-1}$), I_{30} is the maximum 30 minute rainfall intensity ($mm\ h^{-1}$), *j* is an index of the number of years used to produce the average, *k* is an index of the

number of storms in each year, *n* is the number of years used to obtain the average *R*, and *m* is the number of storms in each year.

Soil erodibility factor (K-factor)

Erodibility of a soil is an expression of its inherent resistance to particle detachment and transport by rainfall. It is determined by the cohesive force between the soil particles, and may vary depending on the presence or absence of plant cover, the soil's water content and the development of its structure (Wischmeier and Smith, 1978). The typical range of K value is from about 0.013 to 0.059 SI units or (0.10 to 0.45 US customary units) (Foster *et al.*, 1981).

The K factor is a measure of the inherent erodibility of the soil or surface material at a particular site under standard experimental conditions. The relationship for volcanic soil of Hawaii by El-Swaify and Dangler (1976) equation (10).

$$K = -0.03970 + 0.00311X_1 + 0.00043X_2 + 0.00185X_3 + 0.00258X_4 - 0.00823X_5 \quad \text{Equation 5}$$

Where, X_1 is the percent unstable aggregates <0.250 mm, X_2 is the product of the percent of silt (0.002–0.01 mm) and sand (0.1–2 mm) present in the sample, X_3 is the percent base saturation of the soil, X_4 is the percent silt present (0.002–0.050 mm), and X_5 is the percent sand in the soil (0.1–2 mm). This equation results in a *K*-factor with units of ton acre [hundreds of acre ft. ton f in] $^{-1}$. The recent global data for 225 soils of measured K values obtained from both natural and simulated rainfall studies were pooled into textural classes. Only for less than 10% of rock fragments by weight (less than 2mm diameter size) were considered. The mean values of the soil-erodibility factor for soils within these size classes were then related to mean geometric particle diameter of that class. ln

$$K = 7.594 * \left\{0.0034 + 0.0405 exp\left[\frac{-1}{2}\left[\frac{log(Dg)+1.659}{0.7101}\right]2\right]\right\} \quad (6)$$

$$Dg = exp\left(\sum fi \, ln \frac{(dI+di-1)}{2}\right) \quad (7)$$

Where, K = the erodibility factor expressed as U.S. customary units of ton. acre h (hundreds of acre. ft.- tons in)$^{-1}$ to obtain the K-factor in SI units of t. h. ha ha^{-1} MJ^{-1} mm $^{-1}$ divide the right side of the equations with the factor 7.594.

Dg is the geometric mean particle size, for each particle size class (clay, silt, sand), d_i is the maximum diameter (mm), d_{i-1} is the minimum diameter and f_i is the corresponding mass fraction.

This relation is very useful with soils for which data are limited and/or the textural composition is given in a particular classification system (Shirazi and Boersma, 1984). A similar relation for 138 US soils only with r^2=0.945

$$K=\left\{0.0017+0.0494 exp\left[\frac{-1}{2}\left[\frac{log(Dg)+1.675}{0.6986}\right]2\right]\right\} \ldots \ldots \ldots \ldots \ldots \ldots \ldots \ldots \ldots \ldots \ldots \ldots \ldots \ldots \ldots \ldots \ldots \ldots (8)$$

Slope steepness and slope length factor (LS- Factor)

Slope Length Factor (L)

Plot data used to derive the slope length factor (L) have shown that average erosion for the slope length λ (in ft**.)** varies as

$$L = (\lambda/72.6)^{m} \ldots \ldots \ldots \ldots \ldots \ldots \ldots \ldots (9)$$

Where, 72.6 = the RUSLE unit plot length in **ft.** and m = a variable slope-length exponent (Wischmeier and Smith 1978). The slope length; λ is the horizontal projection, not distance parallel to the soil surface. The slope-length exponent m is related to the ratio β of rill erosion (caused by flow) to interrill erosion (principally caused by raindrop impact) by the following equation (Foster et al. 1977):

$$m = \beta/ (1+\beta)$$

Values for the ratio β of rill to interrill erosion for conditions when the soil is moderately susceptible to both rill and interrill erosion were computed from (McCool et al. 1987)

$$\beta = (\sin \theta/0.0896) / \left[3.0(\sin \theta)^{0.8} + 0.56\right]$$

Where, **θ** = slope angle. Given a value for p, a value for the slope-length exponent m is calculated from equation

L and S factors in RUSLE uses four separate slope length relationships. Three are functions of slope steepness as in the USLE, and of the susceptibility of the soil to rill erosion relative to inter-rill erosion. A separate slope length relationship was developed specifically for the dry farmed cropland region of the Pacific Northwest of the US (McCool et al., 1989; 1993). The major concerns have been expressed over the L-factor than any of the USLE factors, because different users choose different slope length for similar situation. RUSLE includes improved guides for choosing slope length values to give greater consistency among users. The attention given to the L-factor is not always warranted, because soil loss is less sensitive to slope length than to slope steepness. For typical slope conditions, a 10% error in slope length results in a 5% error in

computed soil loss. Revised slope steepness relationships were developed from data from a large number of historical and current research plots (McCool et al., 1987b). Mitasova and Mitas (1999) and Simms et al. (2003) suggested LS factor in Arc GIS raster calculator using the map algebra expression as the following equation.

LS=pow ((Flow Accumulation)*Resolution/22.13, 0.6)*(Sin(slope)*0.0175)/0.896)1.3)……(10)

Cover and management factor (C-Factor)

C factor for RUSLE reflects the effect of plants, soil cover, below-ground biomass, and soil-disturbing activities on soil erosion. Both time-variant (cropping/rotation scenario) and time-invariant (average annual values) modules have been constructed. So, it is the most important RUSLE factor because it represents conditions that can most easily be managed to reduce erosion. The C-Factor is perhaps the most important factor in RUSLE because: (1) it represents surface conditions that are easily managed for erosion control, and (2) the values range from virtually 0 to slightly greater than 1, strongly influencing the soil-loss rate (Toy et al. 1999). Values for C are a weighted average of soil loss ratios that represent the soil loss for a given condition at a given time, to that of the unit fallow plot. Thus, soil loss ratios vary during the year as soil and cover conditions change.

In RUSLE, a sub factor method is used to compute soil loss ratios as a function of four sub factors (Renard et al., 1997) given as:

C = PLU * CC * SC * SR*SM …….. (11)

Where, PLU is prior land use sub factor, CC is crop canopy sub factor, SC is surface or ground cover (including erosion pavement) sub factor and SR is the surface roughness sub factor.

Conservation support practice factor (P-Factor)

Supporting conservation practices like contour farming, strip cropping, terracing, and subsurface drainage on soil loss in an area as they principally affect water erosion by means of modifying the flow pattern, grade, or direction of surface runoff and by reducing the volume and rate of runoff (Renard et al., 1997). Adoption of supporting conservation practices decreases the value of P-factor value as they encourage deposition on uplands locally (Yang et al., 2003).

2.3.2. Comparison of USLE and RUSLE

RUSLE model is more comprehensive and detailed than USLE and is based on empirical- and process-based approaches (Renard et al., 1997). As compared to USLE, it includes more EI values for the western U.S. in addition to those in the eastern U.S. It incorporates soil processes (e.g., freezing and thawing) and changes in water content into the USLE. It uses computer tools to calculate complex LS interactions based on rill and interrill erosion relationships and incorporates information on canopy and surface residue cover and the effects of temperature and soil water on above- and below-ground residue decomposition at short time (1/2 month) intervals.

In USLE, the C values are calculated from tables with data from field experiments, but RUSLE computes these values from four sub-factors, which are the following: prior land use (PLU) factor which accounts for the amount and biomass and tillage practices from previous years, the canopy (CC) factor accounting for the vegetative cover, the surface cover (SC) factor that reflects the amount of residue mulch left on the soil surface, and surface roughness (SR) factor. The RUSLE accounts for the influence of farming across slopes as well as strip cropping and buffer strips within the P factor. The P values are estimated based on slope length and steepness, ridge height, soil deposition, soil infiltration, and the cover and roughness conditions.

Major changes to the USLE incorporated into RUSLE include rainfall erosivity (R-factor**)** is based on new and improved isoerodent maps and erodibility index (EI) distributions for some areas, soil erodibility (K-factor) consider time-variant soil erodibility which reflects freeze-thaw in some geographic areas, in the case of slope length and steepness (LS-factor), new equations developed to account for slope length and steepness separately, cover-management (C factor) accounted additional sub-factors for evaluating the cover and management factor for cropland and rangeland. Finally, conservation support practice (P factor) incorporated new conservation practice values are added for cropland and rangeland (Renald et al., 1997).

2.3.3. Remote Sensing and GIS in Soil Loss risk assessment

Generation of spatial data for application of models is the major difficulty. This is due to the time and budget needed. The advantage of remote sensing technology is, spatial information on input parameters has become more handy and cost-effective. Besides with the powerful spatial processing capabilities of Geographic Information System (GIS) and its compatibility with remote sensing data, the soil erosion modeling approaches have become more comprehensive and robust.

To assess the data on soil type, slope gradient, drainage, geology and land cover, remote sensing is important tool. Multi-temporal satellite images provide valuable information related to seasonal land use dynamics.

Satellite data can be used for studying erosional features, such as gullies, rainfall interception by vegetation and vegetation cover factor. DEM (Digital Elevation Model) one of the vital inputs required for soil erosion modeling can be created by analysis of stereoscopic optical and microwave remote sensing data. Remote sensing can also be used to generate a cover and management factor (C-factor) which is one of the input requirements of erosion modeling (Morgan, 1995; Wischmeier and Smith, 1978).

The factors associated with soil classification such as soil properties, climate, vegetation, topography, and lithology can be potentially mapped with satellite remote sensing to account for spatial differences in erodibility which serve as input data for erosion modeling (Mc Bratney et al., 2003).
Some remote sensing techniques on satellite imagery is NDVI, can be applied for vegetation greenness, biomass, dominant species and leaf area index. The Normalized Difference Vegetation Index (NDVI) is one of the techniques which is useful to separate green vegetation from the background soil brightness. It is the difference between the near infrared and red reflectance normalized over the sum of these bands as shown in equation below by (Rouse *et al*., 1974; Jensen, 2000).

NDVI = (NIR - Red)/ (NIR + Red) ……………………………………………………………… (12)

NDVI values obtained from remotely sensed image can be applied in oil erosion models like RUSLE. This NDVI map can then be classified into vegetation categories and displayed as a vegetation map with different colors representing different levels of vegetation. Then, C-factor can be estimated by applying the relationship used in (Van der Knijff et al.1999, 2000; Van Leeuwen and Sammons 2004): as follows;

$$C = e^{(-\alpha(\frac{NDVI}{\beta - \mathrm{NDVI}})} \ldots \ldots \ldots \ldots \ldots \ldots \ldots \ldots \ldots \ldots \ldots \ldots \ldots \ldots \ldots \ldots \ldots \ldots \ldots \ldots \ldots \ldots \ldots \ldots \ldots \ldots \ldots \ldots \ldots . (13)$$

Where C is the calculated crop-cover management factor; NDVI is the normalized differential vegetation index, α and β are two scaling factors. By applying this relationship, better results are

obtained than using a linear relationship, the values for the two scaling factors α and β are 2 and 1 respectively. Then, the corresponding **C-** factor map was produced**.**

Soil erosion study assumes that there exists a linear correlation between NDVI and C factor, and uses bare soil and forest NDVI values as reference values. Sample NDVI values were collected for bare soil and forest land cover classes from average NDVI image. Since C factor values range from 0 for well-protected soil to 1 for bare soil (Vincent e al., 2007), the C factor values for bare soil and forest land cover were set to 1 and 0, respectively in the regression analysis. The line obtained after analysis is the regression line that describes relationship between C and NDVI values and R shows the correlation coefficient of regression analysis. The regression equation was found as:

C-factor = 1.02 – 1.21 x NDVI ……. (14)

Soil is protected by vegetation cover from rain drop energy before reaching the surface despite the value of C –factor vary with the type, stage of growth and percentage of cover (Gitas et al., 2009). The values of cover and management ranges between 0 and 1 (Tweddales et al., 2000) the C factor values for bare soil and forest land cover were set to 1 and 0, respectively in the regression analysis (Vicente et al., 2007). The goal of regression analysis in mathematical model was used to estimate dependent variable based on independent variable. The linear or non-linear regression equations are constructed using correlation analysis between NDVI values obtained from remotely sensed image and corresponding C factor values obtained from USLE guide tables and related literatures.

2.4. Concepts of Climate and Climate change

Climate is defined as the statistical description of the average weather in terms of the mean and variability of relevant quantities over a period of time ranging from months to thousands or millions of years. Whereas, weather refers to the physical condition of the atmosphere at a certain place over a short period of time which has the principal elements such as temperature, precipitation, pressure, wind and moisture. World Meteorological Organization defined the climate variables average for 30 years classical period. In broader sense climate is the state, including a statistical description, of the climate system (Stone and Knutti, 2011; Philander, 2008). Climate change refers to a change in the state of the climate that can be identified (e.g., by using

statistical tests) by changes in the mean and/or the variability of its properties, and that persists for an extended period, typically decades or longer.

2.4.1. Climate models and Scenarios

Climate models are mathematical representations of the climate system, expressed as computer codes and run on powerful computers. There are different kinds of climate models that range from simple energy balance models to complex earth system models (Stone and Knutti, 2011).

To respond to the needs of decision makers to plan for climate change, a variety of reports, tools, and datasets provide projected climate impacts at spatial and temporal scales much finer than those at which the projections are made. It is important to recognize the variety of assumptions behind the techniques used to derive such information and the limitations they impose on the results

The main tools used to project climate are General Circulation Model (GCMs), which are computer models that mathematically represent various physical processes of the global climate system. These processes are generally well known but often cannot be fully represented in the models due to limitations on computing resources and input data. Thus, GCM results should only be considered at global or continental scales for climatic conditions averaged at monthly, seasonal, annual, and longer time scales.

Atmosphere-Ocean Global Climate Model (AOGCMs) are extensively used for making climate projections. For instance, the climate projections of the Intergovernmental Panel on Climate Change (IPCC) assessment reports have come from these models. AOGCMs provide credible quantitative estimates of future climate change for larger spatial areas (continental or regional scale) and longer time scales. Confidence in these estimates is higher for some climate variables (e.g., temperature) than for others (e.g., precipitation). GCMs are also more skillful at predicting means (averages) of precipitation or temperature than any higher order statistics (i.e., variability).

Socio-economic and emission scenarios provide plausible descriptions of how the future may evolve with respect to a range of variables including socio-economic change, technological change, energy and land use, and emission of greenhouse gases and air pollutants (van Vuuren et al., 2011). These future scenarios of forcing agents (e.g., greenhouse gases and aerosols) are fed in to the climate models as input, and the output of these climate models is

further used in climate change analysis and hence, the assessment of impacts, adaptation and mitigation. Several sets of scenarios including the IS92 scenarios (Legegett et al., 1992), the scenarios from the Special Report on Emission Scenarios (SRES) (Nakicenovic & Swart, 2000) and, more recently, the Representative Concentration Pathways (RCP) (van Vuuren et al., 2011). In the subsequent section, a brief description of RCP scenario is presented.

2.4.2. Climate downscaling

Downscaling is derivation of local to regional-scale (10-100) kilometers) information from larger scale modeled or observed data. To respond to the needs of decision makers to plan for climate change, a variety of reports, tools, and datasets provide projected climate impacts at spatial and temporal scales much finer than those at which the projections are made. It is important to recognize the variety of assumptions behind the techniques used to derive such information and the limitations they impose on the results.

The main tools used to project climate are General Circulation Model (GCMs), which are computer models that mathematically represent various physical processes of the global climate system. These processes are generally well known but often cannot be fully represented in the models due to limitations on computing resources and input data. Thus, GCM results should only be considered at global or continental scales for climatic conditions averaged at monthly, seasonal, annual, and longer time scales. Many of the processes that control local climate, e.g., topography, vegetation, and hydrology, are not included in coarse-resolution GCMs. The development of statistical relationships between the local and large scales may include some of these processes implicitly (Viner, 2012). Global climate models (GCMs) are typically run at coarse spatial resolutions and result in mismatch between available climate change projections and the scale of interest to most applications (Brown et al, 2008). Climate downscaling techniques are used to bridge the spatial and temporal resolution gaps between what climate modelers are currently able to provide and what impact assessors require (Wilby & Dawson, 2007a). There are two main types of downscaling – techniques.

Dynamic downscaling is by explicitly including additional data and physical processes in models similar to GCMs but at a much higher resolution and covering only select portions of the globe. This method has numerous advantages but is computationally intensive and requires large volumes

of data as well as a high level of expertise to implement and interpret results, often beyond the capacities of institutions in developing countries (Daniels et al., 2012).

The GCM output is provided as boundary conditions, which are the values at the edges of the spatial domain of the RCM. Horizontal resolution for most RCMs is in the order of tens of kilometers which could capture important orographic and physical geography details to the simulations. In terms of temporal resolution, RCMs are usually most skillful at monthly or coarser timescales (Brown et al, 2008).

Statistical downscaling consists of modeling the statistical relationships between large-scale climates features that GCMs and local climate characteristics provide. In contrast to the dynamical method, the statistical methods are easy to implement and interpret. They require minimal computing resources but rely heavily on historical climate observations and the assumption that currently observed relationships will carry into the future. However, high quality historical records often are not available in developing countries. However, this approach relies on the critical assumption that the relationship between present large scale circulation and local climate remains valid under different forcing conditions of possible future climates (Zorita and von Storch, 1999). However both downscaling methods have their own advantages and disadvantages, the consensus of model inter–comparison studies is that dynamical and statistical methods have comparable skill at estimating surface weather variables under present climate conditions (Wilby and Dawson, 2007b).

2.4.2.1. Representative Concentration Pathway (RCP) Emission scenarios

Among the research community, recently there has been an increasing interest in scenarios that explicitly explore the impact of different climate-policies in addition to the no-climate-policy scenarios such as SRES (Moss et al. 2010). The need for new scenarios prompted the IPCC to request scientific communities to develop a new set of scenarios for the assessment of future climate change. Therefore a set of new scenarios is constructed containing emission, concentration and land-use trajectories referred to as "**R**epresentative **C**oncentration **P**athways" (RCPs). In its name, the word "representative" signifies that each of the RCPs represents a larger set of scenarios in the literature. This implies that this set of RCPs should be compatible with the full range of emission scenarios (with and without climate policy) available in the current scientific literature. The word "concentration pathway" emphasizes that these RCPs are not the final new, fully integrated scenarios (i.e. they are not a complete package of socio-economic, emission and climate

projections), but instead are internally consistent sets of projections of the components of Radiative forcing that are used for the input to climate models. The word "concentration" also emphasizes that instead of emissions, concentrations are used as the primary product of the RCPs, designed as input to climate models. Four RCPs scenarios named according to Radiative forcing target level for 2100 are used. Comparison of CO2 concentrations obtained by SRES and RCP emission scenarios.

$RCP_{2.6}$:- This scenario has also been referred to as RCP3PD representing the radiative forcing trajectory which goes to a peak level of 3 W/m2 (~490 ppm CO_2 eq) before 2100, followed by a decline (PD=Peak-Decline). The selected pathway declines to 2.6 W/m^2 by 2100 (Van Vuuren et al., 2007). It aims at limiting the increase of global mean temperature to 2°C above the preindustrial period. The $RCP_{2.6}$ outputs indicate possible future temperature and rainfall patterns with climate change policy.

$RCP_{4.5}$:- This scenario describes the stabilization without overshoot pathway to 4.5 W/m^2 (~650 ppm CO_2 equivalent) at stabilization after 2100 (Clarke et al., 2007). RCP4.5 corresponds to that category scenarios in AR4 which contains the far majority of the scenarios assessed.

$RCP_{4.5.}$ It is a stabilization scenario in which total Radiative forcing is stabilized shortly after 2100, without overshooting the long-run radiative forcing target level Tis scenario was an intermediate stabilization scenario leading to 4.5 W/m^2

RCP_6:- This scenario is also similar to RCP4.5, with stabilization without overshoot pathway to 6W/m2 (~850 ppm CO_2 equivalent) at stabilization after 2100 (Fujino et al. 2006). The number of mitigation scenarios leading to 6 W/m^2 in the literature is relatively low however, at the same time many baseline scenarios (no climate policy) correspond to this forcing level.

$RCP_{8.5}$: This scenario corresponds to the rising radiative forcing pathway leading to 8.5 W/m^2 (~1370 ppm CO_2 equivalent) by 2100 (Riahi et al., 2007). It corresponds to a scenario with no-climate policy baseline and comparatively high greenhouse gas emissions.

RCP $_{8.5}$: Under $RCP_{8.5}$ scenario, GHG emissions continue to increase rapidly through the early and mid-parts of the century and then stabilized at just under 30 Gt of carbon compared to around 8 Gt in 2000. This scenario is highly energy intensive with total consumption continuing to grow throughout the century reaching well over 3 times current levels. Land use continues current trends

with crop and grass areas increasing and forest area decreasing. $RCP_{8.5}$ scenario has no any policy or restriction to minimize the emission of GHG at the end of 21st century or it is business-as-usual (BAU) $RCP_{8.5}$ scenario.

$RCP_{8.5}$ was developed using the MESSAGE model and the IIASA (Integrated Assessment Framework by the International Institute for Applied Systems Analysis (IIASA), Austria. This RCP is characterized by increasing greenhouse gas emissions over time, representative of scenarios in the literature that lead to high greenhouse gas concentration levels (Riahi et al., 2007). This scenario was a very high emission scenario leading to 8.5 W/m^2 (Riahi et al., 2007). It corresponds to a scenario with no-climate policy baseline and comparatively high greenhouse gas emissions.

2.4.2.2.Climate change projections

Due to the inherent uncertainty of the climate system and the inevitable existence of model errors, multi-model ensembling is the recommended approach for climate change projections. IPCC has used several models in its coupled model inter-comparison projects (e.g. CMIP3, CMIP5) to make the various projections. There are also regional model inter-comparison projects, like The Coordinated Regional Climate Downscaling Experiment (CORDEX). CORDEX project (http://wcrp-cordex.ipsl.jussieu.fr/) is an initiative of the World Climate Research Program (WCRP) performed with the intention of producing an ensemble of high resolution climate change projections by dynamically downscaling GCM simulations from Coupled Model Inter-comparison Project Phase 5 (CMIP5) data archive (Jones *et al.*, 2011).

The major aims of the CORDEX initiative are to provide a quality controlled dataset of downscaled information, coordinated model evaluation framework, and an interface to the applicants of the climate simulations for further climate change impact, adaptation, and mitigation studies (Giorgi *et al.*, 2009). Recent analysis in relation to CORDEX simulations over Africa can be found in (Nikulin *et al.*, 2012; Hernández-Diaz *et al.*, 2013). Nikulin *et al.* (2012) evaluated the ability of ten RCMs over Africa and concluded that all RCMs simulate the seasonal mean and annual cycle quite accurately. Likewise, it is verified that the mean of multi-model outputs do better than individual simulation. Hernández-Diaz et al. (2013) strengthened the achievement of (Nikulin *et al.*, 2012). They successfully reproduce the overall features of geographical and seasonal distribution over most Africa. In their report, CORDEX simulations

succeed in reproducing the average distribution of precipitation and its large geographical differences.

2.4.3. Impacts of Climate Change on soil erosion

Climate change will influence soil and water resources throughout the world. Global changes in temperature and precipitation patterns will impact soil erosion through multiple pathways, (IPCC, 2007). It is expected to affect soil erosion based on a variety of factors. Increased precipitation amount and intensity has impacts not only on soil moisture and plant growth, but also direct fertilization effects on plants (Nearing, 2001; Zhang and Nearing, 2005). Increased temperature, altered precipitation patterns, snow cover change and seasonal snow melting by climate change are also potential causes of soil erosion (Beniston M., 2006), changes in the magnitude and frequency of extreme events with potential consequent effects on erosion and sediment yield (Fowler and Hennessey 1995). The most direct impact of climate change on soil erosion is the change in the erosive power of rainfall (Favis and Boardman, 1995; Pruski and Nearing, 2002; Mullan et al., 2012).

An increase in precipitation variance is accompanied by an increase in occurrence of heavy storms, which often have high intensity and therefore result in severe soil erosion (Zhang et al., 2004; Zhang and Nearing, 2005). Nearing et al., (2005) have shown that soil erosion was quite sensitive to changes in total rainfall amounts associated with changes in either storm intensity or duration, and soil erosion was more sensitive to those changes than runoff. In tropics, El-Nino Oscillation Southern (ENSO) events and sea surface temperature (SSTs) enhance intense precipitation. To date most soil erosion trends under climate change reported are from model simulations without an explicit spatial downscaling of GCMs projections (Zhang, 2005). This type of approach tends to provide a first order sensitivity of regional response to climate change (Hewitson, 2003**;** Zhang and Liu 2005; Zhang, 2005).

Even though soil erosion is a natural and inevitable process, the accelerated rates of soil loss, represent a serious environmental problem. For example, decline in agricultural productivity (Bakker et al., 2007).

3. MATERIALS AND METHODS

3.1. Description of study area

3.1.1. Location

The study area, Neri watershed is situated in the lower part of the Omo Ghibe basin southwestern, Ethiopia. Geographically, it lies between 5.63^0 and 5.93^0 North, and 36.31^0 and 36.67^0 East. The study area is about **465.46** km^2. There are about eighteen Kebeles (smaller administrative units), Jinka town and parts of Mago national park.

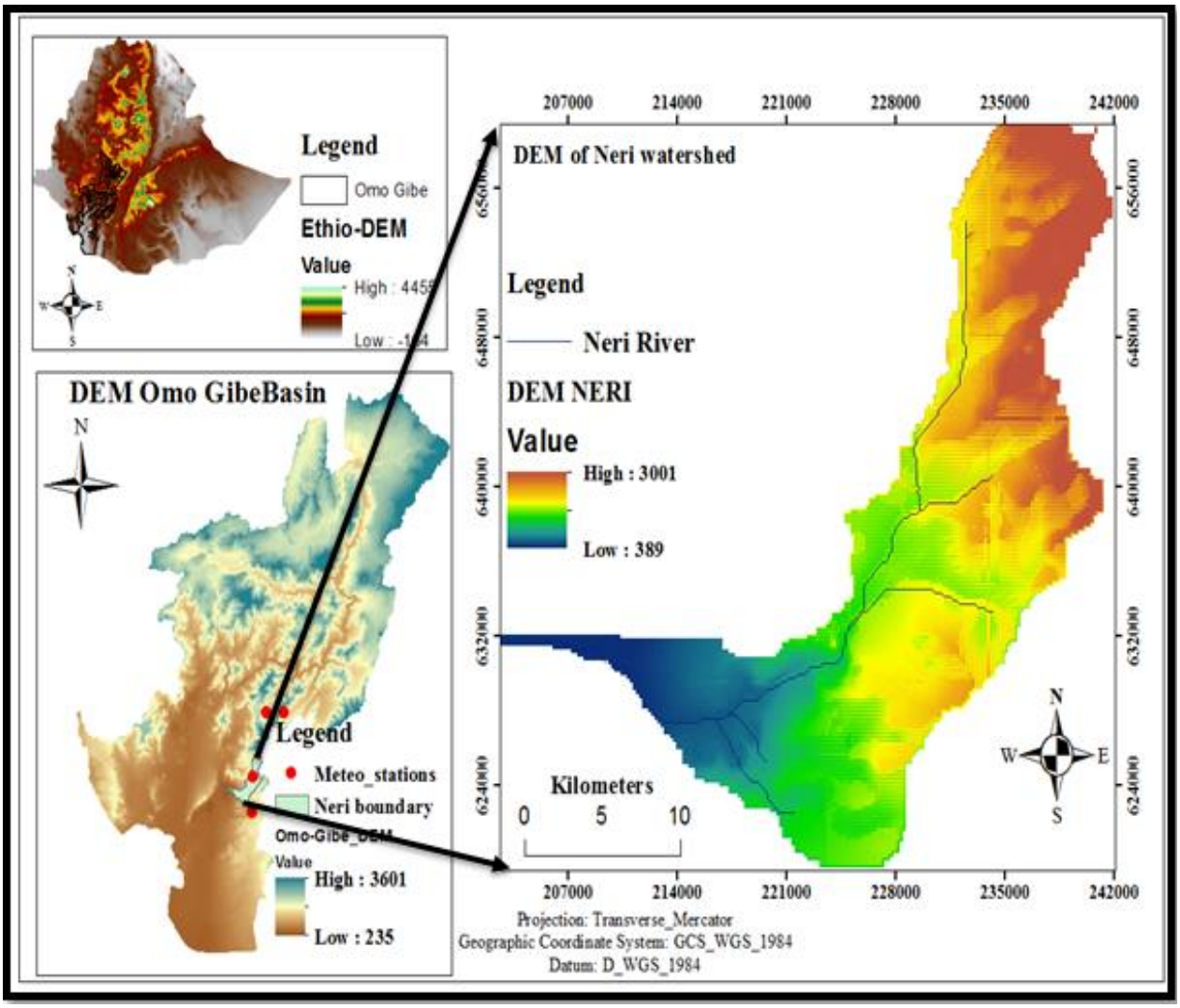

Figure 1:- Location map of the Neri watershed

3.1.2. Climate

The climate of Neri watershed has diverse nature due to the variation in altitude based on elevation. It varies from cool at humid highlands ('Dega') to warm at semi-arid lowlands (Kolla) according

to traditional zone (USDA, 2003; Alemayehu, 2006). Mainly rainfall and temperature are the major climatic elements which are important factors in determining geomorphic processes, soil formation, and the bio-physical environment in general at a given geographical environment.

The long term annul average rainfall of the study area is 1342.033 mm see Figure 2 below and characterized by bimodal type. The mean monthly rainfall of the study area is summarized below in Figure 2. It decreases, but temperature increases throughout the watershed with a decrease in elevation. (Appendix1 Table 2) and Figure 2 below show that, the maximum and minimum monthly average temperatures of the study area are 27.61 and 16.3°C, respectively.

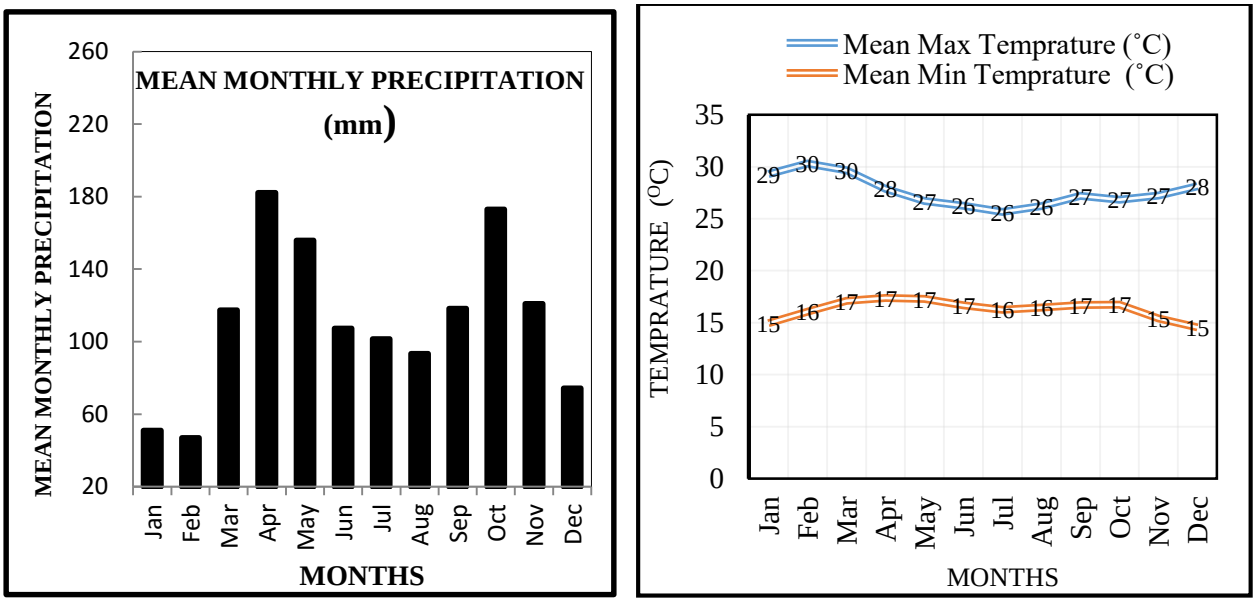

Figure 2:-Monthly average rainfall, and maximum and minimum temperature (1988-2017).

(Source: Regional Meteorological Agency)

3.1.3. Soil types of Neri Watershed

According to FAO (2012) soil classification, soils of the study watershed are classified as Orthic solonchaks, calcic xerosols, haplic xerosols, leptosol, Eutric cambisols, Eutric fluvisols, Orthic acrisols, Dystric nitisols and Dystric fluvisols. Dominant soil of the watershed is Orthic solanchaks followed by Calcic Xerosols as shown in 'Figure 3' and 'Table 6'. Moreover, upper catchment is characterized by variety of soil types i.e. Orthic acrisols, Dystric nitisols, Calcic Xerosols, Dystric fluvisols, leptosol and Orthic solonchaks. Calcic Xerosols and Orthic solonchaks are predominant in the middle catchment. Whereas the remaining three soil types (Eutric cambisols, Eutric fluvisols and haplic xerosols) are found to the lower catchment of the study area.

Table 1:- Soil types of the watershed with their area coverage

No.	Soil type	Area coverage (ha)	Percentage (%)
1	Orthic acrisols	2327.3	5%
2	Eutric fluvisols	4189.14	9%
3	Dystric nitisols	1396.38	3%
4	Leptosols	5120.06	11%
5	Calcic xerosols	7912.82	17%
6	Orthic solonchaks	13032.88	28%
7	Dystric fluvisols	930.92	2%
8	Haplic xerosols	6981.9	15%
9	Eutric cambisols	4654.6	10%

Soil types towards south of Jinka town, middle catchment are structurally weak. This reflects their young age development, and friable consistency. These soils are also characterized as well drained non-calcareous soils (MoWR, 1996).

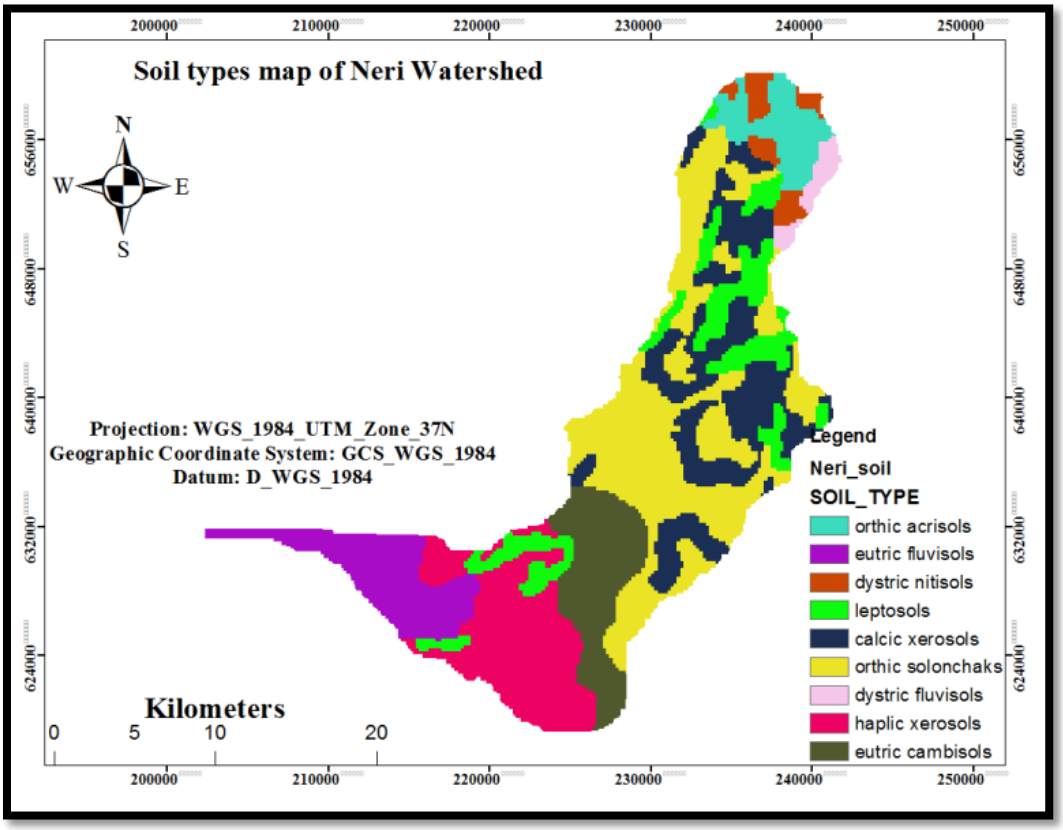

Figure 3:- Soil type map of Neri watershed

3.1.4. Land use/ Land cover types and Farming practices

The land use land cover classes with their area coverage are not discussed here. Further discussion of the land use in the Neri watershed follows on Figure 9. The rural dwellers in Neri watershed are subsistence farmers and animal breeders. With respect to crop types, mostly this area is known to produce crops like maize, wheat, barley sorghum and vegetables. Maize and sorghum are being the commonest at mid to lower catchments and upper catchment is known by wheat and barley production. Among these crops, maize (Zea mays), haricot bean, potato and sorghum (Sorghum bicolor) are cultivated in 'belg' season whereas, wheat, barely in 'meher' season of Ethiopia. Maize is cultivated in both seasons.

Neri watershed has sparse vegetation which is due to patches of agricultural activity. Multipurpose trees species such as Mango (Mangifera indica), Avocado (persea Americana)

Gorka (podocurpus falcatus), coffee, cata-edulis (chat) and Moringa stenophetala in home garden. These species are also sparsely observed on-farm lands with crops.

3.1.5. River characteristics and Topography of Neri Watershed

Among the main river sub basins of Omo-Gibe basin, Mago sub basin is mainly contributed from Neri, Sara and Berso rivers. The study site is known as the Neri watershed; with the catchment area of 465.46 km^2 and is chosen as a pilot test area to quantify soil losses under current and future climate change conditions. Neri river system of the watershed raises from the highest peak of south omo zone Shanghama Mountain, the elevation peak of 3,418m and mainly drains highlands of South Ari woreda and BenaTsemay woredas in its administrative boundary.

The highest and lowest altitude of Neri watershed 3001 meter and 389 meter above sea level respectively. This watershed is generally characterized by rugged topography and degraded ecosystems due to deforestation, overgrazing and poor land management.

3.2. Methods of data collection and parameter determination for estimation of baseline soil loss

The Revised Universal Soil Loss Equation (RUSLE) using GIS and remote sensing technique was used to estimate the mean annual soil loss occurred in Neri Watershed. RUSLE is an empirical model developed by Renard et al. (1997) to estimate soil loss. Laflen and Molden (2003) confirmed its applicability on areas where soil loss by water is a problem.

3.2.1. Rainfall erosivity (R factor) estimation method

The rainfall acts as the force for sheet and rill erosion without protection. The high rate of rainfall with large drop size can erode the soil particles faster than normal rainfall. Precipitation data sets were collected from the National meteorological agency (NMA) from 1988 to 2017 for four meteorological stations namely; Jinka (the station within the watershed), Bulkimender, Sawla and Keyafer rainfall gauging stations which are nearby to Neri watershed. The data of these four stations were used to estimate the erosivity factor for baseline condition as well as data bias check for projected data for future.

Prior to application of historical data to hydrological impact assessment and application in to erosion modelling, missing data was filled by IDW method, checked for outliers and the data homogeneity was tested by means of a frequency analysis.

RAINBOW Version 2.2, (software package by (Raes et al., 2006) which is responsible for hydro meteorological testing the homogeneity and frequency analysis of historical data sets was used. The performance of distributions was evaluated by R-square test and Kolmogorov-Smirnov test (K-S).

As result, four stations (Jinka, Bulkimender, Sawla and Keyafer) data homogeneity and goodness test was accepted (R^2 = 0.97, 0.95, 0.96 and 0.98) respectively at (α = 0.05) (See Appendix 1, Table 3).

Erosivity can be predicted by a suitable regression equation in a case of insufficient rainfall records (FES, 2009).

Even though different regression equations have been developed in Ethiopia that estimate rainfall erosivity (R-value), R factor was determined using regression (Equation 15) calibrated by (Kaltenrieder, 2007) for Ethiopian highlands as also used in Tegegn and Biniam (2017).

$$\mathbf{R = (0.55*P) - 4.7} \quad \mathbf{(15)}$$

Where, R is rainfall erosivity factor, P is mean annual rainfall in (mm)

Estimation of future climate change projection data provided by CORDEX do not provide the type of detailed storm information needed to directly calculate predicted R-factor changes. In the same manner to that of baseline period (1987-2017), bias corrected mean annual rainfall was used projected rainfall erosivity under climate change for each scenarios ($rcp_{2.6}$, $rcp_{4.5}$ and $rcp_{8.5}$) per two future time slices (2021-2050), (2051-2080).

The mean annual rainfall for four gauge stations, and geographical coordinates were used to create a point shape file using Arc Catalog. The created shape file was displayed on Arc Map and the attribute fields for mean annual rainfall data was added to point shape file. Then the average rainfall data for each gauge stations was added to the attribute column. Finally, the point data shape file was interpolated using IDW method and raster rainfall data for study area was obtained. The raster rainfall data of the study area was converted to erosivity map of the study area by using raster calculator for (Equation 15).

3.2.2. Soil erodibility (K factor) estimation method

K values reflect the rate of soil loss per rainfall-runoff erosivity (R) index. There are properties of soil that control erosion are as stated by Fangmeier et al.(2006) the structure, texture, organic matter, clay mineralogy, density, and water content of the soil. Hence, in this study soil texture (particle size distribution) analysis was applied. In soil texture analysis context soil general erodibility nature indicated is to identify relative proportion of different grain sizes of particles (Brady and Well, 2002). Lal and Elliot (1994) also confirmed the importance of the method.

Once the soil types map of the study area is clipped in the ArcGIS environment, 35 field soil composite samples with depth of top (0-20 cm) were collected following representativeness of the nine soil type in the watershed (Table 1) and taking land use types in to account. For estimation of soil erodibility factor values, these soil samples were merged based on soil types of similar 35 samples were brought to particle size distribution analysis by soil sieve method in laboratory.

3.2.2.1. Particle size distribution analysis

Particle size distribution was done by soil sieve based on U.S. Department of Agriculture (USDA) soils taxonomy. Even though there are numerous systems of classifying separates into different size classes, USDA is among the most commonly used systems. Based on the size distribution, primary particles (textural fractions) or soil separates having diameter size limits less than 2.00 mm are usually divided into three classes, sand, silt, and clay. Diameter limits of soil separates are sand (2.00 -0.05 mm), silt (0.05 - 0.002 mm) and clay (<0.002mm). Prior to mechanical sieving, soil samples were dispersed to remove binding agents. During sieving the dispersed soil suspension pass through a nest of sieves of different sizes above. The amount retained on a particular sieve represents the fraction that is larger than the sieve size on which it is retained but

smaller than that of the preceding sieve in diameter size and weighted to represent the percentage of respective soil separates (Lal and Elliot, W., 1994; Shukla, M., 2005).

Afterwards, soil erodibility (K-factor) has been calculated by means of the following formulae which were developed from global data of measured K values, obtained from 225 soil classes (Renard et al. 1997).

$$K=\left\{0.0034+0.0405exp\left[\frac{-1}{2}\left[\frac{log(Dg)+1.659}{0.7101}\right]2\right]\right\} \quad \text{(16)}$$

$$Dg=\exp\left(\sum filn\frac{(dI+di-1)}{2}\right) \text{ with } R^2 = 0.983$$

Where,

Dg is the geometric mean particle size, for each particle size class (clay, silt, sand),

d_i is the maximum diameter (mm),

d_{i-1} is the minimum diameter and

f_i is the corresponding mass fraction.

This relation is very useful with soils for which data are limited and/or the textural composition is given in a particular classification system.

Using Equations (16), soil erodibility factor (K) was calculated for each soil samples. Finally using krigging interpolation method in ArcGIS (version 10.3.1) software which is widely used in several researches (Smith et al., 1993; Wang et al., 2001; Rodriguez et al., 2007; Vaezi et al., 2010 Bonilla et al ., 2012) in this field, soil erodibility factor map was constructed for inter study area.

Thus to obtain soil erodibility raster map of the study area shown in Chapter 4, spatial point K-factor values were interpolated to the watershed area extent by krigging method under spatial analyst tool. Erodibility values were classified according to the erodibility ratings (from low to high) in (Rosewell and Loch, 2002).

3.2.3. Topographic (L and S factors) estimation method

For this study LS factor was derived from DEM of ASTER 2014 with a spatial resolution of 90m was collected from Ethiopian Geological Survey office. DEM preprocessing was done for cones using spatial analyst >Hydrology >FILL tool based on the conceptual boundary of the study watershed prior to obtaining appropriate size. Then the appropriate size of the study area was

delineated by ArcSWAT (Soil and Water Assessment) tool ArcGIS extension (Arnold et al., 1998). By using this watershed area polygon, DEM of study area was clipped with the help of spatial analyst raster tool.

The values of flow accumulation and slope gradient were derived from DEM. Flow accumulation was derived from the DEM after conducting Flow Direction processes. Moreover slope in degree also directly derived from the DEM using ArcGIS 10.3.1 software.

This study therefore employed the following advanced LS factor computation method based on up slope contributing area suggested by (Desmet & Govers, 1996a; 1996b, Moore & Burch, 1986a, 1986b; Moore & Wilson, 1992; Mitasova & Mitas, 1999; Simms et al., 2003)

$$LS = \left({}^{AS}/_{22.13} \right)^{0.6} \left(sin \frac{\beta}{0.0896} \right)^{1.3} \quad \ldots\ldots (17)$$

Where, LS is slope steepness–length factor, As is the specific catchment area, i.e. the upslope contributing area per unit width of contour drains to a specific point (flow accumulation*cell size), and β is the slope angel. LS-factor was computed in Arc GIS raster calculator using the map algebra expression in (Equation 18) suggested by Mitasova and Mitas (1999) and Simms et al., 2003).

LS = pow ([flowaccumulation]*cellsize/22.13,0.6)*pow(sin([slope]*0.01745)/0.0896,1.3)………..(18)

3.2.4. Cover-management (C-factor) estimation method

The C- factor represents the relation between the soil loss in certain agricultural or cover conditions and the erosion that would be obtained from a standard fallow parcel (bare soil). Strict application of this factor as RUSLE guidelines is difficult on data shortage and large scale condition. To estimate C factor by traditional method, simply assigning values to land cover classes has also its own limitations since all pixels in a particular land use land cover class have the same C factor value, those pixels cannot represent spatial variation of this class over the study area (Wang et al., 2001). So that, for C-factor estimation two maps (LULC and NDVI) are generated. NDVI is a simple graphical indicator that can be used to analyze remote sensing measurements and assess whether the target being observed contains live green vegetation or non-vegetation area. Its value ranges from -1 for bare soil to 1 for forest. Both map layers were generated step by step as shown in work flow chart in (Figure 4).

To obtain land use types map of the study area, satellite image from Landsat 8 Operational Land Imager (OLI) TIRS (Thermal Infrared Sensor) with acquisition date of January 17th 2017, accessed

free of charge from US Geological Survey (USGS) and center for Earth Resources Observation and Science through **http://earthexplorerusgs.gov/.** was used.

Image preprocessing tasks including band ratio, NDVI (from band 4 and 5), PCA, tasseled cap, re-projection was performed to correct the surface features reflectance characteristics. Supervised classification procedure was used by Erdas emagine. 2010 software with maximum likelihood algorithm. Field surveys with the help of GPS (Garmin-78) provided the ground information about the types of land-use and land-cover classes was complemented to classification method.

To create training samples were used. They were created using standard procedure through ArcMap 10.3.1 Image Classification tool by drawing them over the areas of each of distinguished land cover. A total of 147 reference points were used for land cover classification. Later, the training samples were used to generate signature files for supervised classifications. Then each cell of composites was assigned to the classes represented in the signature files proportionally to the number of cells apprehended by each signature.

Accuracy assessment was carried out to verify to what extent the produced classification is compatible with what actually exists on the ground based on (overall accuracy and kappa). In this study, Confusion Matrices were used to assess classification accuracy of remotely sensed data. Outputs of the classification method were compared against ground truth data. To accomplish this, Arc Map 10.3.1, spatial analyst extraction tools and Microsoft Excel were used (Verbyla, 2013). It involves the production of references (samples) that evaluate the produced classification. In this study, reference test samples were selected from GPS data that were collected from the ground for the satellite image.

Based on the land cover classification map, a corresponding C factor values from land cover classes according to (Hurni, 1985; BOECM, 1998; Kaltenreider, 2007; Bakker et al., 2008; CGIP, 1999) were assigned in ArcGIS 10.3.1 with the help of join and relate. These values are preferred since they are suitable and suggested for Ethiopian Highland conditions that is dominated by cultivated land and represents a good estimation of cover factor values. Then the C value was converted to raster by Analyst conversion tool method from polygon to raster.

NDVI map generation in bands correspond to the red band (Red) and the near-infrared (NIR) for Landsat 8 Operational Land Imager (OLI) are band 4 and band 5 respectively. By means of Map

algebra, raster calculator on Arc GIS 10.3.1 software, NDVI was calculated by applying the equation (12) by (Rouse *et al*., 1974; Jensen, 2000).

Therefore, regression model ((Knijff et al., 1999; Asis & Omasa, 2007; Durigon et al., 2014) was employed to make correlation analysis between C factor values of land cover classes and NDVI values. This done by assuming that in soil erosion modelling NDVI and C-factor are inversely correlated each other. Then, regression equation given in 'Figure 7' was obtained. Hence, this equation was applied for generation of final C factor map with the help of Spatial Analyst tool of ArcGIS 10.3.1.

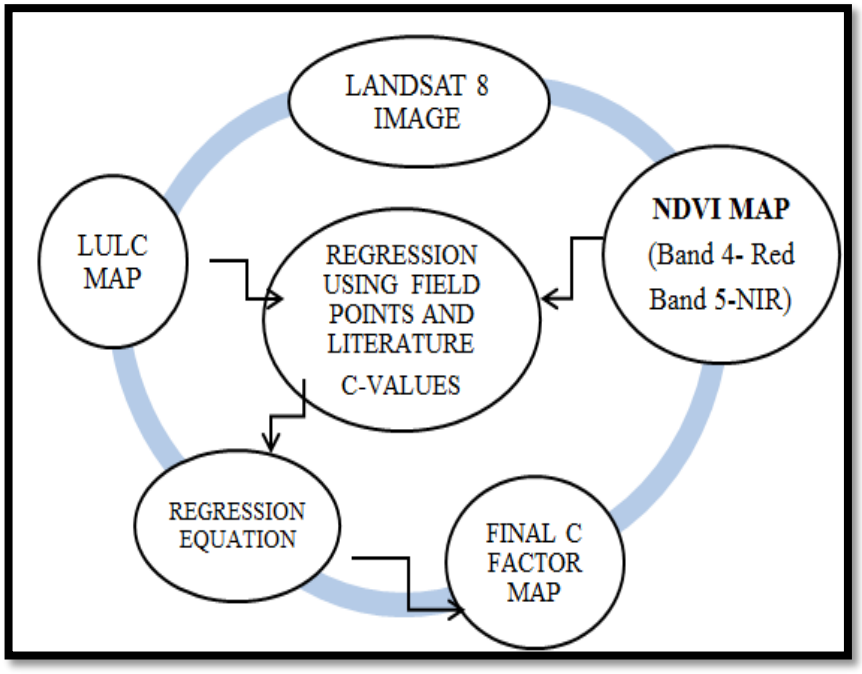

Figure 4:-Workflow of C factor estimation using NDVI and Table values

3.2.5. Support practice (P_ factor) estimation method

Support practice (P-factor) reflects the impact of specific erosion management practices on the corresponding erosion rate with values between 0 and 1. No soil or water conservation measures are applied to the study area, except the start of mass mobilization works through agricultural extension program of the government for terracing though there is no maintenance. Considering the nonexistence of conservation practices in the watershed, P values were analyzed based on the land-use map for different slope gradient classes (Wischmeier and Smith, 1978).

Slope gradient class map (%) derived from ASTER DEM by ArcGIS 10.3.1 spatial analyst hydrology and surface tools. Slope map of the study area was then reclassified by and the P-factor values listed under 'Table 2' were assigned to each land use – slope class combination grid cells. Finally, the assigned P-factor values were lookup in Spatial Analyst Tool extension, first reclassified in to six classes. Then land use land cover map was combined with slope

Table 2:-Conservation support practice (P- Factor Value) (Wischmeier and Smith, 1978)

Land use type	Slope (%)	P-factor value
	0-5	0.1
Agricultural land	5-10	0.12
(cultivated land)	10-20	0.14
	20-30	0 0.19
	30-50	0.31
	50-62.199	0.43
Other land	All	1

In Arc GIS10.3.1, the original land use land cover map obtained by supervised classification of LULC from in a vector format was first reclassified in to two categories (i.e. Agricultural land and other land) then it was converted in to raster format. In Spatial Analyst Tool extension Local the new raster land use was combined with slope class map (%) derived from DEM to get a combined land use – slope map of the study area and the P-factor values listed under 'Table 1' were assigned to each land use-slope class combination grids. Finally with the help of conversion tool, P-factor raster map was obtained by choosing assigned P-value for value field.

3.3. Soil loss estimation method

Revised Universal Soil Loss Equation (Renard et al. 1997), an empirically based model was applied for this thesis work. Its applicability has been confirmed including Ethiopian condition Kaltenrieder (2007); Woldeamlak and Ermias (2009) because of its simplicity and limited data

requirement. The advent of geographical information system (GIS) technology has allowed the equation to be used in a spatially distributed manner because each cell in a raster image comes to represent a field-level unit.

Individual GIS files were built for each RUSLE factor and they were projected with UTM Zone 37N using the WGS 1984 datum; these correspond to standards used by the Ethiopian Mapping Agency. These factor raster combined on a cell by cell-grid modeling procedure in ArcGIS 10.3.1. to predict soil loss in a spatial domain. These factor raster maps that were resampled with 30m by 30m cell size and while the final model output was set to 100m by 100m to obtain the annual soil loss yield per hectare per year.

The resultant annual soil loss rate was determined by a cell-by-cell analysis of the soil loss surface by multiplying the respective RUSLE factor values interactively in ArcGIS 10.3.1 spatial analyst, raster calculator based on equation (5).

3.4. Parameter determination for estimation of future soil loss

One of the main objective of this study is the assessment of soil loss response to the impact of climate change and anticipated management practices. Among RUSLE model parameters, soil erodibility factor (K-factor) and topographic factors (LS-factors) were assumed to be constant in immediate future (2021-2050) and mid future (2051-2080) for all management scenarios. Three scenarios (No-action, Medium-action and comprehensive) management scenarios were simulated based on the nature and assumptions of factors, cover and erosion management practices. These scenarios outputs were obtained as stated in detail following sub sections.

3.4.1. Estimation of rainfall erosivity (R-factor) for future climate change condition

For estimation of future R-factor, predicted rainfall data series were obtained from regional climate multi model outputs of CORDEX-Africa for three RCP scenarios (RCP2.6, RCP4.5 and RCP8.5). RCP8.5 scenario gives predictions that correspond to the business-as-usual development pathways. The $RCP_{2.6}$ outputs indicate possible future temperature and rainfall patterns with climate change policy. The $RCP_{4.5}$ represents the middle situation.

These data was dynamically downscaled with spatial resolution of (0.44°*0.44°) and temporally 1951-2005 for historical and 2006-2100 for future by Coordinated Regional Climate Downscaling Experiment (CORDEX) project from CMIP5 model (Coupled Model Inter-comparison Project fifth phase) (Nikulin *et al.*, 2012; Hernández D. *et al.*, 2013). To extract future projected

precipitation data, geographical coordinates of four meteorological stations of the study area (Jinka, Bulkimender, Sawla and Keyafer) were associated with CORDEX – AFRICA domain grid cells to the periods 2030s (2021-2050) and 2060s (2051–2080).

Due to the fact that simulations of climate variables (temperature and precipitation) often show significant biases because of systematic model errors or discretization and spatial averaging within grid cells, which hampers the use of simulated climate data as direct input data for hydrological models. Observed data sets after they are checked for missing, homogeneity and outlier were used in the bias correction procedures.

The variables precipitation and temperature were subjected to a delta change approach bias correction procedure (Mpelasoka and Chiew, 2009) as follows:

$$P^{scen}_{dm} = P^{obs}_{dm} \left(P_{\mu}^{GCMscen} / P_{\mu}^{GCMcon}\right) \quad \text{Equation (19)}$$

$$T^{scen}_{dm} = T^{obs}_{dm} + \left(T_{\mu}^{GCMscen} - T_{\mu}^{GCMcon}\right) \quad \text{Equation (20)}$$

Where, P^{obs}_{dm} and T^{obs}_{dm} are observed daily precipitation and temperature, P_{μ}^{GCMcon} and T_{μ}^{GCMcon} are mean monthly GCM precipitation and temperature of control period $P_{\mu}^{GCMscen}$ and $T_{\mu}^{GCMscen}$ are mean monthly GCM precipitation and temperature of scenario period.

It has been highlighted that the change signals between GCM baseline and scenario period were derived from mean monthly values but also were applied to the daily time series in order to avoid considerable variability in the day-to-day change signals which would have occurred when using daily change factors.

Application of mean monthly delta factors with the same daily rainfall distribution as historical (baseline) conditions was executed. To correct the mean and temporal variability of GCM output in accordance with the observations (Hawkins et al., 2013; Ho et al., 2012):

To systematically investigate the change in climatic elements, the erosive events (rainy days count) were compared with that of baseline period. Different daily quantitative values of erosive events were proposed. According to Xie Y. et al. (2016), an erosive rainfall event was initially defined as one with rainfall amount $\geq$12 mm/day. However, a best fit threshold of daily rainfall between days to classify as erosive and non-erosive which is 9.7 mm, suggested by Xie Y. et al. (2016) was applied in this study.

Finally, for the determination of R factor from mean annual rain fall of two future time slice in each of the three RCP scenarios, the same procedure in the case of baseline period as elaborated (section 3.2.1.) was followed.

3.4.2. Estimation of future management factors (C and P) by Simulation of scenarios

Scenario simulation is needed to investigate the adaptation strategy for soil erosion risk due to the future climate change situation. Because of the inherent complexity of the environmental and socioeconomic processes that drive land-use and land-cover change, it is not possible to predict future land-cover change in the long-term with a great degree of certainty (Liu et al., 2007).

Scenarios do not predict the future, but rather present collections of alternative for plausible futures, which can provide insight on the range of possible outcomes (Schwartz, 1991). So scenario simulation for future management could be important for such like modelling (Thorn et al., 2017).

Scenarios simulation consists of key source of information regarding alternate futures in combination of literature review, key informant interviews, and collaboration with subject matter experts. These traditional methods, alongside literature review, are well suited for collaboration with experts and can be used in combination with diverse modeling methods (Mallampalli et al., 2016).

The following three scenarios of anticipated management practices only for this particular aim were simulated to be integrated with high, medium and low radiative forcing climate change RCP scenarios in the watershed scale as in (Samal et al., 2017). The aim of these scenario simulation is to investigate the state of management which reduces the risk of soil loss which could be exacerbated due to climate change or in other words to provide multiple facets of erosion management to abate.

Scenario 1 - No management action

This scenario implies that, there is no implementation of anticipated erosion control and cover (crop – management) practices in the future time 2021 through 2080. The future condition is assumed similar such that the model parameters except rainfall erosivity are constant. Inclusion of this scenario, is with the aim of assessing the impact of climate change on soil loss rate, in such a way that the factors erosion model in this study except rainfall erosivity were considered the same as in baseline condition. So that, the soil erosion is looked in silence for changing fortune erosivity energy.

Scenario 2- Progressive erosion control (Medium-action situation)

The scenario condition under which there is an assumption of the community tries to increase to increase productivity by crop selection and physical terraces construction on steeply slope areas (>8%) only due to fear of erosion catastrophes without the recognition of tillage systems and selection of crops for food security in turn this tackle the erosion movement with the aim to copping up the risk. This is the case in which physical terraces constructed on steeply slope areas (>8%) only due to fear of erosion catastrophes without the recognition of tillage systems and but selection of crops for food security (Appendix 3). No more deforestation of currently available forests.

The major characteristics of this scenario are terrace construction and selecting crop for production are taken as the only an archaic actions. No strong regulations of state to SWC practice including structure maintenance.

Scenario 3 – Erosion control scenario or (Control)

Under this scenario, there is added effort of implementing erosion control and cover (crop management) practices in the two future time slices, (2021-2050) and (2051-2080.

Strong regulations or efforts formulated Community Based Participatory Watershed Development Guideline. Physical SWC measures on steep slopes based on their design specification (Lakew et al., 2005), these measures will benefit from vegetative stabilization with grass and legumes, application of compost (particularly close to the bund area where the soil is deeper and the moisture is high), contour plowing, a correct crop rotation, relay cropping, intercropping and other soil management and agronomic measures as per the agro-climatic conditions and farming system of the area.

Crop-management practices were assumed to occur at a constant rate on agricultural fields plus management practices suitable for nonagricultural lands are supposed to be applied in constant rate based on scenario period 2021 through 2080, in such a way that the soil loss rate is reduced to tolerable value.

For cropland, the support practices considered included contouring, strip-cropping, terracing, and subsurface drainage (Renald et al., 1997).

3.4.2.1. Determining cover/crop-management factor (C-factor) input data

An investigation of an anticipated future crop-management and support practices that are responsible for shaping the erosion situation on watershed field condition. The crops and cropping

systems that are recognized to be relevant in the future development opportunities were chosen. For this purpose, an important information from key personal communication from agricultural sectors (SOZDARN. 2017) was collected such that the cropping system under which soil loss is considered to be minor. So that, the possible future cropping types selected. It is also important to under previous information gaps on land suitability. Likewise, effective management practices on other frequently disturbed land use classes (open forests, scrub, grazing, barren and settlement/& urban areas) (Appendix 3) were taken in to account for "if/then" analysis.

The erosion-science literatures were also reviewed to determine suitable C and P values for management practices supposed for to be implemented watershed based on assumptions of scenarios.

Determination of C factor is by following the selection of crop type and cropping system for agricultural lands and management practices for non-agricultural land cover classes. Accordingly, C factor values were obtained from (Kaltenreider, 2007) for with and without contouring based on requirements of management scenarios. For non-agricultural fields, the C-factor values in (Table 4 of Appendix:-3) were taken from (Kaltenreider, 2007; Wischmeier and Smith, 1978; Cooley and Williams (1985; cited in El-Swaify et al., 1985: 509)) based on the suitability of assumptions set and field condition.

Then, final output C-factor values maps were generated with the help of ArcGIS10.3.1 'Conversion tool' under 'Analyst', and adjustments were made based on the regression equation gained as in the case of base of baseline period.

Determination of support practice factor (P-factor), the support practices considered included contouring, strip-cropping, terracing, and subsurface drainage (Renald et al., 1997). Information on the important support practices for the Neri watershed (terraces and contouring) have being announced by government were selected during fieldwork and supplemented by other sources of literature (see Table 5 in Appendix 3). For these selected support practices values considered were contouring and conservation terraces constructed based on cropping systems for the slope gradient classes based on (Deoer, 2005). Whereas, for non-agricultural fields the value of 1 is used (Morgan, 2005). The values were assigned to each land use-slope class combination grids because, these management activities vary on the slopes of the agricultural land.

Finally, with the help of 'Conversion tool under Analyst' in ArcGIS10.3.1, P-factor raster maps were obtained by choosing the assigned as P-value for value field. This procedure was similarly applied for each of the management scenarios conditions.

3.5. Soil loss estimation under future climate change and Management

An important component of the research was to predict soil loss rate under climate change and to investigate its response in a condition at which the management practices come to pass. The two future periods resultant soil loss maps were generated by integrating the parameter outputs for the three RCP scenarios rainfall erosivity (R-factors) and three management practices including (no-action) for (C & P factors) with the remaining non changed, RUSLE soil erodibility (K) and topographic (LS) factors.

Individual GIS files were built for each RUSLE factor and they were projected with UTM Zone 37N using the WGS 1984 datum; these correspond to standards used by the Ethiopian Mapping Agency. These factor raster combined on a cell by cell-grid modeling procedure in ArcGIS 10.3.1 to predict soil loss in a spatial domain. These factor raster maps that were resampled with 30m by 30m cell size and while the final model output was set to 100m by 100m to obtain the annual soil loss yield per hectare per year.

Finally, the same procedure with the one stated in (section. 3.3) with advent of geographical information system (GIS) technology was applied to obtain soil loss change due to climate change and added management practices in each future time slices. Investigation of the difference in a condition to what if the erosion management practices come to pass.

Then, the predicted mean annual soil loss value change in percent and amount based on baseline future from the watershed. Besides Scenario, resulted in percentage reduction of soil loss rates under RCP scenarios were compared within themselves with and with-out management practices. To enable choose the state of management in future, percentage change in soil loss relative to baseline period were compared.

3.6. Identification of Priority areas for intervention

Based on an objective of identifying priority areas of conservation planning, the study watershed was divided into eleven sub-watersheds by using Arc SWAT 2012.10_3.1. Therefore, grids

receiving flow contribution from areas a grid based procedure for discretization of the sub-watersheds wais adopted in the present study (Wicks & Bathurst, 1996). Hence, delineation of sub watersheds as erosion prone areas was done to identify the severity level of soil loss.

Prioritization was given according to WBISPP (2001) soil los severity classes for a targeted and cost-effective conservation planning (Kaltenrieder, 2007). The delineated eleven (11) sub-watersheds with respect to drainage area and for the ease of pointing out administrative areas contributing higher sol loss risk, the nineteen(19) kebeles shape files were used to extract soil loss rate under baseline period condition.. Then, the weighted average soil loss to area was executed. Finally, the based on principle of watershed management, sub-watersheds having mean annual soil loss more than soil loss tolerance (SLT) were ranked one to eleven.

4. RESULT AND DISCUSSION

4.1. Individual RUSLE Factors Outputs under baseline condition

The estimated quantitative out puts of RUSLE individual factors are depicted below in 'Figures 4, 5, 6, 7, 8 and 9'. RUSLE factor six parameter out puts are discussed as follows.

4.1.1. R-factor output for baseline condition

The erosivity factor estimated ranges from 707.3 MJ mm ha^{-1} h^{-1} yr^{-1} (Keyafer station) to 884.43MJ mm ha^{-1} h^{-1} yr^{-1} (Bulkimender station). The R-value of Jinka station which is within the study watershed is 733.42MJ mm ha^{-1} h^{-1} yr^{-1}. Thus, this value has great weight to the R-value of the watershed see 'Table 2' below.

As discussed in Section 3, the R-factor data calculated for four stations were interpolated by Inverse distance weighted (IDW) method so as to estimate the R-value of each grid cells. Therefore, the result of this interpolation gave R-factor values of the study area with the range between 713.084 and 754.427MJ mm h^{-1} ha^{-1} yr^{-1}. This result gives an idea that there is no significant spatial variation of erosivity value in the watershed with standard deviation of 7.27. But, cell by cell look show the upper catchment of the study area received relatively higher rainfall erosivity values than its lower catchment indeed.

Table 3. Meteorological stations and their mean annual rainfall with calculated rainfall

Source: National Meteorological Agency (Computed).

No.	Meteorological Stations	Year	P(mm)	R –Factor (MJ mm h^{-1} ha^{-1} yr^{-1})
1.	**Jinka**	(1988-2017)	1342.03	733.42
2.	**Bulki mender**	(1988-2017)	1616.59	884.43
3.	**Sawla**	(1988-2017)	1332.3	728.1
4.	**Keyafer**	(1988-2017)	1294.52	707.3

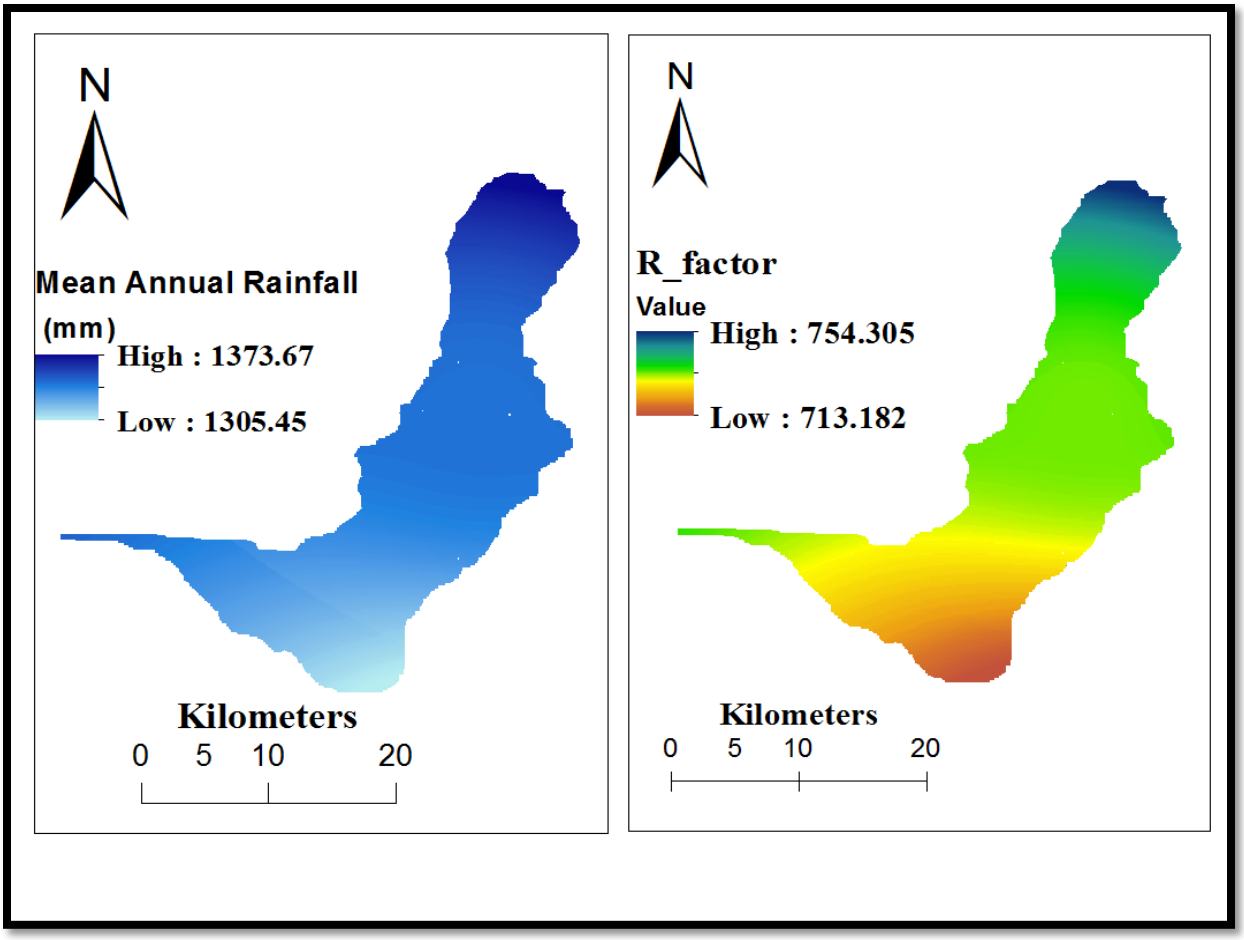

Figure 5:- Mean Annual rainfall (mm) left and Rainfall erosivity factor map right

4.1.2. K-factor output

Soil particle size distribution

Based on soil particle size distribution analysis, primary particles (sand, silt and clay) distribution defined. In the 'Figure 6', soil erodibility factor (K) as the function of geometric mean diameter size (Dg (mm)) is stated. Solid line shows the soil erodibility factor value calculated for 35 field samples whereas, vertical lines represent K-values in each Dg class plus or minus one stand deviation. Soil erodibility is low for extremely lowest and highest values of mean soil particles diameter size. Soils with high sand and high-clay content are having the lower K-values and high-silt content soils having the higher K-values. This reflects that, soil samples that are bearing higher percentage of medium sized soil separate (textural classes) are susceptible for detachment and transport by water. This is due to the weaker strength of bonds between soil particles (aggregate

stability) ease to transport (Murphy and Flewin, 1993). Whereas, clay are more cohesive and sand require high transportation energy.

Soil primary particles (silt, sand and clay) distribution maps constructed using kriging interpolation method in Arc Map10.3.1 are shown in Appendix 2, Figure 1). These maps show that the soil textural classes of Neri watershed based on top samples excluding soil separates diameter size greater than 2 millimeter ranges from clayey to sandy clay loam. The weight based percentage of sand, silt and clay respectively are (21.6-43) %, (21.25-33.3) % and (21-62) %. The spatial distribution of these textural classes as shown in map reveals that the middle catchment is characterized by lesser sand coverage but upper and lower catchments are having higher sand content as shown in three map figures under appendix-2. It indicates that silt coverage shows smooth incremental from upper to lower parts of this watershed. Unlike sand, clay content in north and south of study area is more than central parts. This could be soils south of Jinka are structurally weekly developed reflecting their young age, consistencies are friable. These soils are well drained, non-calcareous and weekly structured (MoWR, 1996).

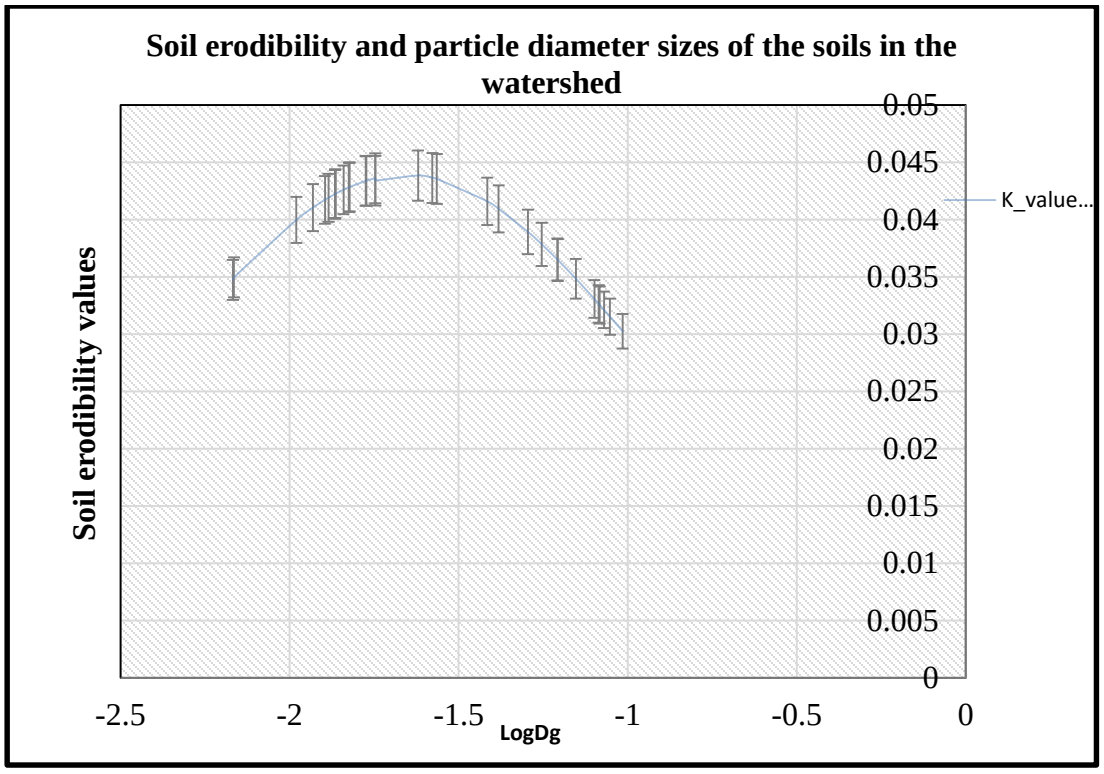

Figure 6. Relationship between soil erodibility values and their geometric mean diameter size

Soil erodibility factor map in the 'Figure 7' is the result of kriging interpolation of calculated spatial K-values based on equation (11) and (12). K-factor values in the study watershed differed from (0.0306– 0.044) Mg h MJ^{-1} mm^{-1}. Annual average soil erodibility factor was estimated to be 0.0385 Mg h MJ^{-1} mm^{-1}, with standard deviation of interpolated K factor map was 0.002 Mg h MJ^{-1} mm^{-1}.

According to (Rosewell and Loch, 2002), soil erodibility values of this study area are categorized under moderate to high ranges. Based on this, about 72% (33513.1ha) of the study area is categorized under moderate erodibility class (<0.04 Mg h MJ^{-1} mm^{-1}) whereas, 28% (13032.9 ha) area is high range (>0.04 Mg h MJ^{-1} mm^{-1}).

The higher the K values, the greater susceptibility of the soil to rill and sheet erosion by rainfall. High soil erodibility factor values greater than 0.04 Mg h MJ^{-1} mm^{-1} from the background soil types of Orthic solonchaks, Calcic Xerosols and highland Dystric Nitisols. These area are the middle catchment of the watershed where lower clay content area with moderate silt content as (Appendix 2 Figure 1) of textural classes and 'Figure 7' below of soil erodibility map. The remaining 43% (15 soil samples) are within the range of (0.023-0.02955) Mg h MJ^{-1} mm^{-1}. Eutric Cambisols, Dystric fluvisols, Haplic Xerosols, Eutric Fluvisols, Leptosols and Orthic Acrisols soils types under this study have moderate K values. This result could be due to, usually soil containing large amounts of coarse silt and fine sand are the most erodible (Manrique, 1988). Soils with high-sand and high-day content are soils having the lower erodibility values, whereas high-silt content are soils having the higher values. (Foster et al., 1981).

Soils with high silt fraction have poor structure and are more erodible (Stern et al., 1991). The nature of the clays in the Cambisols of the watershed are known to be smectic and smectic soils are generally known to be more erodible than soils which contain less smectite and high sesquioxide (Tamirie, 1975; , Piccolo et al., 1996).

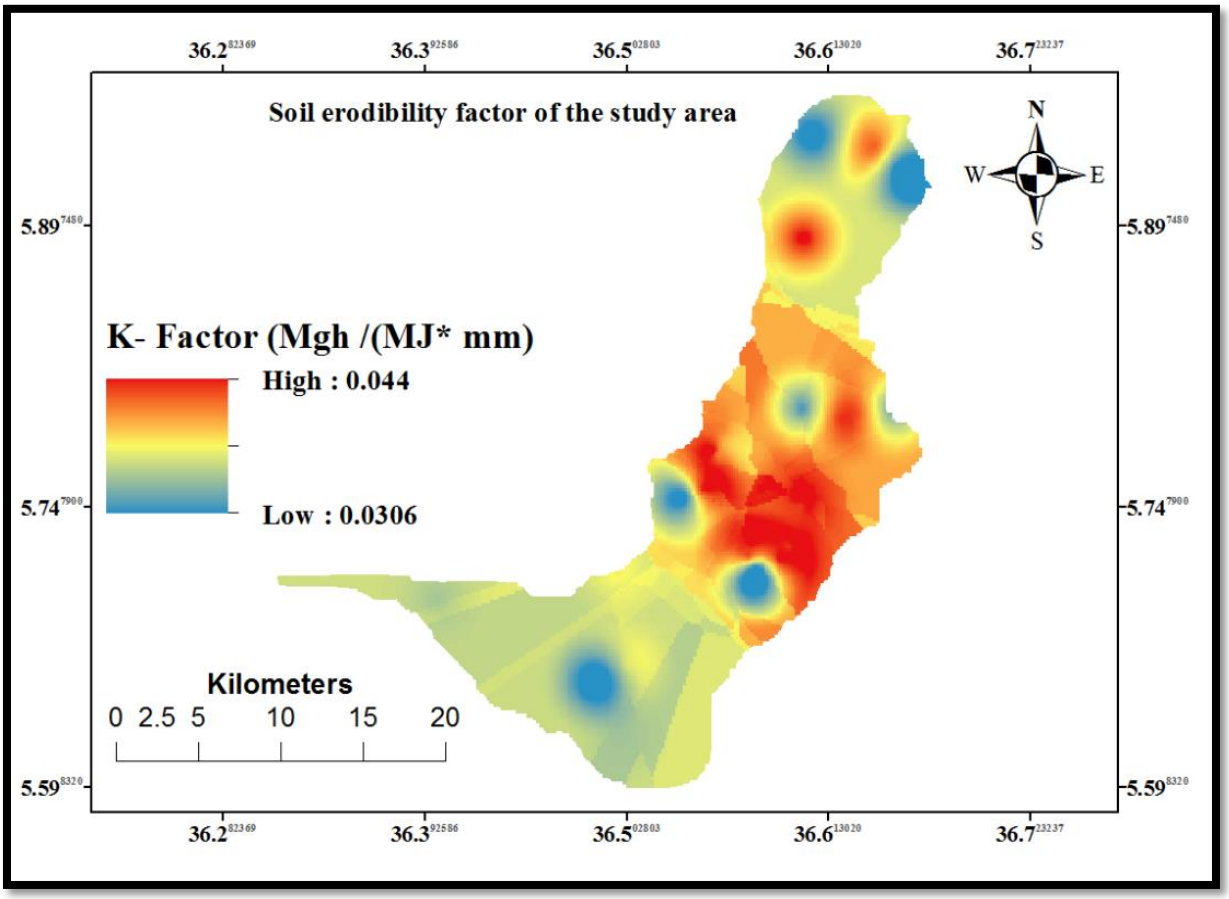

Figure 7:- Soil Erodibility /K_Factor/ Map of the study area

4.1.3. LS-factor output

The combined LS factor indicates the effect of slope length and slope steepness on soil loss. This indicates that higher the value, greater its potentiality to erode.

The values of the LS factor for Neri watershed ranges from 0 in some flat area to 37.3972 in steeper and longer slope areas of the study area and the mean value of 1.523. It is perceptible that drainage area may favor erosion highly. With respect to the slope gradient (degree), study area ranges from (0-32). This indicates that, the area feature description ranges from straight to moderately convex (Young, 1972).

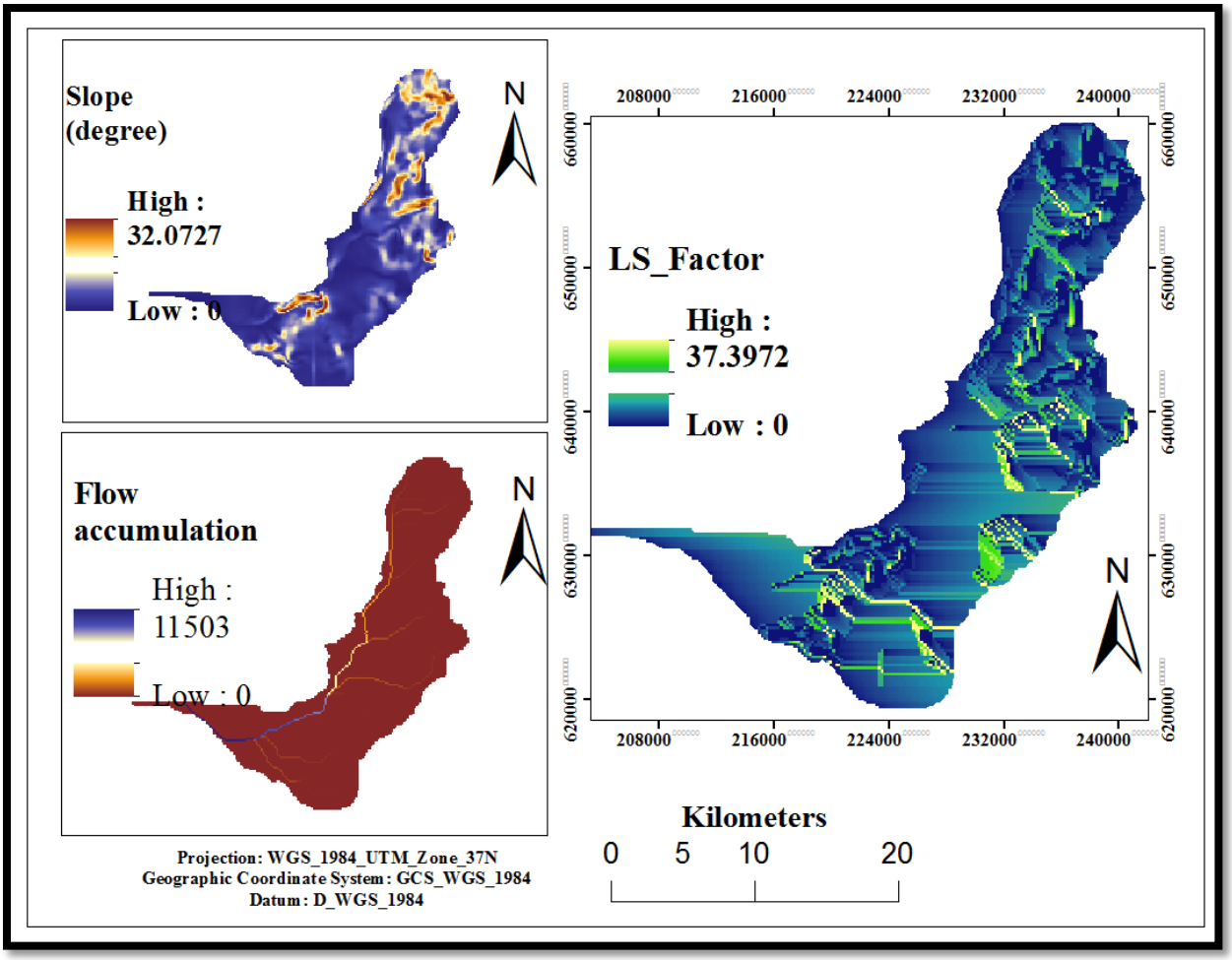

Figure 8:- Derivation of LS-factor from Digital Elevation Model

4.1.4. C-factor output under baseline period

Based on supervised digital image classification technique employed, using ERDAS EMAGINE 10 software which was complemented with field surveys that provided on-the-ground information about the types of land-use and land-cover classes. Six land-use and land cover classes were recognized with the overall classification accuracy. As (Table 3 in appendix-3) highest classification accuracy of forest (100%) and built ups (95%) followed by shrub (93%), agricultural (90%), grass (88%) and barren land (80%). The least accurate is barren land (80%). The overall accuracy 0f 91% and (Kappa = 0.904). The result implies high classification accuracy

On the other hand, the NDVI values map (Figure 11) of this watershed was found to vary between from 0.000745 to 0.499 with mean value of 0.195. After ground verification, it was observed that

the areas having higher value of NDVI have covered green vegetation and area with lower value of NDVI are nearly barren/open land.

C factor values were assigned to pixels of NDVI image through regression equation. Based on an assumption that NDVI and C factor values are inversely correlated each other, the C factor map of Neri river watershed was produced to use in this soil erosion model.

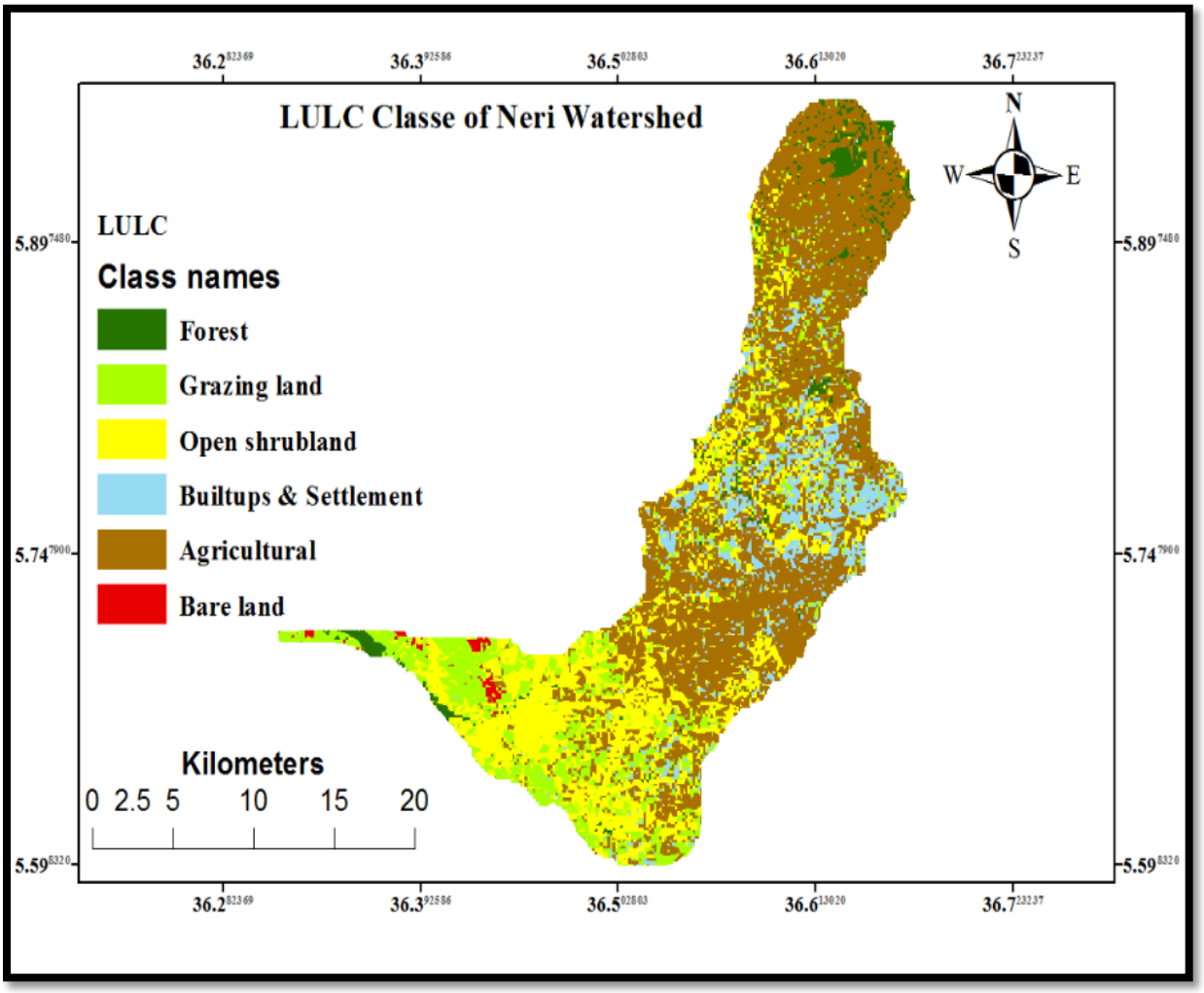

Figure 9 : Map of LULC Classes of Neri Watershed

Table 4:- Land use Land cover classes and their area coverage of the study area

No.	LULC classes	Area coverage (ha)	Percentage (%)
	Agricultural	22514.13	48.4%
	Grazing Lands	6182.31	13.3%
	Forest	1844.11	4.0%
	Shrub and Bush	11561.13	24.8%
	Settlement and built ups	4211.41	9.0%
	Bare lands	232.98	0.5%
		46546	**100%**

Regression model 'Figure 10' presents the variability the C-factor is explained by the explanatory variable (NDVI). The information of C-factor brought by the NDVI and C-factor values form literature is significantly good; given the ($R^2 = 0.974$). The study area possesses high conditions for favoring erosion and low situation for erosion control.

As result of linear regression equation, C-factor output was found to its maximum value of 0.6141, minimum 0.01056 and average 0.385. (std. (±0.072). The vegetative cover condition to reduce erosion in this watershed is less except in the upper and some areas sparsely distributed areas of the watershed (totally 4% of total area). The spatial distribution of cover management factor in the study area is shown in (Figure 11). On this map, lower value of C factor indicates the area possesses good land cover and higher value indicates barren/open land and built up areas.

These results are reliable. According to (Toy et al., 1999) the values range from virtually zero for well-protected soil while slightly greater than 1 for bare soil.

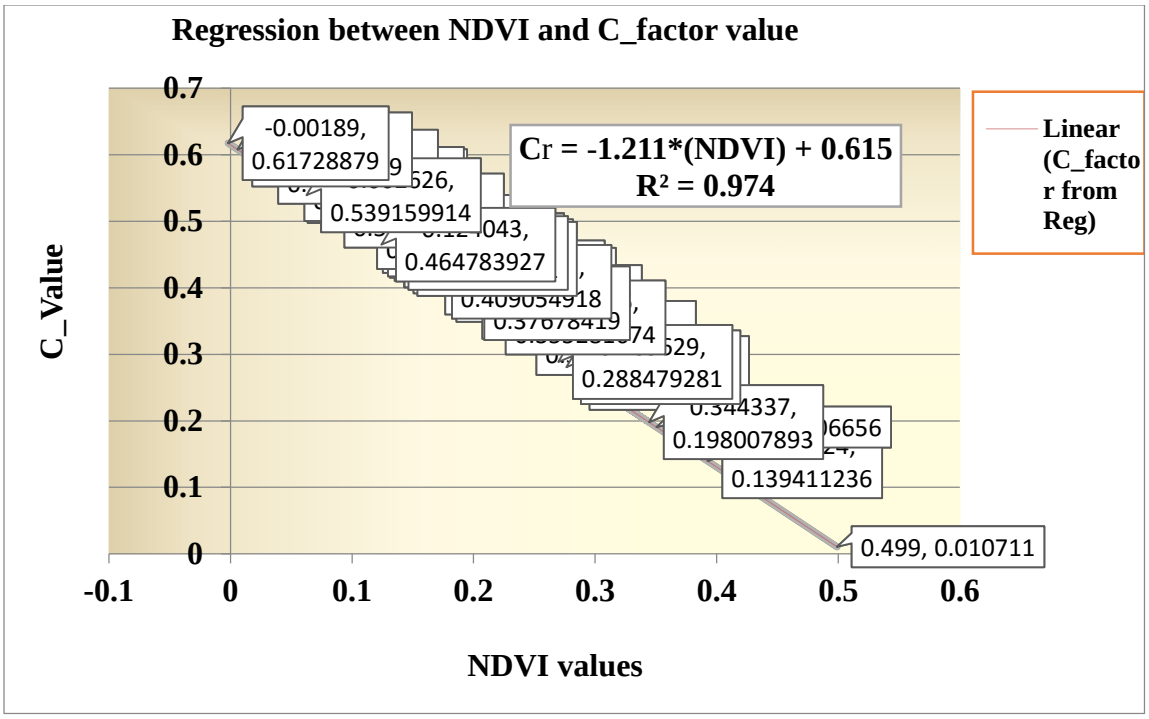

Figure 10: Regression analysis of literature C-factor values NDVI value

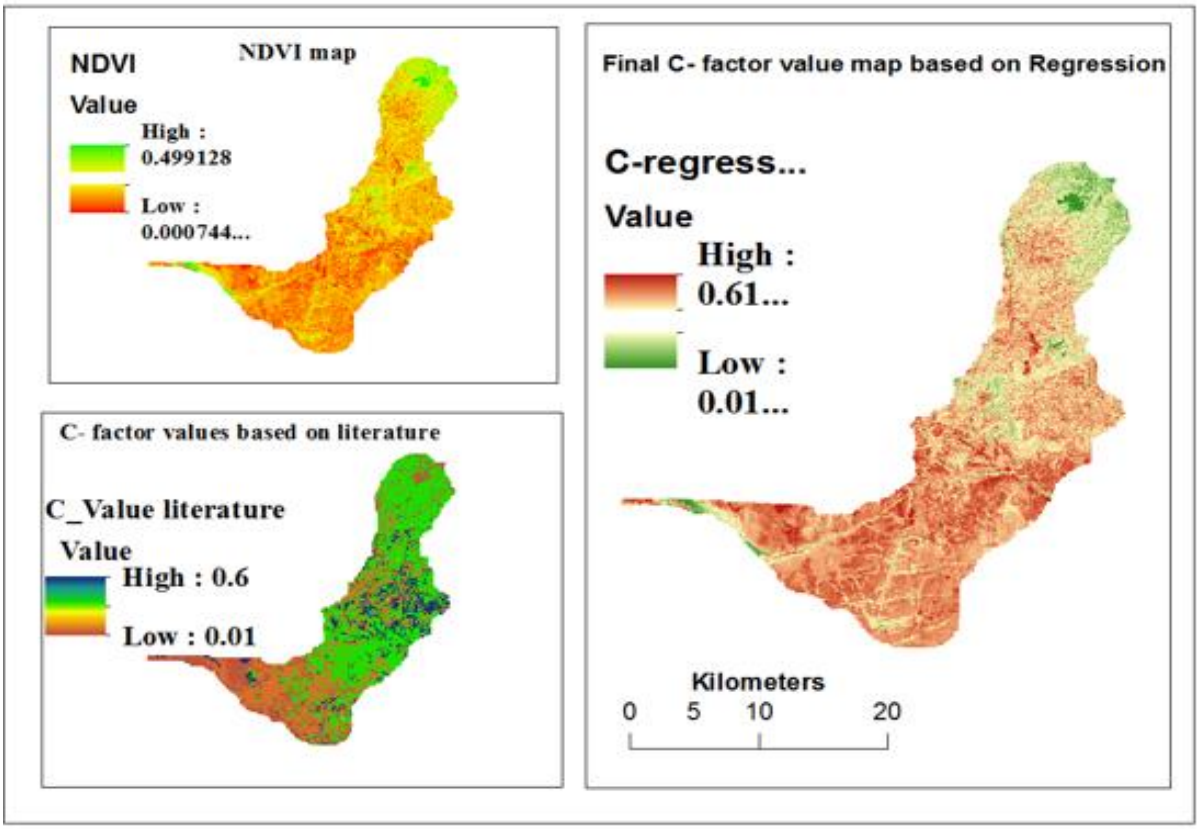

Figure 11: Final RUSLE C-factor map

4.1.5. P-factor output

The P factor values of study area ranges between 0.11 and 1 with mean of 0.591 as shown Figure 12'. No soil or water conservation measures were applied in the study area. So, P values were assigned by the land into grid codes of crop cultivated, open forests, grazing lands, abandoned bare lands, built ups and settlements and shrub land-use classes with intersection to slope gradient classes (percent).

The management activities vary on the slopes of the cultivated lands. Therefore, the crop cultivated land is also sub-divided in to six classes based on the slope percentage, to assign different P value for each slope classes (0–5, 5–10, 10-20, 20–30, 30-50 and > 50 %).

With respect to the P factor in, Land cover types other than agricultural lands about (51.6%) of the area has a value of 1. The lack of cultures in this area has a large influence on the erosion rates. Conservation practices affect erosion mostly by modifying the flow pattern, grade or direction of surface runoff, and by reducing the runoff amount and rate (Renard and Foster, 1983).

Table 5:-P-factor with LULC and slope (Based on Wischmeier and Smith (1978)

LULC classes with their Slope classes (%)	Area coverage (hectare)	Percentage	P-factor (value)
Crop cultivation land with slope (0-5)%	6483.59	13.9%	0.11
Crop cultivation land with slope (5-10)%	5846.61	12.6%	0.12
Crop cultivation land with slope (10-20)%	7159.34	15.4%	0.14
Crop cultivation land with slope (20-30)%	2018.08	4.3%	0.22
Crop cultivation land with slope (30-50)%	970.71	2.1%	0.31
Crop cultivation land with slope (50-62.2)%	35.79	0.1%	0.43
Other land use types with slope (0-62.2)%	24031.87	51.6%	1

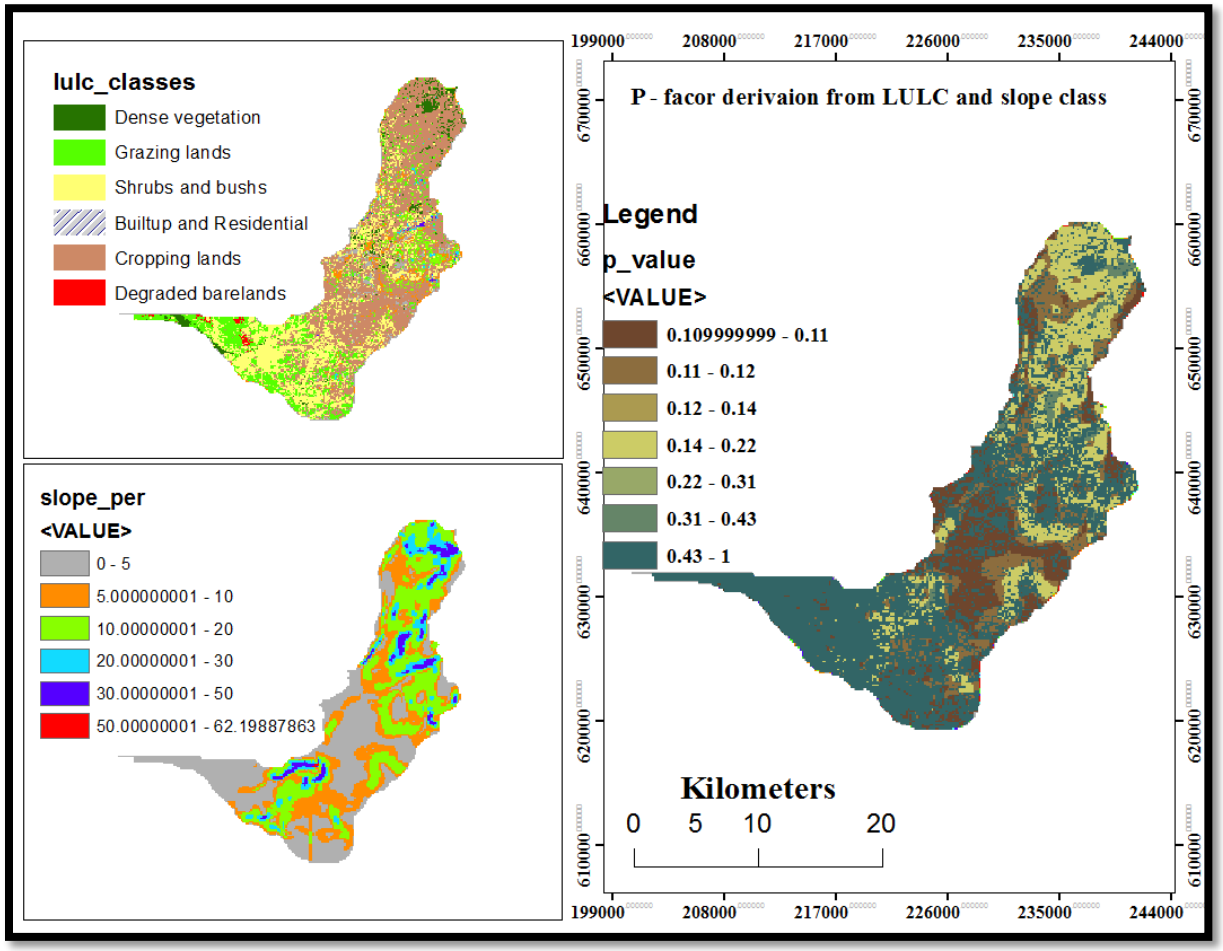

Figure 12:- Derivation and spatial distribution of calculated P values
(Based on Wischmeier and Smith (1978)

4.2. Soil Loss Estimation results under baseline period condition

The RUSLE model output pixel level analysis result of Neri watershed ranges from in the mean (0 ton $ha^{-1}yr^{-1}$) in some plain parts of the studied area (where the LS- factor value of zero) to the maximum amount of (465.16 tons $ha^{-1}yr^{-1}$) at the mid-eastern parts of the watershed. This particular spot is situated at Selmamer administrative kebele, South Ari woreda under (Sub Watershed 6). The very high pixel values (more than 25 tons $ha^{-1}yr^{-1}$) are detected in a distributed manner throughout the watershed. However, the particular maximum pixel value found at much of the steeper slope banks with high LS factor value under city expansion built up areas where poor surface cover condition. The average annual soil loss rate is 9.955 tons/hectare/year from the entire watershed area (46546 hectare). The total amount of soil loss is 463365.46 tons per year.

According to FAO (1986); and Gebreyesus and Kirubel (2009), there are six categories of soil loss risk in the study area, ranging from low (0–5 t ha^{-1} yr^{-1}) to extreme (100–465.16 t ha^{-1} yr^{-1}). Based on the analysis, about 54.88% (25536.8 ha) of the watershed was categorized under low to moderate classes. The remaining 45.12% (21009.2ha) of land area was classified under high to extreme class about several times the maximum tolerable soil loss. Higher soil losses rates were detected as the effect of combination in areas where the convex topography having high LS-factor value, poor vegetation cover, heavy rains, susceptible soils and in a condition without conservation practices. The combined values of these factors are directly related to soil losses; the larger are the values the greater the losses (Renald *et al.,* 1997).

Soil loss in the study watershed is influenced by erosion factors differently. Ordinary least-square regression analysis on 147 locations of the entire watershed indicated that soil loss has high correlation with primarily soil erodibility, followed by cover-management topographic factors, support practice and lastly rainfall erosivity the overall coefficient of determination (R^2) respectively are (0.7674), (0.6801), (0.651), (0.598) and (0.5448).

The result of RUSLE parameter analysis gives you an idea that factors combined effect resulted high soil loss from an area. Single parameter dominancy in contribution was not significantly explained however the leading effect of soil inherent erodibility followed by cover management and slope length and gradient (LS) factor were explained by the soil loss output.

Rainfall erosivity is the powerful driver in overall erosion mechanism having a strong influence on detachment of soil particles as well as bearing on transport through runoff. It has not only a strong influence on detachment of soil particles, but also have bearing on transport through runoff (Lal and Elliot, 1994). Therefore, the high erosivity values in the upper catchment area are of major importance on any poorly vegetated, steep slopes. Despite this truth, the variation in spatial distribution of soil loss in this study is not primarily influenced by rainfall erosivity. This is due to the resultant R factor map of the watershed by interpolation received the greater weight from Jinka meteorological station, the one with in the watershed.

Fortunately, the upper catchment does not necessarily experience high erosion rates. It is apparent that the reason is a vegetation cover at upper catchment to the other parts of the watershed combined with lower erodible soil property at steeply slope spots. The actual erosive power of the rain depends highly on plant cover (Evans, 2000), vegetation on soils reduce the energy of

raindrops (Bochet et al., 1998; Durán et al., 2007) and the inherent nature of soil having lower percentage silt content as well as they are not easily crumbled. For this reason, it is apparent that the surface cover upper catchment area does not necessarily experience high erosion rates.

The estimated mean annual soil loss results in the study area compared with the other previous reports in Ethiopian and particularly in Omo-Gibe basin condition. The mean annual soil loss results in the study area is lower than the annual average soil loss under Ethiopian condition which is 12 tons per hectare per year and about 42t ha^{-1} yr^{-1} from cultivated highland (Hurni, 1993). Similarly, 42 t /ha/y reported by Tegegne and Biniam (2017) at Koga watershed in the highlands of Ethiopia. According to the report by Tadesse and Abebe, (2014), 30.4 t /ha/ y soil loss for Jabi Tehinan woreda in the north western high land. The relatively low estimated average annual soil loss in the current study watershed could be due to mostly the land used for agricultural crops in this study area was located in areas where the least LS value was observed. In the watershed, out of the entire cultivated field shown in 'Table 6', 87% (19587.29 hectare) is area less than 20% slope.

Conversely, the mean annual soil loss rate from this watershed is slightly higher than the previous research report in the case of Gibe-III Dam Catchment which is 7.47 t /ha/ y by Gerawork and Awdenegest (2014) and twice higher than the the mean annual soil loss rate reported by (Bagegnew et el., 2019) which is 4.27 t/ h/y in Karesa Watershed, Dawuro Zone, Omo- Gibe basin. In this case the probable reason could be this study watershed owe low proportion of forest cover than the watersheds in comparison.

The soil loss rate is higher with respect to the soil formation rate for Ethiopia 2 tons per hectare per year, which is very low compared to soil erosion rates (Mahmud *et al.,* 2005).

Table 6:- Area and amount of annual soil loss for each severity class (WBISPP, 2001).

Soil loss ($t\ ha^{-1}\ year^{-1}$)	Equivalent top soil removal (mm)	Soil loss risk class	Area (ha)	Area (%)
(0 - 3.125)	(<0.2.5)	Very Less	25023.13	53.76%
(3.125 - 6.25)	0.2.5 – 0.5	Less	6316.29	13.57%
(6.25 - 12.5)	0.5 - 1	Moderate	10896.42	23.41%
(12.5 - 25)	1 - 2	High	3025.49	6.5%
(> 25)	>2	Very High	1284.67	2.76%
			46546	**100%**

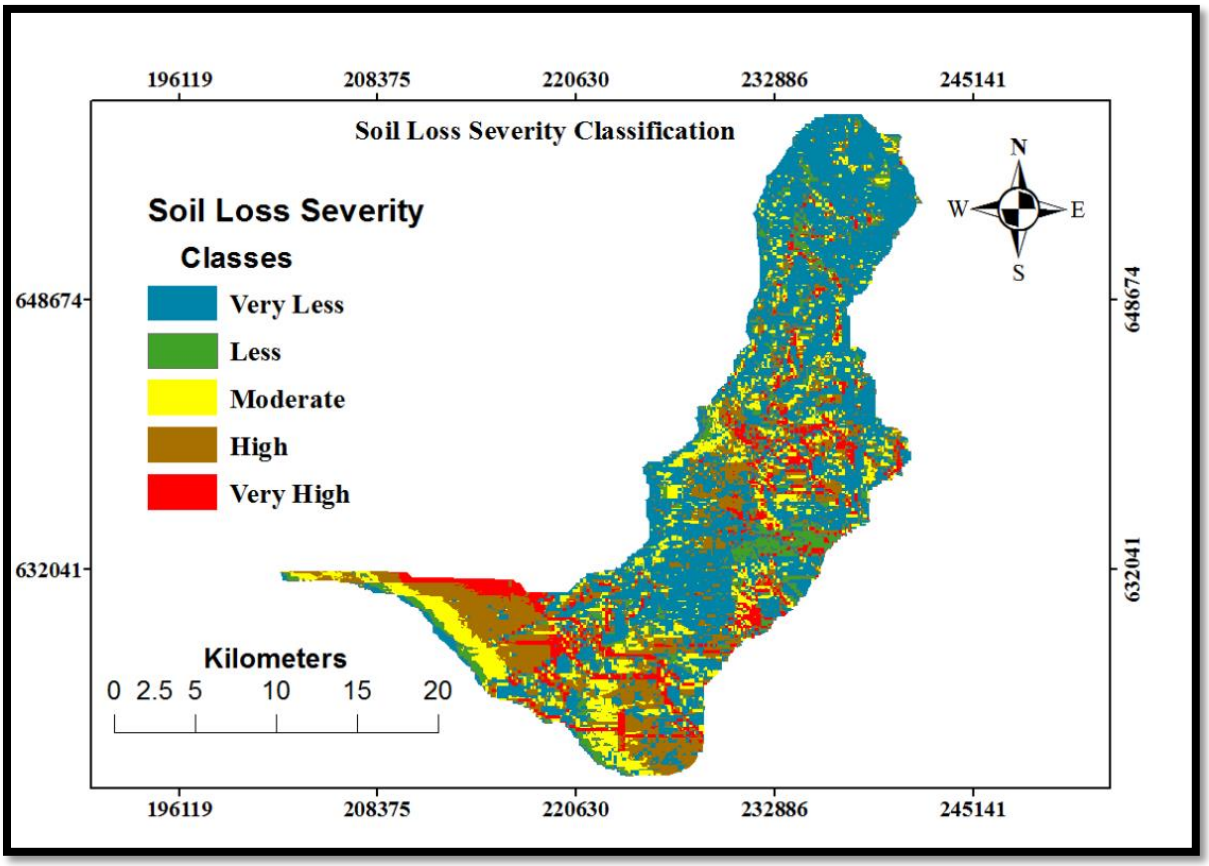

Figure 13:- Soil loss severity classes map of Neri watershed

4.3. Soil loss prediction under future and drawing comparison

Soil loss values computed for each of combined climate change and potential management practice scenarios are also displayed by means of soil erosion prediction maps. The set of maps were obtained to show the impact of climate change on soil erosion and the effects of management

practices on soil erosion. The following sub-sections show the outputs of parameters and resultant soil loss based on purposive scenarios simulated.

Integration of RUSLE parameters soil erodibility and topographic as constants and management practices factors (C and P) with projected R-factor values based on three RCP scenarios resulted in the different soil loss rate maps as shown under their respective sub topics. The scenarios outputs were obtained as stated in detail sub sections (4.4.2), (4.4.3) and (4.4.4).

4.3.1. Individual factor outputs for prediction of soil loss

4.3.1.1. R-factor output based on future climate change RCP scenarios

Rainfall over future time periods over baseline period is higher except in the case of near future $RCP_{2.6}$ as shown in Figure 14.

The result of Inverse Distance Weight method of interpolation gave the mean R-factor value for the year range (2021-2050) in MJ mm h^{-1} ha^{-1} yr^{-1} are (741.91, 745.911 and 733.53 for $RCP_{2.6}$, $RCP_{4.5}$ and $RCP_{8.5}$ respectively. Whereas, the mean outputs for the year (2051-2080) are (724.04, 761.558 and 759.02) MJ mm h^{-1} ha^{-1} yr^{-1} for $RCP_{2.6}$, $RCP_{4.5}$ and $RCP_{8.5}$ respectively. These results are much higher than the R- factor value obtained by baseline condition (1988-2017).

It is perceptible to understand the impact of climate change has contributed to the increase in the power of rain by increasing erosive events. (Appendix 1 table 4) shows that the percentage distribution of rainy days are higher than for that of baseline period with exception to mid future $RCP_{2.6}$ scenario. Undoubtfully, percentage erosive events are linearly correlated ($R^2 = 0.861$) with R-factor. The case of decline in rainfall and rainfall erosivity for $RCP_{2.6}$ scenario in near future (2051-2080) could be considered as reliable due to its consistency with respect to the characteristic of this scenario that lead to very low greenhouse gas concentration levels. This scenario stated as a scenario of 'with climate policy'. It is a "peak-and-decline" scenario; its radiative forcing level first reaches a value of around 3.1 W/m^2 by mid-century, and returns; (and indirectly emissions of air pollutants) are reduced substantially, over time. (Van Vuuren et al., 2007). (Characteristics quoted from VanVuuren et al., 2011).

For all the R-factor maps resulted through IDW method of interpolation, the mean value converges to the calculated R- value of Jinka station. This is due to CORDEX – Grid associated to Jinka meteorological station is the one within the watershed boundary, which has greater weight to the

mean R-value of the watershed than those gauging stations located outside. This behavior is similarly sensed also in baseline period.

This outputs witness that the future is intense, in agreement with past reports based on GCMs. IPCC report in (1995) states several global coupled models indicate that the ENSO-like SST variability they simulate continues with increased CO_2 - associated with the mean increase of tropical SSTs as a result of increased greenhouse gas concentrations, there could be enhanced precipitation variability associated with ENSO events in the tropical continents and an increase in rainfall intensity mainly over tropical land regions and the northern mid-latitudes based on ECHAM3 model (Cubasch *et al.*, 1995).

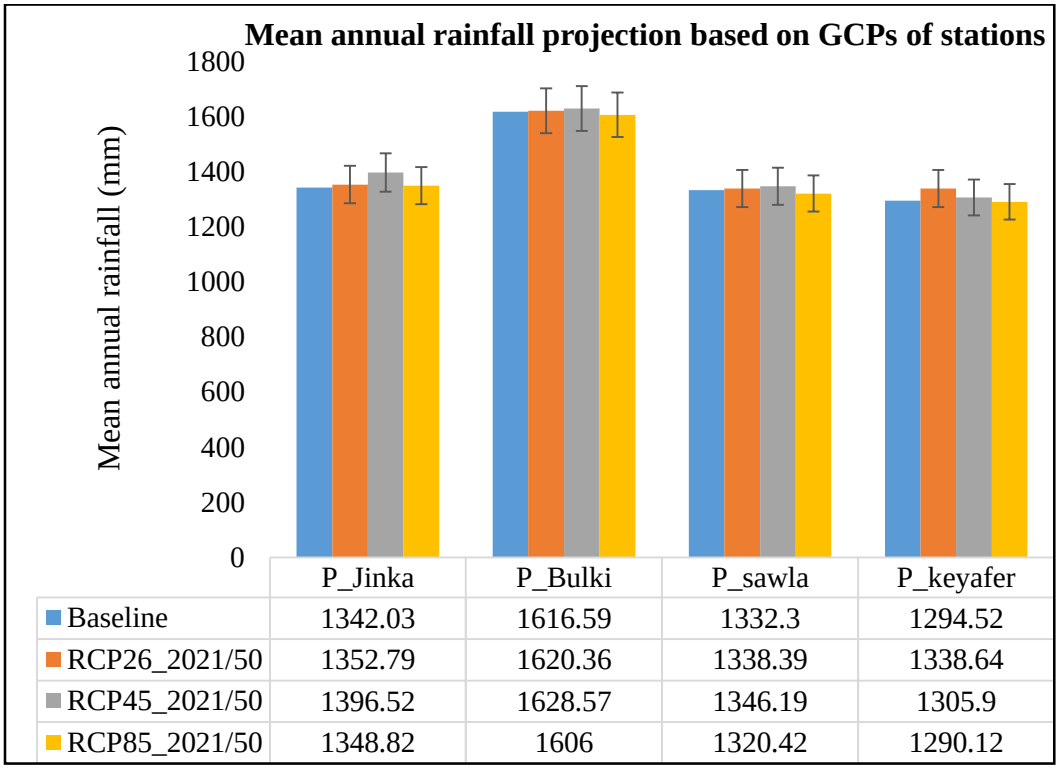

	P_Jinka	P_Bulki	P_sawla	P_keyafer
Baseline	1342.03	1616.59	1332.3	1294.52
RCP26_2021/50	1352.79	1620.36	1338.39	1338.64
RCP45_2021/50	1396.52	1628.57	1346.19	1305.9
RCP85_2021/50	1348.82	1606	1320.42	1290.12

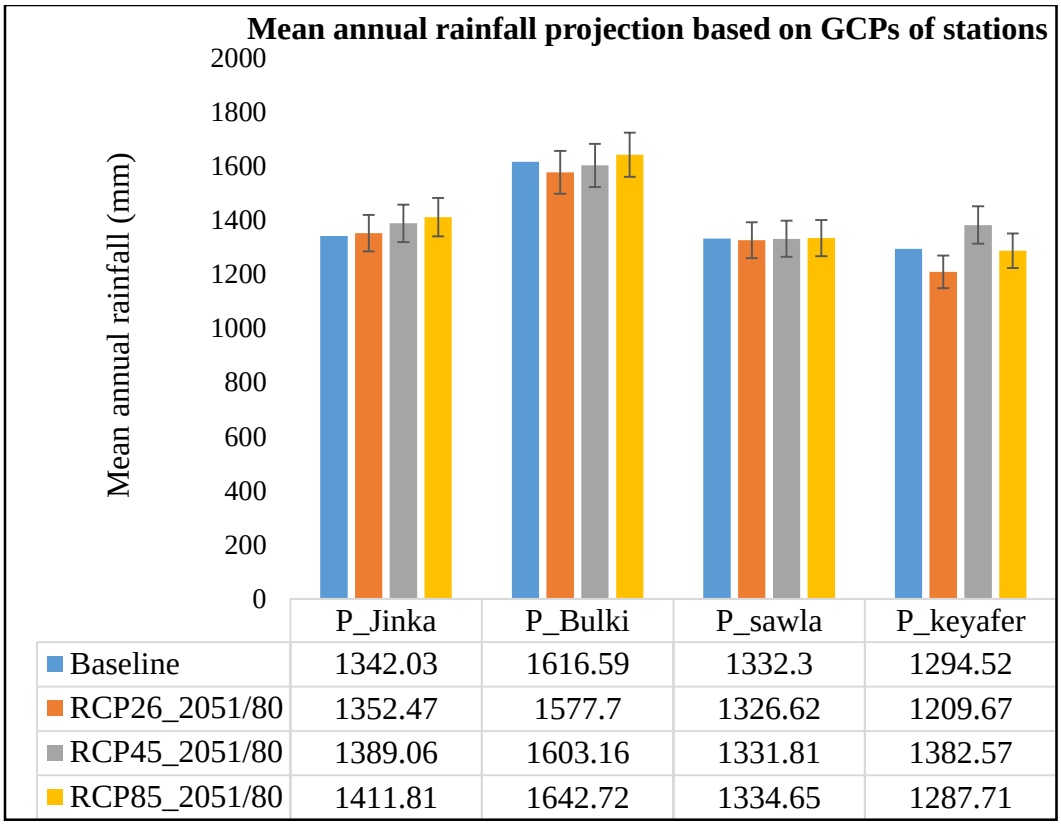

	P_Jinka	P_Bulki	P_sawla	P_keyafer
Baseline	1342.03	1616.59	1332.3	1294.52
RCP26_2051/80	1352.47	1577.7	1326.62	1209.67
RCP45_2051/80	1389.06	1603.16	1331.81	1382.57
RCP85_2051/80	1411.81	1642.72	1334.65	1287.71

Figure 14:- Rainfall projection for two future time slices

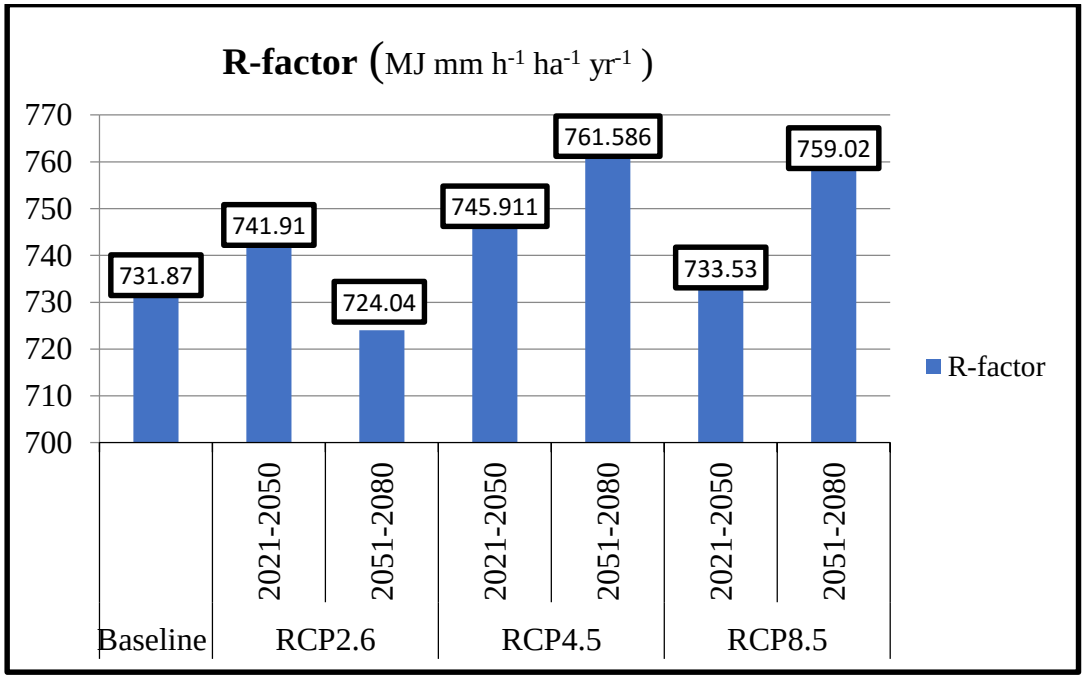

Figure 15 :- Computed R-factor values compared to baseline periods

4.3.1.2. Management practices (C & P factor) outputs for future Scenarios

Scenario-1 (No-action) scenario C-factor and P-factor values are assumed to be equal to the value in the case of baseline condition implies that the situation in the future don't need action.

Based on three scenarios of management practices, crop management (C-factor) values stated in section (3.5.2), In the case of cultivated fields, the C- value varies annually where the cover of the fields varies. However, the mean C-factor values are 0.364 and 0.332 in the cases of scenario-2 and scenario-3 respectively. Both of these values are less than that of baseline period by 5.5% for scenario-2 and 14% for scenario-3. The dominant crops such as maize (Zea-mays), wheat (Triticum-aestivum), sorghum (sorghum bicolor) barely other legumes in the study area, suggested for future, year after year remain the same. The important difference with in the values of these two scenarios cases is by added cropping system (contouring, crop rotation among them, fallow) for (scenario 3) as C-factor (sub-factors) under cultivated fields and supposed management under non-agricultural fields.

The C-values changes per each grid cell for changing cover-management. The lesser values of C-factor, the better cover- management is. This factor reflects the surface protection effect that dissipates the kinetic energy of raindrops before impacting the surface (Erdogan *et al.*, 2006).

Conservation practice factor according to Renald et al. (1997) definition is an expression of supporting conservation practices such as contour farming, strip cropping, terracing, and subsurface drainage on soil loss at a particular site, which principally affect water erosion by modifying the flow pattern, grade, or direction of surface runoff and by reducing the volume and rate of runoff.

Hence, the output P-factor mean values under (Scenario 2 and 3) respectively are 0.566 and 0.563. These values are less than the mean outputs under baseline period by almost 5%.

4.3.2. Soil loss rate under No- management action scenario

The amount of soil loss varies due to changes in erosivity (R-factor) under three RCP emission scenarios for two future time periods. Prediction results clearly show that the higher soil loss values compared to baseline period. With a mean annual soil of (10.12, 10.26 and, 9.98 ($t.ha^{-1}yr-1$)) are estimated under $RCP_{2.6}$, $RCP_{4.5}$ and $RCP_{8.5}$ scenarios respectively in immediate future (2021-2050). With the exception to $RCP_{2.6}$ (2051-2080), the predicted mean amounts are again greater

than that of baseline condition. The mean annual soil loss rates estimated for near future period (2051-2080) are 9.88, 10.41and 12.14($t.ha^{-1}yr^{-1}$) $RCP_{2.6}$, $RCP_{4.5}$ and $RCP_{8.5}$ respectively. It is perceptible that the rise in erosivity (R- factor value) has resulted in soil loss increment linearly given ($R^2 = 0.914$) correlated.

As it is clearly seen in Table 8 below RUSLE model outputs show that, the rate of mean and total annual soil loss per year smoothly increase with exception for the case in $RCP_{2.6}$ (2051-2080) which is slight decline (-0.75%).

The highest (21.95%) average yield increment over baseline is predicted by $RCP_{8.5}$ (2051-2080) followed by 4.57% rise in the case of $RCP_{4.5}$ (2051-2080). Overall, on average of all three scenarios, in immediate an erosivity increase by 1.17% and near future (2021-2050) by 2.23% whereas, for mid future (2051-2080) is a 2.2% rise in erosivity yields 9% incremental soil loss. This result is nearly in agreement with research report by (Nearing et al., 2004) which stated that when rainfall increases, runoff and erosion increase at an even greater rate. For instance, a 1% increase in annual precipitation can increase erosion by 1.7 percent, if other factors are equal. The other report in Wisconsin stated that in the absence appropriate adaptation action soil erosion could more than double by 2050 relative to 1990s (WICCI, 2011).

Table 7 Soil loss rate change RCP scenarios with (No – action management scenario)

Scenario (RCP)	Period	Mean R-factor	Percent (%) erosivity rise relative to baseline	Mean annual Soil loss ($t\ ha^{-1}\ yr^{-1}$)	Total annual soil loss ($ton\ yr^{-1}$)	Percent (%) soil loss rise
Baseline	1988-2017	731.87	---	9.955	463,365.4	--
$RCP_{2.6}$	2021-2050	741.91	1.4%	10.12	471,045.5	1.66%
	2051-2080	724.04	-1.1%	9.88	459,874.5	-0.75%
$RCP_{4.5}$	2021-2050	745.911	1.9%	10.26	477,562.0	3.06%
	2051-2080	761.558	4.1%	10.41	484,543.9	4.57%
$RCP_{8.5}$	2021-2050	733.53	0.2%	9.98	464,529.1	0.25%
	2051-2080	759.02	3.7%	12.14	565,068.4	21.95%

4.3.3. Soil loss under medium-action/progressive state of mgmt. /scenario.

The predicted soil loss results only by applying terrace based on the slope classes are lesser than in the cases of baseline and future no action scenario. As it is clearly shown in the (Appendix 4 and Table 9), the mean annual soil loss rate ranges from (8.94 tons/hectare/ year) $RCP_{2.6}$ (2051-2080) to that of higher value of (9.5 tons/hectare/ year) under the case of $RCP_{4.5}$ (2051-2080). When compared to the estimated result in baseline period (9.955 tons/ha/ yr.), implementation of terraces and crop selection has brought at least the least reduction 4.6% ($RCP_{4.5}$ (2051-2080)) to the higher reduction 10.2% (($RCP_{2.6}$ (2051-2080)). Similarly, the comparison of the model out puts under this scenario with the prediction results in the case of no-action scenario gives an insight to the role of applying conservation practices to reduce erosion however the reduction is not likely to cope-up fully the erosion aggravated due to climate change.

Table 8:- Soil loss rate change under climate change with (Medium action management)

Management Scenario	**Scenario (RCP)**	**Period**	**Mean annual Soil loss (t/ha/ yr.)**	**Total soil loss (ton/ yr)**	**(%) Change in soil loss Compared with**	
					Baseline	Scenario_1
	Baseline	1988-2017	9.955	463365.4	--	--
Scenario 2 (medium-action)	$RCP_{2.6}$	2021-2050	9.25	430550.5	7.08 % ↓	9.4% ↓
		2051-2080	8.94	416121.2	10.2% ↓	10.5% ↓
	$RCP_{4.5}$	2021-2050	9.36	435670.6	6.0% ↓	9.6% ↓
		2051-2080	9.5	442187.0	4.6% ↓	9.6 % ↓
	$RCP_{8.5}$	2021-2050	9.12	424499.5	8.4% ↓	9.4 % ↓
		2051-2080	9.41	437997.9	5.5% ↓	20.9% ↓

4.3.4. Soil loss rate results under comprehensive management scenarios

Proposed management practices integrated whatever the climate effect by increasing rainfall erosivity appears, the rate of soil loss estimated decreases. The predicted soil loss results by applying crop-cover management by selection of cropping system by contouring (Kaltenrieder, 2007) complimented with conservation terraces constructed based on (Deoer, 2005) are lesser than in the cases of baseline and future no management action scenario.

Table 10 states that, the predicted soil rate results under management (scenario 2) under three RCPs combination in both future time slices are lesser than the outputs of baseline as well as no-

management. The lowest output or the greatest decline (17.9%) relative to reference period is generated by $RCP_{2.6}$ (2051-2080) and the highest output or the least decline (13.0%) is by $RCP_{4.5}$ (2051-2080).

Based on comparison with no management action scenario, $RCP_{8.5}$ (2051-2080) has resulted at maximum situation by 41.2% less result relative to $RCP_{8.5}$ (2051-2080) under the case of it's no management action condition. In the other cases of RCPs the reduction is by about (20%) relative to no management action scenarios with in themselves.

The predicted soil loss results in this scenario condition are generally realistic with what can be observed in the field based on previous studies. For instance, the research finding by (Zhang et al., 2012) supports current result; which confirmed the runoff and soil erosion on rangelands for three future climate emission scenarios (A2, A1B, and B1) might increase significantly even if total annual or seasonal rainfall amounts were to remain unchanged or decrease in the condition of no implementation of management practice.

The crop management factor represents the ratio of soil loss under a given crop to that from bare soil. Since soil loss varies with the erosivity and the morphology of the plant cover. These results are reliable surface cover, such as the rocks and residue composition, is considered as one of the most sensitive factors controlling erosion (Renard et al., 1991; 1994; Evans, 2000).

Table 9:- Soil loss rate change under climate change with (Comprehensive management)

Management Scenario	Scenario (RCP)	Period	Mean annual Soil loss (t/ha/ yr.)	Total soil loss (ton/ yr)	Change in soil loss percent (%)	
					Compared with Baseline	Compared Sc_1
	Baseline	1988-2017	9.955	463365.4	--	--
Scenario 3 (Comprehensive management scenario)	$RCP_{2.6}$	2021-2050	8.44	392848.2	15.2% ↓	19.9% ↓
		2051-2080	8.17	380280.8	17.9% ↓	20.9% ↓
	$RCP_{4.5}$	2021-2050	8.54	397502.8	14.2% ↓	20.1% ↓
		2051-2080	8.66	403088.4	13.0% ↓	20.2% ↓
	$RCP_{8.5}$	2021-2050	8.31	386797.3	16.5% ↓	20.1% ↓
		2051-2080	8.60	400295.6	13.6% ↓	41.2% ↓

4.4. Prioritization for Soil Conservation Planning

Identifying priority areas for intervention is one of the main objective of this thesis. The base for this is soil loss tolerance. According to (Gebreyesus and Kirubel, 2009; FAO and UNEP., 1984), soil loss tolerance (SLT) denotes the maximum allowable soil loss rate that will sustain an economic and a high level of productivity. It is the normal soil loss tolerance values range from (5–11) tones/hectare/year (Renald *et al.,* 1996). An argument according to Morgan (1995) also is 10 ton ha-^{1}yr-^{1} as an appropriate boundary measure of soil loss over which agriculturalists should be concerned. The assignment of a range depended on the judgment of how much erosion would be harmful to the soil.

Hence, for this particular study due to lack of soil formation rate information for the soils of Neri watershed, (WBISPP, 2001) classification of soil loss classes which is for Southern Ethiopia was used and the extent of soil erosion in the study area was classified into five erosion hazard classes (Figure 13 and Table 5). Tabular representation for area coverage in hectare and percent proportion the soil erosion potential categories. Based on the analysis, the total area with a soil loss potential higher than the SLT, i.e. greater than 6.25 tons ha^{-1}yr $^{-1}$, was (19,241ha.), which comprises 32.67% of the total study area and the remaining 67.33%, (31339.42 hectare is not under erosion hazard zone. Intervention priorities needs to identify where at the first and then to follow are needed.

4.4.1.1. Soil Loss rate at sub watersheds

To prioritize conservation planning, judgment of mean annual and total annual soil loss for sub watershed based identification was applied. To do this, geographical information system (GIS) technology has allowed the equation to be used in a spatially distributed manner because each cell in a raster image comes to represent a field-level unit. Even though the equation was originally meant for predicting soil erosion at the field scale, its use for large areas in a GIS platform has produced satisfactory results (Mellerowicz *et al.,* 1994).

By delineating sub-watersheds as erosion prone areas according to the severity level of soil loss, priority was given for a targeted and cost-effective conservation planning (Kaltenrieder, 2007). Accordingly, Neri watershed was sub divided in to eleven (11) sub watersheds. The output under (Table 10) clearly shows that, the mean annual soil loss rates from sub watersheds range from 1.923 ton ha^{-1} yr^{-1} to 20.08 ton ha^{-1} yr^{-1}. The situation for sub watersheds numbered (SW_4, SW_5, SW_6, SW_7, SW_8, SW_9, SW_{10} and SW_{11}) is beyond the soil loss tolerance (>6.125 ton ha^{-1} yr^{-1} according to (WBISPP, 2001) and the remaining are not. Hence, for prioritization of conservation

planning, their area weighted average was applied for ranking to take area coverage of these sub watershed in to account.

4.4.1.2. Soil Loss rate at administrative level

Neri watershed consists of about 19 Kebeles administrations of 2 Woredas, i.e. South Ari and BenaTsemay, an attempt was made to see which of these 19 kebeles highly affected by soil erosion in order to prioritize them for conservation planning. The average annual soil loss rate of the study area Kebeles ranges from 1.54– 19.02 tons/ha/yr^{-1} Table 11. Out of the total 19 Kebeles, 10 (Alga, Arkisha, Aydfo, Bako, Dell, Dordora, Gazer, Gedir, Goldia, Goyd, Jinka town, Kaysa, MNP, Pola, Senegal and Selmamer) produce a mean annual soil loss more than tolerable loss rate category (>6.125 tons per hectare per year) and the rest 9 kebeles are below the maximum mean annual soil loss tolerable limit. As shown in figure 12, the average annual soil loss rate of these ten Kebeles are 7.96, 9.70, 6.46, 14.09, 6.41, 16.37, 13.33, 15.09, 19.02 and 14.35 tons per hectare per year respectively.

However, in terms of the total annual soil loss these Kebeles generate of 440,790.456 ton /year comprising 95% of the total annual soil loss from the entire watershed. Among the above listed Kebeles Goldia accounts the highest total annual soil loss 172647.43 tons per year (37.3%) followed by Arkisha 67871tons per year (14.6%). The remaining Alga, Senegal, Selmamer, Kaysa, MNP, Jinka town and Goyd account for 24188.52671 tons yr^{-1} (3.00%), 24542.27499 tons yr^{-1} (3.10%), 16500.67672 tons year^{-1} (2.10%), 107471.0408 tons year^{-1} (13.50%), 8989.242285 tons year^{-1} (1.10%) and 57360.43064 tons year^{-1} (7.20%) respectively. In addition to their area coverage, the topographic ruggedness, lack of conservation measures, and poor vegetation cover during critical periods of the year (i.e. at the beginning of main rainy season) coupled with erosive rainfall contributes to the high rate of soil erosion in the above prioritized.

Table 10:- Soil loss rates by Sub watersheds.

Sub Watershed	**Local names (tributaries)**	**Mean annual soil loss**	**Area (hectare)**	**Weight of Area (%)**	**Total annual soil loss (t/yr.)**	**Weighted average**	**Rank** weighted average
SW_1	Neriweset	1.923	3024.025	6.50%	5815.02	12.5%	10th
SW_2	Zomba	3.358	2395.130	5.15%	8042.82	17.3%	9th
SW_3	Uti	5.620	7686.820	16.51%	43197.91	92.9%	7 th

SW_4	Afia	12.845	4788.774	10.29%	61512.94	131.8%	3rd
SW_5	Shaleka	7.316	3180.054	6.83%	23263.92	50.0%	8th
SW_6	Gamayso	10.015	7799.139	16.76%	78104.71	167.7%	1st
SW_7	Hacheker	11.305	5436.154	11.68%	61454.59	132.2%	2nd
SW_8	Argon	20.080	184.749	0.40%	3709.73	8.0%	11th
SW_9	kibsh	14.045	4047.001	8.69%	56840.78	121.8%	6th
SW_10	Beso	16.867	3475.749	7.47%	58623.93	126.2%	5th
SW_11	Ufiker	13.432	4528.407	9.73%	60826.72	130.6%	4th
Total			**46546**	**100%**	**463,365.46**		

Table 11. Soil loss rates by small administrative units

No.	Name of Administrative Kebeles	Average Annual Soil Loss (ton/ha/yr)	Area (hectare)	Area (%)	Total Annual soil loss (ton/yr)	Percentage of soil loss/total
1	Alga	7.96	5113.3263	11.0%	40712.77	8.8%
2	Arkisha	9.70	7000.0579	15.0%	67871.00	14.6%
3	Aydo	1.54	222.2191	0.5%	341.91	0.1%
4	Bako	6.46	1813.4222	3.9%	11708.58	2.5%
5	Dell	2.86	954.8981	2.1%	2733.08	0.6%
6	Dordora	1.89	1580.2734	3.4%	2987.49	0.6%
7	Gazer	2.10	147.0273	0.3%	308.82	0.1%
8	Gedir	2.10	1898.7752	4.1%	3987.44	0.9%
9	Goldia	14.09	12256.688	26.3%	172647.43	37.3%
10	Goyd	6.41	2177.9349	4.7%	13956.32	3.0%
11	Jinka	16.37	889.4369	1.9%	14557.01	3.1%
12	Kaysa	13.33	1072.8883	2.3%	14297.31	3.1%
13	MNP	15.09	4041.7772	8.7%	60996.13	13.2%

14	Pola	3.08	323.8607	0.7%	996.24	0.2%
15	Senegal	19.02	285.3593	0.6%	5428.41	1.2%
16	Selmamer	14.35	2690.1142	5.8%	38615.50	8.3%
17	Sh/weset	1.70	1083.0168	2.3%	1842.49	0.4%
18	Shepi	4.47	520.2985	1.1%	2325.74	0.5%
19	Zomba	2.85	2474.6289	5.3%	7055.69	1.5%
	Total		**46546.002**		**463369.34**	**100%**

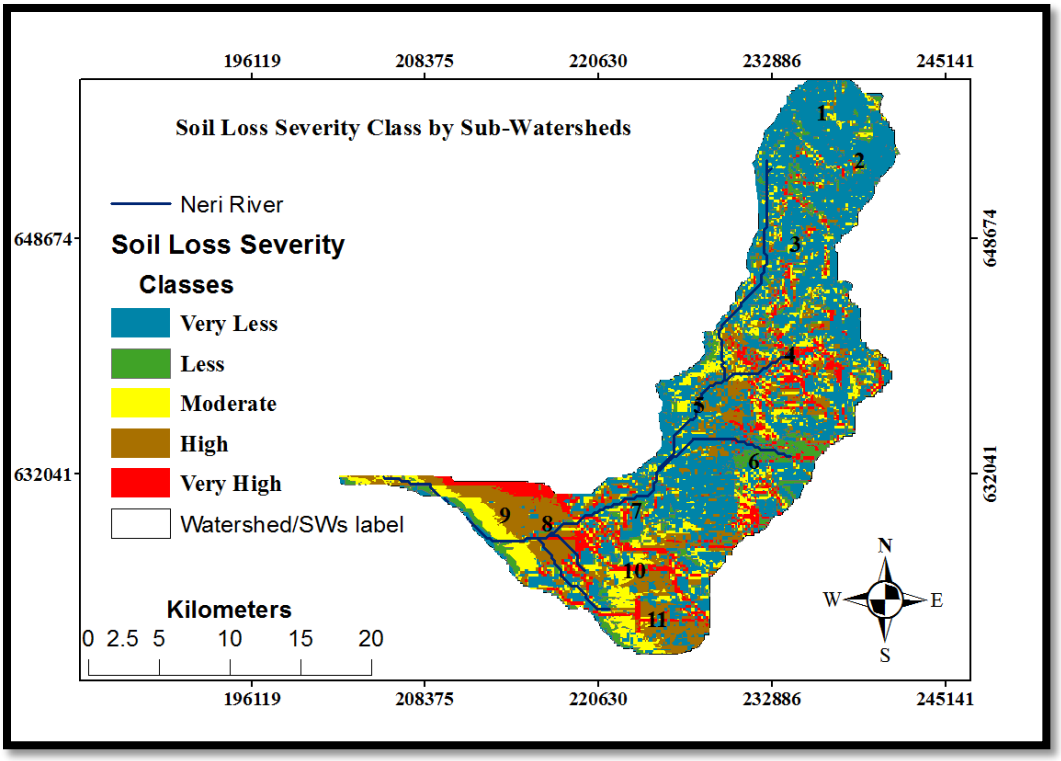

Figure 16:- Soil loss severity classes by sub watershed

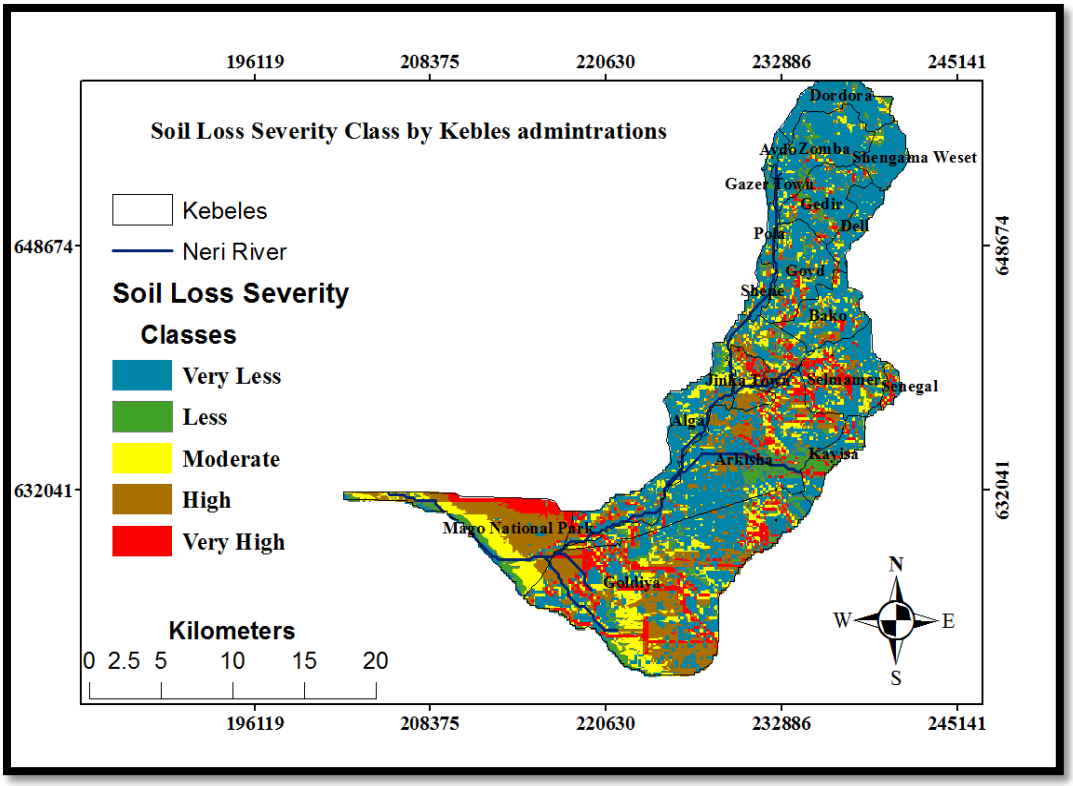

Figure 17 : - Soil loss rate severity class distribution based on administrative Kebeles

5. SUMMARY AND CONCLUSION

The application of RUSLE model (Renard et al., 1997) over the Neri watershed with the aid of GIS and remote sensing applications to generate soil loss estimation maps. Moreover, the study was an attempt to estimate average annual soil loss at this watershed, to predict the consequences in terms of soil loss under future conditions of climate change and state of management practices to identify areas of intervention.

Despite the difficulties for strict application of RUSLE model, some algorithms have been forced into a simplification in order to adapt them to the data availability. For the conditions of data base shortage, remotely sensed satellite imagery was used. Besides, for future soil loss estimation, dynamically downscaled rainfall projection by GIS-based approach enabled to estimate watershed-based soil loss rate. This model provided great advantage to achieve above aims for this watershed with complex topographic feature.

The resulting baseline period soil loss map produced by overlaying of grid maps of the six factors showed that the soil loss rate of the watershed ranged from 0 – 465.16 t ha-^{1} year^{-1} with a mean annual soil loss rate of 9.95 t ha-^{1}yr-^{1} and overall total annual amount of 463,365.46 t/yr. So that, it is perceptible that this watershed is under risk of soil erosion.

However different reports suggested different soil loss tolerance (SLT) and use various soil loss severity classification, this study used soil loss severity classification based on (WBISPP, 2001), the one more suitable for this study. As result, about more than 6.25 tons ha^{-1}yr $^{-1}$, was (19,241ha.), which comprises 32.67% of the total study area and the remaining 67.33%, (31339.42) hectare is lesser, which is recognized as area not zone of a great danger of soil erosion. The highest soil loss recorded spots are areas of long steep slope areas at middle-eastern parts of the watershed where no or low existence of surface cover, without support practice and highly erodible soil and erosive rain combined.

The immediate (2021-2050) and near (2051-2080) future soil loss response for changing climate under anticipated management practices was conducted through application of predicted rainfall data series obtained from regional climate multi model outputs of CORDEX-Africa for three RCP scenarios (RCP $_{2.6}$, RCP$_{4.5}$ and RCP$_{8.5}$) for R-factor and three simulated management scenarios for C and P factor. To highlight an understanding of changing precipitation due to climate change

impact on soil erosion, the no management action scenario of C and P factor were complimented. As result prediction, mean annual soil loss rate clearly show that the higher soil loss values compared to baseline period except for $RCP_{2.6}$ (2051-2080) which show the characteristic of little decline in (-0.75%). The highest rise (21.95%) on average yield increment over baseline is predicted by $RCP_{8.5}$ (2051-2080) followed by 4.57% rise in the case of $RCP_{4.5}$ (2051-2080).

The resultant soil loss in the rest condition of management practices scenarios (2 and 3) highlighted that the relative merits of management actions by counteracting the risk of soil erosion relative to baseline/reference/ period (1988-2017) and future no-management scenario situation. Both management action scenarios (2&3) in near term future (2051-2080) complimented with $RCP_{2.6.}$ Scenario, resulted in high reduction of soil loss i.e. (10.2% ↓) for scenario-2 and (17.9% ↓) for scenario-3 compared with the baseline period. However as soil loss rates under RCP scenarios were compared within themselves with and with-out management practices as well as the two states of management scenario cases each other. Based on computation, Scenario-3 has brought the highest reduction of soil loss by (41.2%) for $RCP_{8.5}$ (2051-2080) and nearly by half of this much percentage reduction for the other RCPs.

In general, the averaged (means of three RCP scenarios) under no management scenarios situation has predicted a higher annual average soil loss. Which is (15.3%) and (15%) in immediate and mid future respectively relative to reference period output. The implication of this is percentage reduction potential management practice in the case of scenario-3 for all (RCPs) has twice higher advantage of (23.73% over scenario-1) minimizing the soil loss relative to scenario-2 management (11.57%) over scenario-1). The mean annual soil loss rate is beyond the soil loss tolerance SLT (6.25 t $ha^{-1}yr^{-1}$) in Neri watershed under baseline as well as future periods.

As a further matter, for the prioritization of intervention, the soil loss map of baseline period was used to extract the soil loss per nineteen (19) kebele administrative units and eleven (11) sub-watersheds (SWs). But sub-watersheds having greater than SLT were chosen. Based on the analysis, sub-watersheds (SW-4, SW-6, SW-7, SW-9, SW-10 and SW-11), greater than SLT in their order of area weighted average soil loss were identified for priority intervention.

Based on the findings of this study, to ensure sustainable resource use, management practice like contour cropping with selected high biomass bearing ones complimented with soil and conservation practices in agricultural fields and with giving special attention to climate change through strong policy measures, erosion minimization in non-agricultural land use classes are of paramount importance. Further study to understand the land suitability that consider the climate change is needed.

6. REFERENCES

Anderson, J.R., 1971. Land use classification schemes used in selected recent geographic applications of remote sensing: Photogrammetric Eng., v. 37, no. 4, p. 379-387.Arnold, J.G., Srinivasan, R. Muttiah, S., and Williams, J.R. 1998. Large area hydrologic modeling and assessment part I: model development. Journal of American Water Resources. Association 34(1):73-89.

Angima S.D., Stott, D.E., O‟Neill, M.K., Ong CK, Weesies, G.A. 2003. Soil erosion prediction using RUSLE for central Kenyan highland conditions. Agriculture, ecosystems and environment 97(1-3):295- 308.

Arnold, J.G., R. Srinivasan, R.S. Muttiah, and J.R. Williams. 1998. Large area hydrologic modeling and assessment part I: model development. J. American Water Resources Association 34(1):73-89.

Asis, A.M., Omassa, K. 2007. Estimation of vegetation parameter for modeling soil erosion using linear spectral mixture analysis of Landsat ETM data. ISPRS Journal of Photogrammetry and Remote Sensing, v.62, p.309-324.

Aster, D. 2004. Use of geospatial technologies for environmental protection in Ethiopia. Environmental Protection Authority. United Nations/European Space Agency/Sudan. In Proceedings of Remote Sensing Workshop on the Use of Space Technology for Natural Resources Management Environmental Monitoring and Disaster Management. April 4–8, 2004 Sudan, Khartoum.

Bagegnehu, B., Alemayehu, M., Nigatu, W. 2019. Geographic Information System (GIS) based soil loss estimation using Universal Soil Loss Equation Model (USLE) for soil conservation planning in Karesa Watershed, Dawuro Zone, South West Ethiopia International Journal of Water Resources and Environmental Engineering, 2141-6613.

Bai, Z., Dent, D.L., Olson, L., Shaepman M.E., 2008. Proxy global assessment of land degradation. Soil use and Management, 24, 223-234.

Beniston, M. 2006. Mountain weather and climate: A general overview and a focus on climatic change in the Alps. Hydrobiology**,** 562**,** 3–16.

Blanco CH, Lal R. 2008. Principles of soil conservation and management. Springer Science and Business Media B.V, Berlin P 240.

Beyene, T., Lettenmaier D.P. and Kabat P.2009. Hydrologic impacts of climate change on the Nile River Basin: Implications of the 2007 IPCC scenarios. Climate Change, 100, 433-461.

Bochet, E., Rubio J.L., Poesen J. 1998. Relative efficiency of three representative matorral species in reducing water erosion at the micro scale in a semi-arid climate, Geomorphology 23, 139–150.

BCEOM.2006. Abay river basin integrated development master plan project. Data collection and site investigation survey and analysis on environment and soil conservation. Sectorial studies Section II, Phase 2. Vol. XIII.

Beasley D.B., Huggins L.F., Monke E.J., 1980. ANSWERS: a Model for Watershed Planning. Transactions of the American Society of Agricultural Engineers 23 (4): pp938–944.

Bonilla, C.A. and Johnson, O.I. 2012. Soil Erodibility Mapping and Its Correlation with Soil Properties in Central Chile. Geoderma, 189-190, 116-123.

Brown, L.C.; Foster, G.R., 1987. Strom erosivity using idealized intensity distributions. Trans. American Society of Agricultural Engineering, 30, 372–386.

Brown, C., Greene, A, Block, P. and Giannini, A. 2008. Review of downscaling methodologies for Africa climate applications. International Research Institute for Climate and Society ColumbiaUniversity.

Chiew, F.H.S., Teng, J., Kirono, D., Frost, A., Bathols J, Vaze J, Viney N, Young W, Hennessy K and Cai W.2008a. Climate data for hydrologic scenario modelling across the Murray-Darling Basin. A report to the Australian government from the CSIRO Murray-Darling Basin Sustainable Yields Project. CSIRO, Australia.

Christensen, J.H., Hewitson, B., Busuioc, A., Chen, A., Gao, X., Held, I., Jones, R., Kolli, R.K., Kwon, W.-T., Laprise, R., Magaña Rueda, V., Mearns, L., Menéndez, C.G., Räisänen, J., Rinke, A., Sarr A., and Whetton. P. (2007). Regional Climate Projections. In Solomon, S., Qin, D., Manning,

Clarke, L., Edmonds J., Jacoby H., Pitcher H., Reilly J., Richels R., 2007. Scenarios of Greenhouse Gas Emissions and Atmospheric Concentrations. Sub-report 2.1A of Synthesis and Assessment Product 2.1 by the U.S. Climate Change Science Program and the Subcommittee on Global Change Research. Department of Energy, Office of Biological & Environmental Research, Washington DC. USA, 154 pp.

Cooley, K. R. & Williams, J. R., 1985: Applicability of the universal soil loss equation (USLE) and the modified USLE to Hawaii, In El-Swaify, S. A., Moldenhauer, W. C. & Lo, A. (eds.), International conference on soil erosion and conservation, “Malama Aina 83”, Soil Conservation society of America, University of Hawaii, Department of Agronomy and Soil Sience, Honolulu, HI, pg 509-522.

El-Swaify, S. A. & Dangler, E. W., 1976: Soil erosion prediction and control, Soil conservation society of America, Iowa, Ankeny.

Daniels, A. E., Morrison, J. F., Joyce, L. A., Crookston, N. L., Chen, S. C., & McNully, S. G. (2012). Climate projections FAQ. General Technical Report. Fort Collins, CO, U.S. Department of Agriculture, Forest Service, Rocky Mountain Research Station: 1-32.

De Jong, S.M. 1994. Application of Reflective Remote Sensing for Land Degradation Studies in a Mediterranean Environment (Utrecht: Netherlands Geographical Studies, University of Utrecht.

De Jong, S.M., Paracchini, M.L., Bertolo, F. Folving, S., Megier, J., de Roo, A.P.J, 1999. Regional assessment of soil erosion using the distributed model SEMMED and remotely sensed data. Catena, 37, 291–308.

Deore, S.J. 2005. Prioritization of micro-watersheds of upper Bhama Basin on the basis of soil erosion risk using remote sensing and GIS technology. Ph.D Thesis. University of Pune, India.

Desmet, P.J.J. and G. Govers, 1996a. A GIS Procedure for Automatically Calculating the USLE LS factor on Topographically Complex Landscape units. Journal of Soil and Water Conservation. 51(5):pp427-433.

Desmet P.J.J., and Govers , G. 1996b. Comparisons of Routing Algorithms for Digital Elevation Models and Their Implications for Predicting Ephemeral Gullies. International Journal of Geographical Information Systems. 10(3):pp311-331.

Durán Z.V.H., Rodríguez P.C.R., Francia M.J.R., Cárceles R.B., Martínez R.A., Pérez G.P. 2007. Harvest intensity of aromatic shrubs vs. soil-erosion: an equilibrium for sustainable agriculture (SE Spain), Catena (in press) available on line at: www.sciencedirect.com.

Durigon, V.L., Carvalho, D.F., Antuness, M.A.H., Oliveira, P.T.S., Fernandess, M.M. 2014. NDVI time series for monitoring RUSLE cover management factor in a tropical watershed. International Journal of Remote Sensing, v.35, p.441-453.

Erdogan, E., Erpul, G., Bayramin, I. 2006. Use of USLE/GIS Methodology for Predicting Soil Loss in a Semiarid Agricultural Watershed. Env. Monit. Assess. 131: 153-161.

Fangmeier, D.D., Elliot, W.J., Workman, S.R., Huffman, R.L. and Schwab, G.O. 2006. Soil and Water Conservation Engineering. 5th ed. Thomson Delmar Learning. New York. P35.

Favis M D.T.; Boardman, J. 1995. Nonlinear responses of soil erosion to climate change: A Modelling study on the UK South Downs. Catena, 25, 365–387.

Federal Democratic Republic of Ethiopia (FDRE). 2011. Green economy strategy Ethiopia's Climate-Resilient Green Economy. GTP-I.

Feng, X. Wang, Y. Chen L. Fu, B. Bai G. 2010. Modelling soil erosion and its response to land-use change in hilly catchments of the Chinese Loess Plateau. Geomorphology, 118, 239–248.

Flanagan D.C. & Nearing M.A. (eds), 1995 - USDA – Water erosion Prediction Project (WEPP): Hill slope profile and watershed model documentation. USDA-ARS National Soil Erosion Research Laboratory, West Lafayette (NSERL Report No. 10).

Food and Agricultural Organization (FAO) and UNEP, 1984. Provisional Methodology for Assessment and Mapping of desertification.

Food and Agricultural Organization (FAO).1986. Highland reclamation study: Ethiopia. Final Report. Food and Agriculture Organization of the United Nations, Rome, Italy.

Food and Agriculture Organization (FAO). 2012. A National Soil Model of Ethiopia A geo statistical approach to create a national soil map of Ethiopia on the basis of an SRTM 90 DEM and SOTWIS soil data.

Foster G.R., 1981. Conservation practices in erosion models. In Soil Conservation: Problems and Prospects, ed. Morgan, R.P.C., 273-278. New York: John WILLYand Sons.

Foster, G.R.; McCool, D.K.; Renard, K.G.; Moldenhauer, W.C, 1991. Conversion of the Universal Soil Loss Equation to SI metric units. Journal of Soil Water Conservation, 36, 355–359.

Fowler AM, Hennessey. KJ. 1995. Potential impacts of global Warming on the frequency and magnitude of heavy precipitation. Natural Hazards, 11: 283-303.

Fujino, J., Nair R., Kainuma M., Masui T., Matsuoka Y. 2006. Multi-gas mitigation analysis on stabilization scenarios using AIM global model. Multigas Mitigation and Climate Policy. In: The Energy Journal, 3 (Special Issue).

Ganguly, S., Friedl, M.A., Tan, B., Zhang, X.Y., Verma, M, 2010. Land surface phenology from MODIS: Characterization of the collection 5 global land cover dynamics product. Remote Sens. Environ, 114, 1805–1816.

Gebreselasie, E.D., 1996. Soil erosion hazard assessment for land evaluation. MSc Thesis, University of Bern.

Gebreyesus, B. and Kirubel, M., 2009. Estimating Soil Loss Using Universal Soil Loss Equation (USLE) for Soil Conservation planning at Medego Watershed, Northern Ethiopia. Journal of American Science: 5(1), pp58-69. Marsland Press

Gerawork, B.and Awdenegest, M. x x 2014. Spatial Erosion Hazard Assessment for Proper Intervention in the case of Gibe-III Dam Catchment, Southwest Ethiopia. MSc Thesis, Haramaya University.

Geremew, S., Agizew, N. 2015. Climate Modelling of the Impact of Climate Change on Sugarcane and Cotton for Project on 'a Climate Resilient Production of Cotton and Sugar in Ethiopia' Climate Change and Modelling. EDRI Research Report 21. Addis Ababa: Ethiopian Development Research Institute.

Girod, B. Wiek, A., Mieg, H., Hulme, M. 2009. The evolution of the IPCC's emission scenarios. Environmental Science & Policy 12, 103-118.

Gitas I Z, Douros K, Minakou C, Silleos G N, Karydas C G., 2009. Multi-Temporal Soil Erosion Risk Assessment Using Modified USLE Raster Model. Earsel proceedings 8: 1:40-52.

Gregory, K.J. and Walling, D.E. 1973. Drainage basin form and process. Edward Arnold, London.

Hellden, U., 1987. An Assessment of Woody Biomass, Community Forests, Land Use and Soil Erosion in Ethiopia, Lund University Press, Lund.

Hernández-Díaz L, Laprise R, Sushama L, Martynov A, Winger K, Dugas B. 2013. Climate simulation over CORDEX Africa domain using the fifth-generation Canadian Regional Climate Model (CRCM5). Clim. Dyn. 40: 1415–1433,

Houghton, P. D., and Charman, P. E.V. 1986. Glossary of Terms Used in Soil Conservation. Soil Conservation Service of New South Wales: Sydney.

Hudson and Smith D., 1978. Predicting Rainfall Erosion Losses: A Guide For conservation Planning-USDA Agricultural Hand book No 537, Washington, DC.

Hulme, M., Doherty, R., Ngara, T., New, M. and Lister, D. 2001. African climate change: 1990–2100. *Climate Res.* 17, 145–168.

Hurni H. 1985. Erosion - Productivity - Conservation Systems in Ethiopia. Proceedings 4th International Conference on Soil Conservation, Maracay, Venezuela pp. 654- 674.

Hurni, H. 1990. Degradation and conservation of soil resources in the Ethiopian highlands. Mountain Research and Development 8: 123-130.

Hurni, H. 1993. Land degradation, fine, and land resource scenarios in Ethiopia. In: Pimenta (edition.),

Hurni, H, Herweg K, Portner B, Liniger H. 2008. Soil Erosion and Conservation in Global Agriculture. In Land Use and Soil Resources. Springer, Dordrecht pp. 41-71.

IPCC, 1990a. Climate Change- The IPCC Scientific Assessment, Houghton, J.T., Jenkins, G.J., Ephraums, J.J. (eds.) Cambridge University Press, Cambridge, UK.

IPCC, 1990b. Emissions scenarios. Response Strategies Working Group (Ed.). IPCC.

IPCC, 2007. Climate Change- The Physical Science Basis. Contribution of Working Group I to the Fourth Assessment Report of the Intergovernmental Panel on Climate Change [Solomon, S., Qin, D., Manning, M. et al.(eds)] Contribution of Working Group I to the Fourth Assessment Report of the Intergovernmental Panel on Climate Change. Cambridge University Press, Cambridge, UK.

IPCC, 2013. Climate Change-The Physical Science Basis. Contribution of Working Group I to the Fifth Assessment Report of the Intergovernmental Panel on Climate Change [Stocker, T.F., D. Qin, G.-K. Plattner, M. Tignor, S.K. Allen, J. Boschung, A. Nauels, Y. Xia, V. Bex and P.M. Midgley (eds.)]. Cambridge University Press, Cambridge, United Kingdom and New York, USA, 1535 pp.

Jensen. J.R. 2000. Remote Sensing of the Environment: An Earth Resource Perspective Prentice Hall, New Jersey.Joshi VU, Nagare Land use change detection along the Pravara River Basin in Maharashtra, using Remote Sensing and GIS Techniques. AGD Landscape Environ 3:71–86.

Jones C, Giorgi F, Asrar G. 2011. The Coordinated Regional Downscaling Experiment: CORDEX An international downscaling link to CMIP5. CLIVAR Exchanges 16: 34–40.

Kaltenrieder J. 2007. Adaptation and Validation of the Universal Soil Loss Equation (USLE) for the Ethiopian Eritrean Highlands. MSc Thesis, University of Berne, Centre for Development and Environment Geographisches Institute.

Kariyeva, J.; Van Leeuwen, W., 2011. Environmental drivers of NDVI-based vegetation phenology in Central Asia. Remote Sens, 3, 203–246.

Karl, T.R., and R.W. Knight. 1998. Secular trends of precipitation amount, frequency, and intensity in the United States. Bulletin of the American Meteorological Society 79(2):231-241.

King C., Delpont G., 1993. Spatial Assessment of Erosion: Contribution of Remote Sensing. Remote Sensing Reviews 7: pp223– 232.

Knijjf, J.M. van der; Jones, R.J.A.; Montanarella, L, 1999. Soil erosion risk assessment in Italy. Brussels: European Commission. 58p.

Kouli, M., Soupios, P. and Vallianatos, F. 2009. Soil erosion prediction using the Revised Universal Soil Loss Equation (RUSLE) in a GIS framework, Chania, Northwestern Crete, Greece. *Environmental Geology* 57: 483-497.

Lakew D., Carucci, V., Asrat W. and Yitayew A., (eds). 2005. Community Based Participatory Watershed Development: A Guideline. Ministry of Agriculture and Rural Development, Addis Ababa, Ethiopia.

Lal, R. & Elliot, W. 1994: Erodibility and erosivity, In Lal, R. (ed.), *Soil Erosion research Methods*, St. Lucie Press, Delray Beach, Florida, pp 181-207.

Leggett J., Pepper W.J., Swart R.J. 1992. Emissions Scenarios for IPCC: an update. In Climate Change 1992. The Supplementary Report to the IPCC Scientific Assessment [Houghton, J.T., B.A. Callander & S.K. Varney, (eds)]. Cambridge University Press, Cambridge, UK. 69–95.

Lillesand T.M., and Kiefer, R.W., 2000. Remote Sensing and Image Interpretation. 4th ed. John Wiley and Sons Inc. New York.

Liu, J., Dietz, S., Carpenter, M., Alberti, C., Folke, E., Moran, A., Pell, P., Deadman, T., Kratz, J., Lubchenco, E., Ostrom, Z., Ouyang, W., Provencher, C., Redman, S., Schneider, H. and Taylor,W. 2007. Complexity of coupled human and natural systems. *Science* 317(5844):1513-1516.

López Vicente, M.; Navas, A. 2010. Routing runoff and soil particles in a distributed model with GIS: Implications for soil protection in mountain agricultural landscapes. Land Degrad. Dev., 21,100–109.

Mahmud Y., Alemu M., Menale K. and Pender J., 2005. Cost of Land degradation in Ethiopia: A Critical Review of Past Studies. Environmental Economics Policy Forum in Ethiopia, and International Food Policy Research Institute, Addis Ababa, Ethiopia.

Manrique, L. A., 1988. Land Erodibility Assessment Methodology, Manrique International Agro technology, Honolulu.

McBratney A.B., Santos M.L.M., Minasny B. 2003. On Digital Soil Mapping. Geoderma. (117), 3 – 52.

McCool D.K., Brown L.C. and Foster G.R., 1987. Revised Slope Steepness for the Universal Soil Loss Equation. *Trans. ASAE*.30: pp1387-1396.

McCool, D. K., G. R. Foster, K. G. Renard, D. C. Yoder, and G. A. Weesies. 1995. RUSLE: revised universal soil loss equation. Tecnologies to Address Soil Erosion on Department of Defense Lands San Antonio, TX.

McTainsh GH. 1971. Stream bank erosion, Banks Peninsula, New Zealand. Unpublished MA thesis (Geography), University of Canterbury, Christchurch, New Zealand.

Mellerowicz, K.T., Ress, H.W., Chow, T.L., and Ghanem, I., 1994. Soil conservation planning at the watershed level using the Universal Soil Loss Equation with GIS and microcomputer technologies: A case study. Journal of Soil and Water Conservation 49: 194-200.

Merritt W.S., Letcher R.A., and Jakemna A.J., 2003. A Review of Erosion and Sediment Transport Models. Environmental Modeling and Software 2003; 18(8-9): 761-799.

Michael, A.; Schmidt, J.; Enke, W.; Deutschlander, T., Maltiz, G. 2005. Impact of expected increase in Precipitation intensities on soil loss results of comparative model simulations. Catena, 61,155–64.

Mitasova, H., and Mitas, Z. 1999. Modeling soil detachment with RUSLE 3D using GIS. IL, USA: University of Illinois at Urbana –Champaign.

Moore, D., & Wilson, J. P. 1992. Length–slope factors for the revised universal soil loss equation: simplified method of estimation. Journal of Soil and Water Conservation, 47(5), 423–428.

Moore, I. D., & Burch, G. J. 1986a. Physical basis of the length-slope factor in the universal soil loss equation. Soil Science Society of America Journal, 50(5), 1294–1298.

Moore, I. D., & Burch, G. J. (1986b). Modeling erosion and deposition: topographic effects. Transactions of the Asae, 26, 1624–1630.

Morgan, R.P.C. 1995: Soil Erosion and Conservation, second edition, Longman Group Limited, London.

Morgan, R.P.C., 2005. Soil Erosion and Conservation, third ed. Blackwell Science Ltd., 304ISBN: 1-4051-1781-8.

Moss, R. H., et al. (2010). The next generation of scenarios for climate change research and assessment. Nature, 463, 747–756.

Mpelasoka, F.S., Chiew, F.H.S., 2009. Influence of rainfall scenario construction methods on runoff projections. J. Hydrometeorol. 10, 1168–1183

Ministry of Water Resources (MoWR). 1996. Integrated Development of Omo-Gibe River Basin Master Plan Study, vol. 11 (F1, F2, F3, Addis Ababa, Ethiopia).

Mullan, D.; Favis-Mortlock, D.T.; Fealy, R. 2012. Addressing key limitations associated with modelling soil erosion under the impacts of future climate change. Agriculture Forest. Meteo, 156, 18–30.

Murphy, B. W., and Flewin, T. C. 1993. Rill erosion on a structurally degraded sandy loam surface soil. Australian Journal of Soil Research 31, 419–436.

Musgrave G W.1947. The quantitative evaluation of factors in water erosion. A first approximation. Journal Soil and Water Cons, 2:133-138.

Nakicenovic, N., Swart R. 2000. IPCC Special Report on Emissions Scenarios, 599 pp., Cambridge Univ. Press, New York.

Nearing M.A., Lane L.J. and Lopes V.L., 1984. Modeling Soil Erosion. In: R. Lal (ed.); Soil Erosion Research (2nd edition). *Soil and Rainfall Conservation Society*, St. Lucie press pp 127-156

Nearing, A.M. 2001. Potential changes in rainfall erosivity in the U.S. with climate change during the 21st century. J. Soil Water Conservation, 56, 229–232.

Nearing, M.A., Pruski, F.F., and O'Neal M.R. (2004). "Expected climate change impacts on soil erosion rates: A review," Journal of Soil and Water Conservation. 59(1):43-50.

Nearing, M.A., V. Jetten, C. Baffaut, O. Cerdan, A. Couturier, M. Hernandez, Y. Le Bissonnais, M.H. Nichols, J.P. Nunes, C.S. Renschler, V. Souchere, and K. van Oost, 2005. Modeling response of soil erosion and runoff to changes in precipitation and cover. Catena 61(2-3):131-154.

Nikulin G, Jones C, Giorgi F, Asrar G, Büchner M, Cerezo-Mota R, Christensen OB, Déqué M, Fernandez J, Hänsler A, van Meijgaard E, Samuelsson P, Sylla MB, Sushama L. 2012. Precipitation climatology in an ensemble of CORDEX-Africa regional climate simulations. J.Clim. 25: 6057–6078, DOI: 10.1175/JCLI-D-11-00375.1.

Oldeman, L., Hakkeling, R., Sombroek, W., 1990. World map of the status of soil degradation, an explanatory note. International soil reference and information center, Wageningen. The Netherlands and the United Nations Environmental Program, Nairobi, Kenya.

Oldeman LR, 1994. The global extent of land degradation. In: Greenland DJ, Szabolcs I (eds) Land resilience and sustainable land use. CAB International, Wallingford UK, pp 99–118.

Perez-Rodriguez, R., Marques, M.J. and Bienes, R. 2007. Spatial Variability of the Soil Erodibility Parameters and Their Relation with the Soil Map at Subgroup Level. Science of the Total Environment, 378, 166-173.

Petter, P. 1992. GIS and Remote Sensing for Soil Erosion Studies in Semi-arid Environments. PhD Thesis. University of Lund, Sweden.

Pettorelli, N.; Vik, J.O.; Mysterud, A.; Gaillard, J.M.; Tucker, C.J.; Stenseth, N.C. 2005. Using the satellite-derived NDVI to assess ecological responses to environmental change. Trends Ecol. Evol., 20, 503–510.

Philander S. G. 2008. Encyclopedia of Global Warming and Climate Change, Vol. 1-3. SAGE Publications, California

Piccolo, A., Pietramellara, G., Mbagwu, J.S.C. 1996. Use of Humic Substances as Soil Conditioners to Increase Aggregate Stability. Geoderma, 75, 267–277.

Prasannakumar, V., Vijith, H., Abinod, S., Geetha, N. 2012. Estimation of soil erosion risk within a small mountainous sub- watershed in Kerala, India, using Revised Universal Soil Loss Equation (RUSLE) and geo-information technology. Geosci Front 3(2):209–215.

Pruski, F.F., Nearing, M.A. 2002. Climate-induced changes in erosion during the 21st century for eight U.S. locations. Water Resources. Res, 38, 34–44.

Raes, D., Willems, P. and G Baguidi, F. 2006. RAINBOW – a software package for analyzing data and testing the homogeneity of historical data sets. Proceedings of the 4th International Workshop on 'Sustainable management of marginal dry lands'. Islamabad, Pakistan, 27-31 January. (In press).

Raymond, D.J. 2017. Convection in Pacific Inter tropical convergence zone (ITCZ). Geophysical research letter 44: 1,562-568.

Reed, B.C., White, M., Brown, J.F. 2003. Remote Sensing Phenology. In Phenology: An Integrative Environmental Science; Schwartz, M.D., Ed.; Kluwer Academic Publishers: Dordrecht, The Netherlands, pp. 365–380.

Renard KG, Foster GR.1983. Soil conservation: principles of erosion by water. In: Degne HE and Willis WO (Eds.) Dry land Agriculture, Agronomy Monogr. 23, American Soc., Crop Sci. Soc. Am., and Soil Sci. Am Madison, Wisconsin,156-176.

Renard, K.G., Foster, G.R., Weesies, G.A., Porter, J.P., 1991. RUSLE: revised universal soil loss equation. Journal of soil Water Conservation. 46 (1) 30–33.

Renard, K.G.; Fremund, J.R. 1994. Using monthly precipitation data to estimate the R-factor in the revised USLE. *Journal of Hydrology, 157,* 287–306.

Renard, K.G., Foster, G.R., Weesies, G.A., McCool, D.K. and Yoder, D.C. 1996. Predicting Soil Erosion by Water: A Guide to Conservation Planning with the Revised Universal Soil Loss Equation (RUSLE). USDA, Washington, DC.

Renard, K. G., Foster, G. R., Weesies, G. A., McCool, D. K., and Yoder, D. C., 1997. Predicting soil erosion by water: A guide to conservation planning with the Revised Universal Soil Loss equation, Agriculture Handbook No. 703, U.S. Department of Agriculture, Washington, D.C., USA.

Renard, K.G.; Fremund, J.R. 1994**.** Using monthly precipitation data to estimate the R-factor in the revised USLE. Journal of Hydrology, 157, 287–306.

Renschler C., 1996. Soil Erosion Risk Mapping by Means of Geographical Information Systems (GIS) and Hydrologic Modeling. MSc Thesis, Technical University of Braunschweig.

Reusing, M., Schneider, T. and Ammer, U. 2000. Modeling soil loss rates in the Ethiopian highlands by integration of high resolution MOMS-02/D2-stereo data in a GIS. *Remote Sensing* 21(9):1885–1896.

Riahi K., Gruebler A., Nakicenovic N. 2007. Scenarios of long-term socio-economic and environmental development under climate stabilization. In: Technological Forecasting and Social Change 74, 7, 887-935.

Richard Jones, David Hassell, Debbie Hudson, Simon Wilson, and Mitchell, Geoff Jenkins and John. 2003. Workbook on generating high resolution climate change scenarios using PRECIS: Hadley Centre for Climate Prediction and Research, Met Office UK.

Rosewell, C. J., Crouch, R. J, Morse, R. J., Leys, J. F., Hicks, R. W., and Stanley, R. J. 2007. Forms of Erosion. In 'Soils- their properties and management'. 3rd edn. (Eds P. E. V. Charman and B. W. Murphy.) pp. 14–40. (Oxford University Press: Melbourne.)

Rouse, J. W., R. H. Haas, J. A. Schell, and D. W. Deering. 1974. Monitoring vegetation systems in the Great Plains with ERTS, Third ERTS Symposium, NASA SP-351 I, 309- 317.

Samal, N. R., W. Wollheim, S. Zuidema, R. Stewart, Z. Zhou, M.M. Mineau, M. Borsuk, K. H. Gardner, S. Glidden, T. Huang, D. Lutz, G. Mavrommati, A. M. Thorn, C. P. Wake, and Huber, M. 2017. A coupled terrestrial and aquatic bio-geophysical model of the Upper Merrimack River watershed, New Hampshire, to inform ecosystem services evaluation and management under climate and land-cover change. Ecology and Society 22(4):18. https://doi.org/10.5751/ES-09662-220418.

Schwartz, P. 1991. The art of the long view: planning for the future in an uncertain world. First edition. Doubleday, New York, NewYork, USA.

Sertu, S. 2000. Degraded Soil of Ethiopia and their management. Proceeding of FAO/ISCW expert consultation on management of degraded soils in Southern and East Africa. 2nd network meeting, 18-22 September 2000. Pretoria.

Shirazi, M. A. and L. Boersma. 1984. A unifying quantitative analysis of soil texture. Soil Science Society of America Journal 48:142-147.

Sluiter, R. 2009. Interpolation methods for climate data - Literature review: KNMI, R&D Information and Observation Technology De Bilt, (Version1.0).

Smith, J.L., Halvorson, J.J. and Papendick, R.I. 1993. Using Multiple-Variable Indicator Kriging for Evaluating Soil Quality. Soil Science Society of America Journal, 57, 743-749.

Sonneveld, B.G.JS. 2002. Land under Pressure: The Impact of Water Erosion on Food Production in Ethiopia. Shaker Publishing, Maastricht, the Netherlands.

South Omo Zone Department of Agriculture and Natural Resources (SOZDARN). 2017. Annual Report. Amharic (National language) version. Jinka, South Omo, Ethiopia.

South Omo Zone Department of Water and Irrigation development (SOZDWID). 2017. Irrigation development growth and transformation plan (GTP-II) Amharic (National language) version. Jinka, South Omo zone, Ethiopia.

Stern, R., Benhur, M., Shainberg, I. 1991. Clay Mineralogy Effect on Rain Infiltration, Seal Formation and Soil Losses. Soil Sci. 1991, 152, 455–462.

Stocking, M.A. 1986. The cost of soil erosion in Zimbabwe in terms of loss of three major nutrients. FAO Consultants Working Paper 3, AGLS, Rome.

Stone D. and Knutti, R. 2011. Weather and climate. In Modelling. The Impact of Climate Change on Water Resources. Fung, F., Lopez, A., and Mark New, (Eds). Blackwell Publishing.

SWCS. 2003. Conservation implications of climate change: Soil erosion and runoff from cropland. A report from the Soil and Water Conservation Society. Soil and Water Conservation Society, Ankeny, IA.

Tamene, L. 2005. Reservoir siltation in the dry lands of Northern Ethiopia: causes, Source areas, management option. PhD. Thesis, University of Bonn, Germany.

Tamene, L., and Vlek, P.L.G. 2006. Analysis of factors determining sediment yield variability in the highlands of Ethiopia. Geomorpology.76, 76-91.

Tamirie, H. 1975. Chemical and Physical Properties of Major Soils in Alemaya Woreda, Eastern Ethiopia. Agrokemiaest Alajtan Tom, 24, 183–186.

Tegegn, M. and Biniam, S. 2017. Estimating soil erosion risk and evaluating erosion control measures for soil conservation planning at Koga watershed in the highlands of Ethiopia. Solid Earth 8:13-25.

Thorn, A., Wake, C., Grimm, C., Mitchell, M., Mineau, M. and Ollinger, S. 2017. Development of scenarios for land cover, population density, impervious cover, and conservation in New Hampshire, 2010–2100. *Ecology and Society* 22(4):19. https://doi.org/10.5751/ES-09733-220419

Tilahun A., Takele, B. and Endrias, G., 2001. Reversing the Degradation of Arable Land in Ethiopian Highlands. Managing African Soils No. 23. London: IIED.

Toy, T.J., G.R. Foster, and K.G. Renard. 1999, RUSLE for mining, construction and reclamation lands: Journal of Soil and Water Conservation v. 54, no. 2, p. 462-467.

Tweddales S C, Eschlaeger C. R., Seybold W. F., 2000. An Improved Method for Spatial Extrapolation of Vegetative Cover Estimates ((R)USLE C factor) using LCTA and Remotely Sensed Imagery.

United States Department of Agriculture (USDA). 2003. EPIC-Erosion Productivity Impact Calculator-Model Documentation. Technical Bulletin, vol. 1768. Agricultural Research Service, USA.

United States Geological Survey Metadata (USGS). 2017. Metadata. Retrieved from Earth Explore **http://earthexplorerusgs.gov/**metadata/10880/1174275/

Vaezi, A.R., Bahrami, H.A., Sadeghi, S.H.R. and Mahdian, M.H. 2010. Spatial Variability of Soil Erodibility Factor (K) of the USLE in North West of Iran. Journal of Agricultural Science and Technology, 12, 241-252.

Van der Knijff, J., Jones, R., Montanarella, L. 2000. Soil erosion risk assessment in Europe. EUR 19044 EN. Office for Official Publications of the European Communities, Luxembourg.

Van der Knijff, M., Jones R.J.A., Montanarella L. 1999. Soil erosion risk in Italy. EUR19022 EN. Office for Official Publications of the European Communities, Luxembourg.

Van Leeuwen, W.J.D., Sammons, G. 2004. Vegetation dynamics and soil erosion modeling using remotely sensed data (MODIS) and GIS. Tenth Biennial USDA Forest Service Remote Sensing Applications Conference, 5–9 April 2004, Salt Lake City, UT. US Department of Agriculture Forest Service Remote Sensing Applications Center, Salt Lake City.

Van Vuuren D.P., Edmonds J., Thomson A., Riahi K., Kainuma M., Matsui T., Hurtt G.C., Lamarque J-F., Meinshausen M., Smith S. 2011. Representative concentration pathways: an overview. In: Climatic Change, 109, 5-31.

Víctor, H., Durán, Z., Carmen, R. and Rodríguez, P. 2008. Soil-erosion and runoff prevention by plant covers. A review. Agronomy for Sustainable Development, Springer Verlag/EDP Sciences/INRA, 28 (1), pp.65-86.

Vicente M L, Navas A, Machin J. 2007. Identifying erosive periods by using RUSLE factors in mountain fields of the Central Spanish Pyrenees. Hydrol. Earth Syst. Sci. Discuss., (4): 2111-2142.

Verbyla, D. 2013. Estimating Classification Accuracy Using ArcGIS. Retrieved February 2019, from https://www.youtube.com/watch?v=9dGjuEQie7Y&t=2s..

Vrieling, A. 2006. Satellite remote sensing for water erosion assessment: A review. *Catena, 65*, 2–18.

Wang, G., Gertner, G., Liu, X. and Anderson, A. 2001. Uncertainty Assessment of Soil Erodibility Factor for Revised Universal Soil Loss Equation. Catena, 46, 1-14.

Wang. X. & Yin, Z. Y. 1998. A comparison of drainage networks derived from digital elevation models at two scales. SHE hydrologica modelling system. J.Hydrology, 175, 213-238.

Wilby, R.L. and Dawson, C.W. 2007. SDSM:A decision support tool for the assessment of regional climate change impacts. Environmental Modeling Software, 17, 145-157.

Wischmeier, W.H.; Smith, D.D. 1958. Rainfall energy and its relationship to soil loss. Trans. American .Geophysics. Union. , (39), 285–291.

Wischmeier W.H., Johnson C.B. and Cross B.V., 1971. A Soil Erodibility Nomograph for Farm Land and Construction Sites. J. Soil and Water Conserv. 26: pp.189- 193.

Wischmeier W.H. and Smith D.D. 1978. Predicting Rainfall Erosion Losses: A Guide For Conservation Planning-USDA Agricultural Hand book No 537, Washington, DC.

Woldeamlak, B., Teferi, E. 2009. Assessment of soil erosion hazard and prioritization for treatment at the watershed level: Case study in the Chemoga watershed, Blue Nile basin, Ethiopia. Land. Degrad .Dev. 20, 609–622.

Woody Biomass Inventory and Strategic Planning Project (WBISPP). 2001. Southern Nations Nationalities and People's Regional State: A strategic plan for the sustainable development, conservation, and management of the woody biomass resources. Addis Ababa, Ethiopia.

Xie, Y., Shui-qing Y., Bao-yuan L., Mark A. and Nearing Ying Z. 2016. Models for estimating daily rainfall erosivity in China. Journal of Hydrology 535, 547–558.

Yang, D.; Kanae, S.; Oki, T.; Koike, T.; Musiake, K.2003. Global potential soil erosion with reference to land use and climate changes. Hydrology. Process, 17, 2913–2928.

Zemenu D., and Minale, A.S. 2014. Adoption of soil conservation practices in North Achefer District, Northwest Ethiopia. Chinese Journal of population Resources and Environment, 12.

Zhang, X.C. 2007. A comparison of explicit and implicit spatial downscaling of GCM output for soil erosion and crop production assessments. *Climate Change, 84*, 337–363.

Zhang, X.C., Nearing, M.A. 2005. Impact of climate change on soil erosion, runoff and wheat Productivity in central Oklahoma. Catena, 61, 185–195.

Zhang, Y., Hernandez, M., Anson, E., Nearing, M.A., Wei, H., Stone, J.J. and Heilman, P. 2012. Modeling climate change effects on runoff and soil erosion in Southeastern Arizona rangelands and implications for mitigation with conservation practices, Journal of Soil and Water Conservation 67(5):390-405.

Zorita, E. and Von Storch, H. 1999. The analog method as a simple statistical downscaling technique: comparison with more complicated methods. Journal of Climate 12(8), 2474-2489.

APPENDICES

Appendix 1: Climatic data analysis

Table 1:- Mean Monthly and Annual Rainfall (mm) by stations (1988 - 2017)

Months	Jan	Feb	Mar	Apr	May	Jun	Jul	Aug	Sep	Oct	Nov	Dec	Annual av.g
Jinka	51.06	46.96	117.31	182.23	155.89	107.31	101.42	93.42	118.23	172.97	120.92	74.30	**1342.02**
Bulki	52.16	38.79	161.65	232.09	173.88	132.71	152.93	163.66	146.06	176.12	114.04	70.70	**1614.79**
Sawla	49.71	27.38	129.49	204.66	168.06	109.92	109.73	120.52	124.21	150.68	87.44	50.49	**1332.29**
Keyafer	55.64	37.70	137.49	197.19	150.90	82.13	90.74	96.50	105.79	150.68	110.45	79.31	**1294.52**

Table 2. Computed Mean monthly Temperatures of meteorological stations

Source: National Meteorological Agency (2018)

Station	Variable	Jan	Feb	Mar	Apr	May	Jun	Jul	Aug	Sep	Oct	Nov	Dec
	T_max(^{0C})	29.29	30.31	29.65	27.89	26.70	26.26	25.65	26.23	27.20	26.84	27.23	28.13
Jinka	T_min(^{0C})	14.97	16.07	17.10	17.39	17.29	16.67	16.25	16.46	16.72	16.73	15.40	14.56
	T_Avg(^{0C})	22.13	23.19	23.38	22.64	22.00	21.46	20.95	21.34	21.96	21.78	21.31	21.34
Bulkimender	T_max(^{0C})	22.13	23.58	22.91	21.76	21.44	20.55	19.45	19.62	20.46	21.00	21.88	22.27
	T_min(^{0C})	11.05	11.50	11.57	11.37	11.36	11.00	10.74	10.75	10.88	10.97	10.69	10.65
	T_Avg(^{0C})	16.59	17.54	17.24	16.57	16.40	15.78	15.10	15.18	15.67	15.98	16.28	16.46
Sawla	T_max(^{0C})	31.99	33.06	32.08	29.95	29.04	28.05	26.99	27.38	28.67	29.06	30.06	30.84

Table:-3 Observed precipitation data homogeneity test of four stations before use (Rainbow software)

Probability Of Exceedance (%)	Magnitude Event (mm) by stations				Return period (year)
	Jinka	**Bulkimender**	**Sawla**	**Keyafer**	
10	1623.088	1927.3843	1485.6	1637.9	10.00
20	1526.546	1822.2098	132.9	1520.0	5.00
30	1456.935	1746.3746	1395.0	1434.9	3.33
40	1397.495	1681.6203	1362	1362.3	2.50
50	1342.033	1621.1983	1362.5	1294.5	2.0
60	1286.570	1560.7763	1332.3	1226.7	1.67
70	1227.131	1496.0220	1269.6	1154.1	1.43
80	1157.520	1420.1867	1231.7	1069.1	1.25
90	1060.978	1315.0123	1179.0	951.1	1.11
Mean (μ)	μ=1342.033	μ=1616.59	μ=1332.3	μ=1294.5	
Stdev (σ)	σ =219.278	σ=238.8852	σ =119.6	σ=267.9	
Performance Evaluation	R2 =0.98 (K-S): 0.0757	R2 =0.95 (K-S) : 0.1804	R2 =0.96 (K-S) :0.0548	R2 =0.98 (K-S) : 0.0771	

Table 4:- Percentage frequency distribution changes of total rainy days and erosive events between baseline and projected 2030s (2021-2050), 2060s (2051-2080).

PCP (mm) intervals	Percent days/total						
	Baseline period	$RCP_{2.6}$		$RCP_{4.5}$		$RCP_{8.5}$	
	1988-2017	2021–2050	2051-2080	2021-2050	2051-2080	2021-2050	2051-2080
<1mm/day	65.08%	66.20%	70.93%	68.28%	64.90%	67.79%	63.92%
1-9.7 mm/day	23.37%	19.61%	18.8%	20.5%	19.9%	18.9%	20.200%
>9.7 mm/day	11.55%	14.18%	10.2%	14.2%	15.2%	13.3%	15.880%
Rainy days sum	34.92%	33.8%	29.1%	34.7%	35.1%	32.2%	36.080%

Table: Bias corrected precipitation data for RCP scenarios per meteorological stations associated Grid points (GP)

A) RCP26/2021

Month	BC_P_J_RCP26_2021/50	BC_P_{Bulki}_RCP26_2021	BC_P_{Sawl}_RCP26_2021/50	BC_$P_K$eyafer_RCP26_2021
Jan	51.12	53.30	51.25	58.63
Feb	48.45	43.83	29.24	35.16
Mar	120.22	166.87	131.41	135.57
Apr	181.71	231.34	209.80	210.88
May	152.48	170.26	163.60	165.75

Jun	108.06	129.69	107.33	83.78
Jul	106.15	151.39	109.36	100.26
Aug	92.86	159.79	117.59	81.52
Sep	122.71	143.42	123.61	104.92
Oct	175.89	179.18	152.12	158.80
Nov	121.58	119.02	93.60	115.27
Dec	71.56	72.29	49.47	88.10
	1352.79	**1620.36**	**1338.39**	**1338.64**

N.B.

(BC_P_J_RCP_{26}_2021/50):- stands for (Bias corrected) PJ (rainfall in Jinka (geographic coordinate) in $RCP_{2.6}$ for near term future. Likewise, the subscript letters (J, B, S and) are for four meteorological stations.

Month	BC_P_J_RCP26_2051/80	BC_P_{Bulki}_RCP26_2051/80	BC_P_{sala}_RCP26_2051/80	BC_$P_{keyafer}$_RCP26_2051/80
Jan	53.77	71.23	50.31	1.32
Feb	53.28	66.86	28.54	5.24
Mar	115.81	153.47	127.84	20.43
Apr	186.78	282.75	211.06	212.34
May	150.97	132.36	164.26	433.23
Jun	101.75	66.78	103.86	138.01
Jul	101.81	144.46	108.87	72.74

Aug	82.56	95.25	115.08	11.83
Sep	117.14	151.38	124.14	47.10
Oct	178.54	198.27	150.46	164.67
Nov	146.10	169.68	93.07	100.30
Dec	63.95	45.21	49.12	2.45
	1352.47	1577.70	1326.62	1209.67

RCP45/2021

Month	BC_Pj_RCP45_2021	BC_Pb_RCP45_2021	BC_Ps_RCP45_2021	BC_Pk_RCP45_2021
Jan	54.71	56.83	57.97	55.32
Feb	61.98	41.40	30.17	38.64
Mar	119.69	164.12	129.97	141.02
Apr	190.05	235.79	211.67	201.26
May	150.98	169.53	165.14	147.82
Jun	101.92	130.68	104.11	80.24
Jul	104.98	152.79	109.66	90.78
Aug	90.77	160.23	119.17	93.75
Sep	127.00	147.55	126.89	107.59
Oct	176.68	181.40	149.39	156.58
Nov	143.59	119.67	91.96	115.58

Dec	74.17	68.58	50.07	77.32
	1396.52	1628.57	1346.19	1305.90

RCP45/2051

Month	BC Pj_RCP45_2051	BC_Pb_RCP45_2051	P003_RCP45_2051	BC_Pk__RCP45_2051
Jan	73.76	46.04	53.36	60.78
Feb	48.65	39.93	27.78	39.34
Mar	113.18	162.24	127.57	143.52
Apr	183.15	235.26	207.62	211.67
May	148.17	175.89	161.46	156.22
Jun	101.92	131.98	104.37	84.72
Jul	102.85	152.46	109.24	97.24
Aug	86.96	160.61	117.36	98.68
Sep	118.24	146.14	123.43	112.78
Oct	184.12	172.13	152.78	165.42
Nov	153.04	111.65	95.94	126.52
Dec	75.03	68.82	50.89	85.66
	1389.06	1603.16	1331.81	1382.57

Month	BC_Pb_RCP85_2021	BC_Pb_RCP85_2010	BC_PS_RCP85_2010	PB_Pk_RCP85_2010
Jan	54.20	52.93	50.04	54.22
Feb	49.92	40.00	28.14	37.94
Mar	118.62	161.39	129.27	138.48
Apr	178.41	230.69	204.78	194.87
May	151.81	169.43	163.56	146.40
Jun	101.22	126.65	103.95	77.46
Jul	103.54	152.69	108.81	91.93
Aug	90.10	161.70	118.01	95.46
Sep	121.74	148.72	124.31	109.54
Oct	173.13	174.35	147.26	151.64
Nov	144.13	119.22	93.34	115.32
Dec	62.00	68.23	48.94	76.86
	1348.82	1606.00	1320.42	1290.12

	JINKA	BULKI	SAWLA	KEYAFER
Month	p001_RCP85_2051	P002_RCP85_2051	P003_RCP85_2051	P004_RCP85_2051
Jan	107.15	66.25	56.30	5.36
Feb	42.33	40.29	27.95	5.99

Mar	133.94	160.26	126.88	16.75
Apr	199.24	234.17	206.83	189.65
May	143.42	169.21	161.77	319.95
Jun	74.74	126.11	102.12	91.54
Jul	93.87	154.19	108.85	88.49
Aug	93.81	162.85	118.81	61.98
Sep	108.48	150.14	123.46	67.62
Oct	162.63	183.14	152.60	227.36
Nov	173.60	126.51	99.60	191.53
Dec	78.60	69.60	49.47	21.48
	1411.81	1642.72	1334.65	1287.71

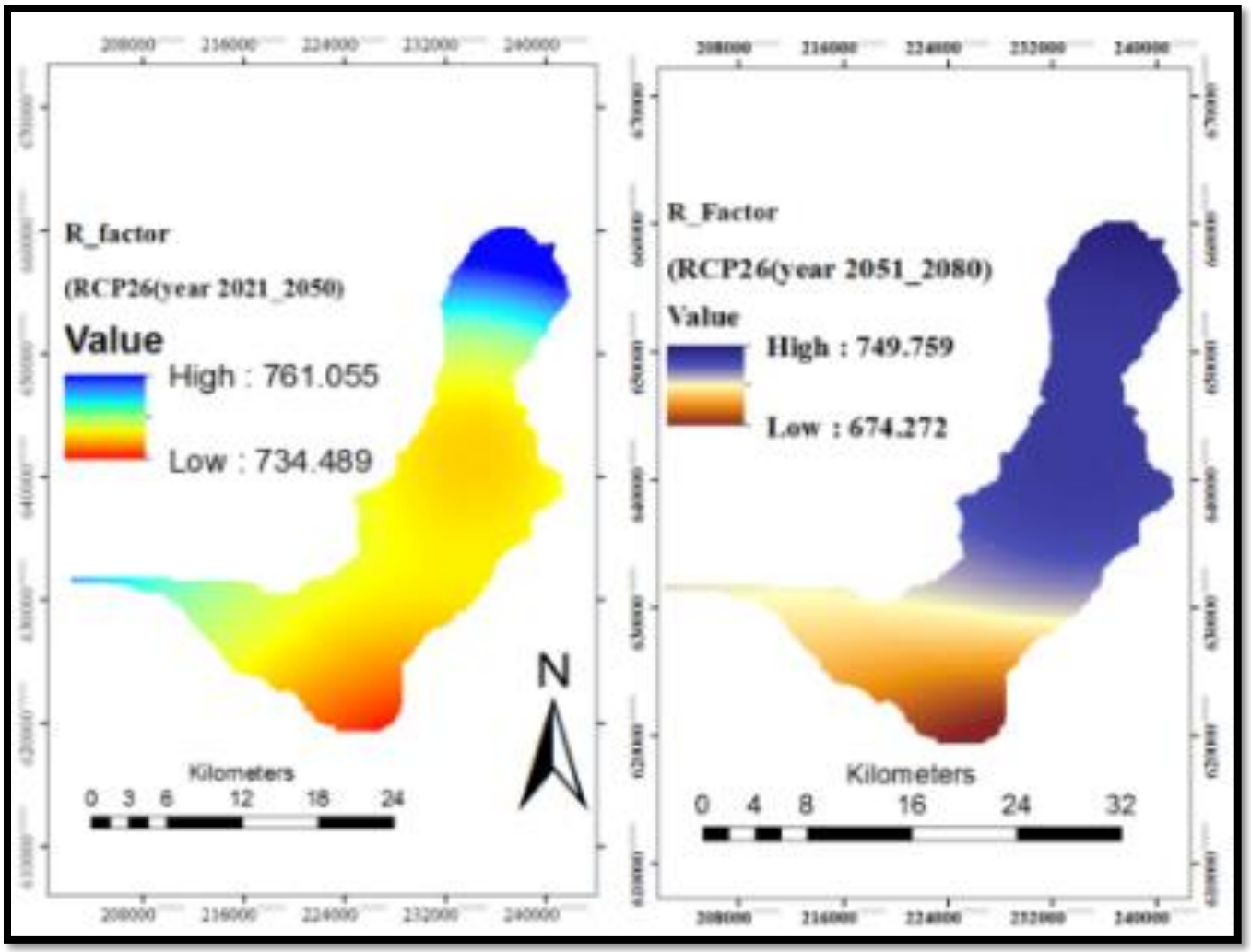
R_factor
(RCP26(year 2021_2050)
Value
High : 761.055
Low : 734.489
N
Kilometers
0 3 6 12 18 24
R_Factor
(RCP26(year 2051_2080)
Value
High : 749.759
Low : 674.272
Kilometers
0 4 8 16 24 32

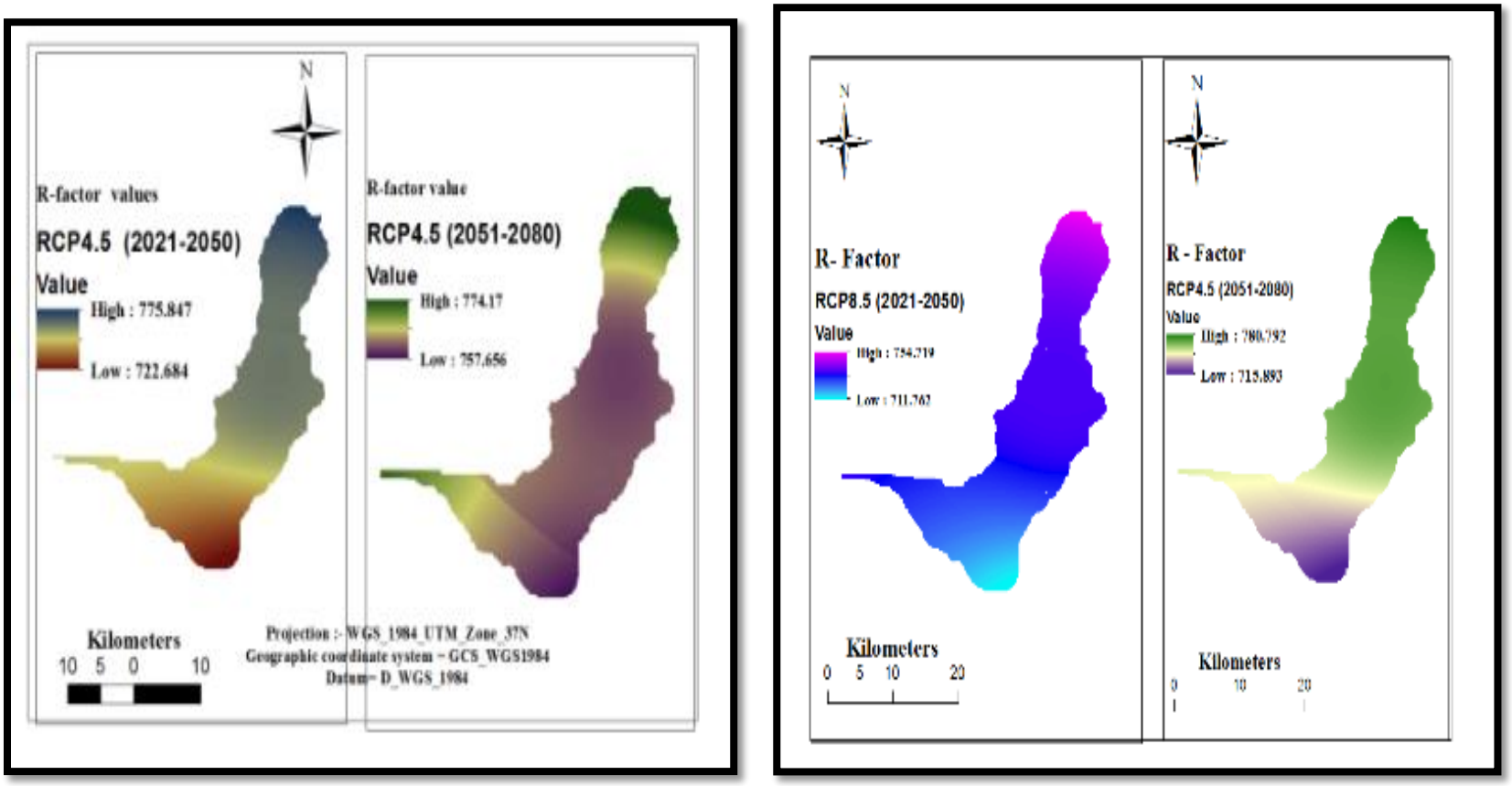

Figure 1:- R_Factor maps for Three RCP scenarios over two future time periods

Appendix 2: Soil data analysis

Table 1:- Computation of soil erodibility (K-Value) computation for each soil samples

No.	**X** (meter)	**Y** (meter)	**sand**	**silt**	**clay**	**Dg**	**Log $_{Dg}$**	**K_value (Mgh/(MJ*mm)**
1	211977.76	630500.90	44%	33%	23%	0.06	-1.21	0.036517422
2	239704.60	641556.23	51%	22%	27%	0.07	-1.15	0.034831206
3	230859.62	632822.00	24%	27%	49%	0.01	-1.90	0.041722462
4	222997.21	622417.21	45%	31%	24%	0.06	-1.21	0.036463852
5	238718.92	657129.15	39%	29%	32%	0.04	-1.42	0.041592456
6	241194.76	654818.30	52%	27%	21%	0.09	-1.05	0.031522117
7	240194.76	655818.30	51%	27%	22%	0.08	-1.08	0.032533157
8	228890.90	638926.78	20%	33%	47%	0.01	-1.93	0.041042294
9	228669.70	639027.31	36%	12%	52%	0.02	-1.75	0.04360045
10	234221.50	641658.99	22%	12%	66%	0.01	-2.17	0.034733942
11	229319.08	640573.52	28%	16%	56%	0.01	-1.93	0.041048633
12	229336.48	639467.01	32%	4%	64%	0.01	-1.98	0.039972227
13	223480.40	626456.81	42%	34%	24%	0.06	-1.25	0.037836761
14	222886.41	632162.06	43%	29%	28%	0.05	-1.30	0.038920016
15	221775.15	625653.30	50%	30%	20%	0.09	-1.07	0.032120618

16	231299.18	631935.02	57%	19%	24%	0.10	-1.02	0.030249722
17	234845.60	657734.09	57%	14%	29%	0.08	-1.09	0.032643069
18	238443.94	656569.92	42%	25%	33%	0.04	-1.38	0.040933132
19	226996.48	636489.72	50%	28%	22%	0.08	-1.10	0.033062059
20	237543.00	641394.00	22%	32%	46%	0.01	-1.88	0.04190794
21	236281.05	641059.60	25%	27%	48%	0.01	-1.87	0.042232255
22	234042.00	636236.00	26%	21%	43%	0.02	-1.62	0.043844865
23	234047.00	635986.00	25%	27%	48%	0.01	-1.87	0.042232255
24	234374.00	635648.00	26%	30%	45%	0.02	-1.82	0.042843303
25	232791.00	632668.00	30%	23%	47%	0.02	-1.77	0.043401979
26	232807.00	632780.00	29%	25%	46%	0.02	-1.77	0.043385742
27	233290.00	633449.00	25%	27%	48%	0.01	-1.87	0.042232255
28	233455.00	633640.00	25%	30%	45%	0.02	-1.82	0.042841929
29	234196.00	633841.00	28%	27%	45%	0.02	-1.77	0.043369252
30	234268.70	651698.00	26%	24%	40%	0.03	-1.58	0.04364056
31	228048.00	636888.00	24%	32%	44%	0.01	-1.82	0.042818643
32	229245.00	638110.00	23%	33%	44%	0.01	-1.84	0.042602663
33	234121.50	641558.99	16%	25%	59%	0.01	-2.16	0.034838218
34	221675.15	625553.30	13%	25%	62%	0.01	-2.25	0.031885124
35	228777.70	639127.31	27%	44%	29%	0.03	-1.56	0.043548725

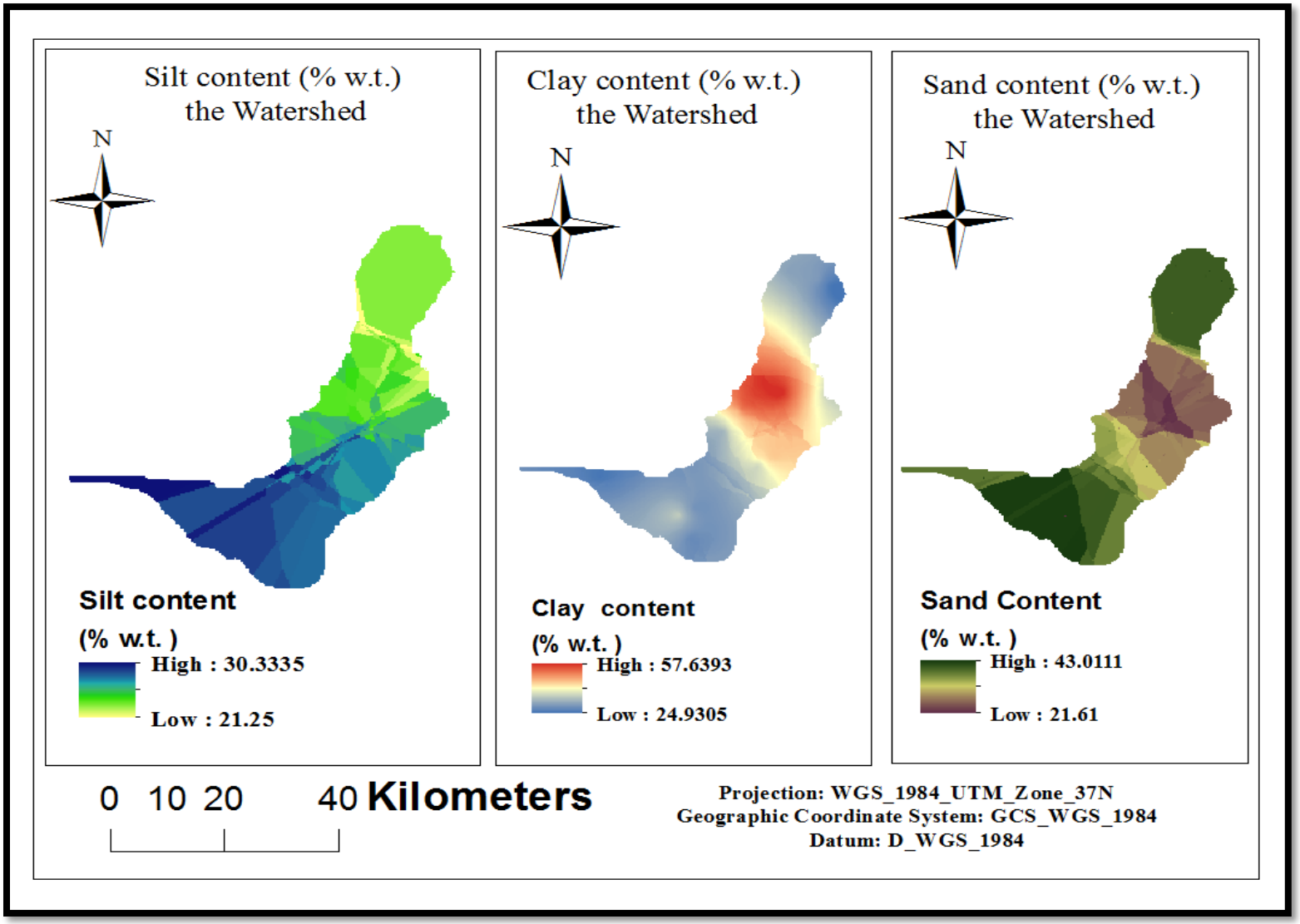
Silt content (% w.t.)
the Watershed
N
Silt content
(% w.t.)
High : 30.3335
Low : 21.25
Clay content (% w.t.)
the Watershed
N
Clay content
(% w.t.)
High : 57.6393
Low : 24.9305
Sand content (% w.t.)
the Watershed
N
Sand Content
(% w.t.)
High : 43.0111
Low : 21.61
0 10 20 40 Kilometers
Projection: WGS_1984_UTM_Zone_37N
Geographic Coordinate System: GCS_WGS_1984
Datum: D_WGS_1984

Appendix 3: Land use land cover and management practices data

3.1. Tables

Table1: Classification Accuracy Matrix

Classified	REFERENCE_1	REFERENCE_2	REFERENCE_3	REFERENCE_4	REFERENCE_5	REFERENCE_6
1	**21**	0	1	0	1	0
2	0	**15**	0	0	1	1
3	0	0	**26**	0	2	0
4	0	1	0	**21**	0	1
5	0	0	1	1	**35**	2
6	0	1	0	0	0	**16**

Classes	**Reference Total**	**Classified total**	**Number of correct**	**Producer's accuracy (%)**	**User's accuracy (%)**
FRST	**21**	23	21	100%	91%
GRSS	17	17	15	88%	88%
SHRUB	28	28	26	93%	93%
BLTP	22	23	21	95%	91%
AGR	39	39	35	90%	90%
BARE	20	18	16	80%	89%
Total	**147**	**147**	**134**		

Over all accuracy of = 91%

Kappa statistic = 0.904

Table 2: - Ground Truth data

Easting	Northings	Land C
234042	636236	FRST
232791	632668	FRST
229245	637502	FRST
223557.3	627392.1	FRST
228901.9	626651.3	FRST
216836.9	629350.1	FRST
232923.6	637287.6	FRST
233048.3	655223.4	FRST
232382.1	638472.8	FRST
232591.7	638038.9	FRST
233331.6	637765.9	FRST
238378.6	637282.7	FRST
230450.5	639303.8	FRST
230810.3	639528.7	FRST
233009.8	640633.8	FRST
232791	632668	FRST
229245	637502	FRST
232791	632668	FRST
234042	636236	FRST
207800.9	631502.6	FRST
208324.7	630645.3	FRST
228048	636888	GRS
227288	638830	GRS
232568.3	631476	GRS
230987.1	632123.7	GRS
234012.9	633076.7	GRS
235683.5	632903.5	GRS
238998.2	637689.8	GRS

232560.1	631459.1	GRS
212773.6	631119.5	GRS
228619.3	626869.5	GRS
235748.5	632737.6	GRS
234723	657900.3	GRS
234020.5	657729.6	GRS
237080.4	659935.5	GRS
234730.9	657887.8	GRS
228620.3	626868.5	GRS
233933.2	657776.7	GRS
208575.4	631816.2	SHRUB
209829.9	630831.2	SHRUB
210810.2	630601	SHRUB
210929.3	630263.7	SHRUB
212021.2	630932.1	SHRUB
215170.1	626017.5	SHRUB
219440.5	627049.4	SHRUB
217980	625779.4	SHRUB
220156	629366.1	SHRUB
227094.6	628302.3	SHRUB
233000.1	630757.6	SHRUB
240712.7	638618.4	SHRUB
240665.1	638666.1	SHRUB
237799.6	640277.4	SHRUB
236250.8	636244.5	SHRUB
229229	640914.3	SHRUB
231081.1	641211.9	SHRUB
230677.6	643566.7	SHRUB
229989.7	641079.6	SHRUB

229361.3	643004.5	SHRUB
229956.6	640973.8	SHRUB
231782.5	632702.9	SHRUB
230504.4	627249.8	SHRUB
232156.7	651847.2	SHRUB
234061.7	651836.6	SHRUB
232109	651794.2	SHRUB
235719.8	632740.4	SHRUB
236085	633835.8	SHRUB
228895	641788	BLTP
231081	638389	BLTP
230238	638110	BLTP
232369	638732	BLTP
231927.5	653401.8	BLTP
232328.3	652139.7	BLTP
229046.5	642546.4	BLTP
229974.8	635757.5	BLTP
229794.4	640155.4	BLTP
227545.4	638851	BLTP
231317.1	637950.9	BLTP
231071	638291	BLTP
238529.9	638300.9	BLTP
238355.3	638110.4	BLTP
234099.8	647936.5	BLTP
231591.1	648127.5	BLTP
232242	648298.2	BLTP
233535.8	646524.2	BLTP
233254	646893.3	BLTP
235451.1	649476.4	BLTP

235954.9	648887.9	BLTP
236731.3	640786.2	BLTP
232370.9	641760.9	AGR
237460.5	656770.9	AGR
236873.8	656100.4	AGR
240243.4	658799.4	AGR
241577.2	654932.9	AGR
235345.6	644485.5	AGR
238326.1	641629.7	AGR
233842.9	638377.6	AGR
207977.5	630630.1	AGR
209930.1	630074.5	AGR
232568.2	637740.6	AGR
240246	658790	AGR
236863.8	656104.4	AGR
240239.5	658789.4	AGR
234042	636236	AGR
232791	632668	AGR
229245	637502	AGR
234005.3	631518	AGR
229245	637502	AGR
223557.3	627392.1	AGR
228901.9	626651.3	AGR
216836.9	629350.1	AGR
232923.6	637287.6	AGR
233048.3	655223.4	AGR
232382.1	638472.8	AGR
232591.7	638038.9	AGR
233331.6	637765.9	AGR
238378.6	637282.7	AGR
230450.5	639303.8	AGR
234701.8	644679	AGR
235819.7	645254.4	AGR
236461.3	644295.3	AGR
235746.9	642297.7	AGR
236180.2	646118.3	AGR
235644.2	641439	AGR
229375.3	636503	AGR
228925.5	637124.8	AGR
234005.3	631518	AGR
234005.3	631518	AGR
214599	631166.4	BARE
214949.6	629942.7	BARE
215462.2	628689.9	BARE
209871.8	631945.5	BARE
209924.7	631707.4	BARE
2160488	628365.7	BARE
235750	649238.5	BARE
209202.5	632000.8	BARE
214279.9	631176.2	BARE
214781.6	631287.5	BARE
214380.2	631281.1	BARE
214875.6	631486.4	BARE
214985.2	629853.8	BARE
204090.2	631836.4	BARE
215824.6	628885.9	BARE
215692.1	628171	BARE
215470.6	628105.9	BARE
215660.7	628070.5	BARE
215796.1	628907.7	BARE
215110.4	631081.6	BARE

Table 2: C-factor values used from other sources in regression model with NDVI values in each LULC classes under baseline period.

LULC classes	C-Factor values	References
Cropping land	0.3 (mean for crops)	Kaltenrieder,2007
Plantation forest	0.01	(Hunri,1988)
Grazing (pasture)	0.02	Bakker et al., 2008
Shrubs & Bush land	0.06	CGIP,1999
BLTP and settlement mix	0.4	BCEOM (1998)
Bare land	0.6	BCEOM (1998)

Table 3:- Crop-cover Management (C-factor) Values for future scenarios.

Crop type	**Senario_2**	**Senario_3**	
	C Factor value	C-factor values in fields ploughed in contour	
Maize	0.05	0.05	These C-Factor values are assigned for supposed management practices in Ethiopian condition Source: Adapted from (Kaltenreider, 2007)
Sorghum	0.05	0.05	
Sweet pot	0.05	0.05	
Field pea	0.1	0.1	
Intercropping	0.1	0.1	
Two crop season	0.15	0.15	
Haricot bean	0.3	0.25	
Barely	0.35	0.30	
Lentil	0.4	0.35	
Wheat	0.4	0.45	
Niger seed	0.5	0.45	
Teff	0.8	0.7	
Other land use		C-values for management scenario expectation and descriptions	

Forest		0.004 “Forests with not less than 75% cover including undergrowth and due to enrichment planting” (Wischmeier Smith (1978)
Grazing lands		0.01 (Kaltenreider,2007)
Shrubs & Bush land		0.038 “short brush with average drop fall height of 0.5m and 80% cover” (Wischmeier and Smith (1978)
settlement areas and BLTP		0.35 Area expected to have Limited cover and moderate runoff (Cooley and Williams, 1985)
Bare land		0.55 Bare soil with low to moderate runoff potential Cooley and Williams (1985; cited in El-Swaify et al., 1985: 509)

Table 4: Supposed support practices (P- factor) based on scenario2 and scenario-3

LULC	Slope (%)	Anticipated Conservation practice	P factor	Referance
Cultivated	(0-8%)	Terracing	0.1	(DEOER,2005)
Cultivated	(9-15%)	Terracing	0.14	
Cultivated	(>15%)	Terracing	0.16	
Other	All	None	1	Morgan, 1995

Supposed support practices (P- factor) based For (Scenario-3)				
LULC	Slope (%)	Anticipated Conservation under Scenario period	P factor	Referance
Cultivated	(3-5%)	Terracing and contouring	0.1	(DEOER,2005)
Cultivated	(6-8%)	Terracing and contouring	0.1	
Cultivated	(9-12%)	Terracing and contouring	0.12	
Cultivated	(13-16%)	Terracing and contouring	0.14	
Cultivated	(>17%)	Terracing and contouring	0.16	
Other	All	None	1	Morgan, 1995

Appendix 4: Soil Loss raster outputs scenarios of Climate change and Management

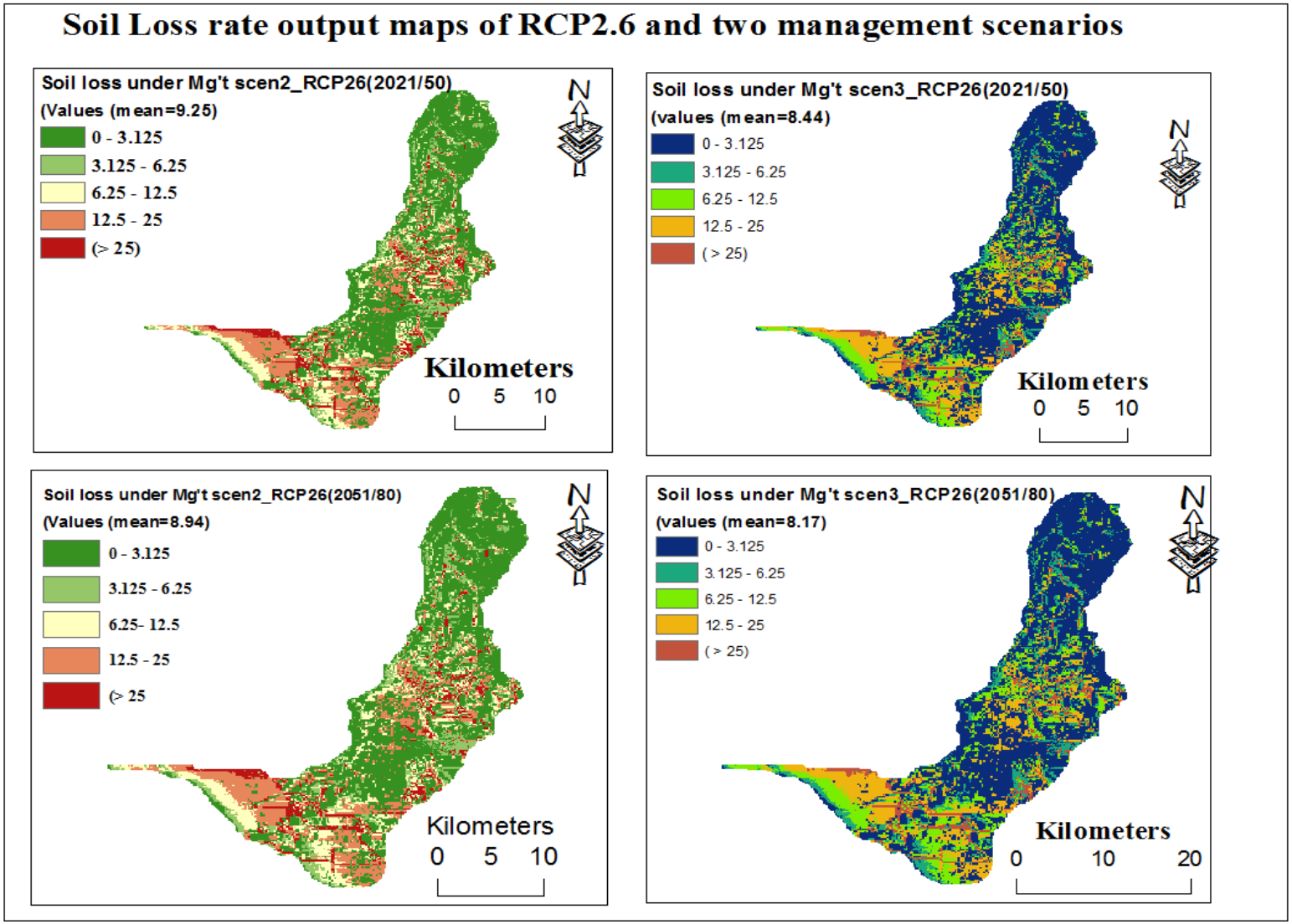

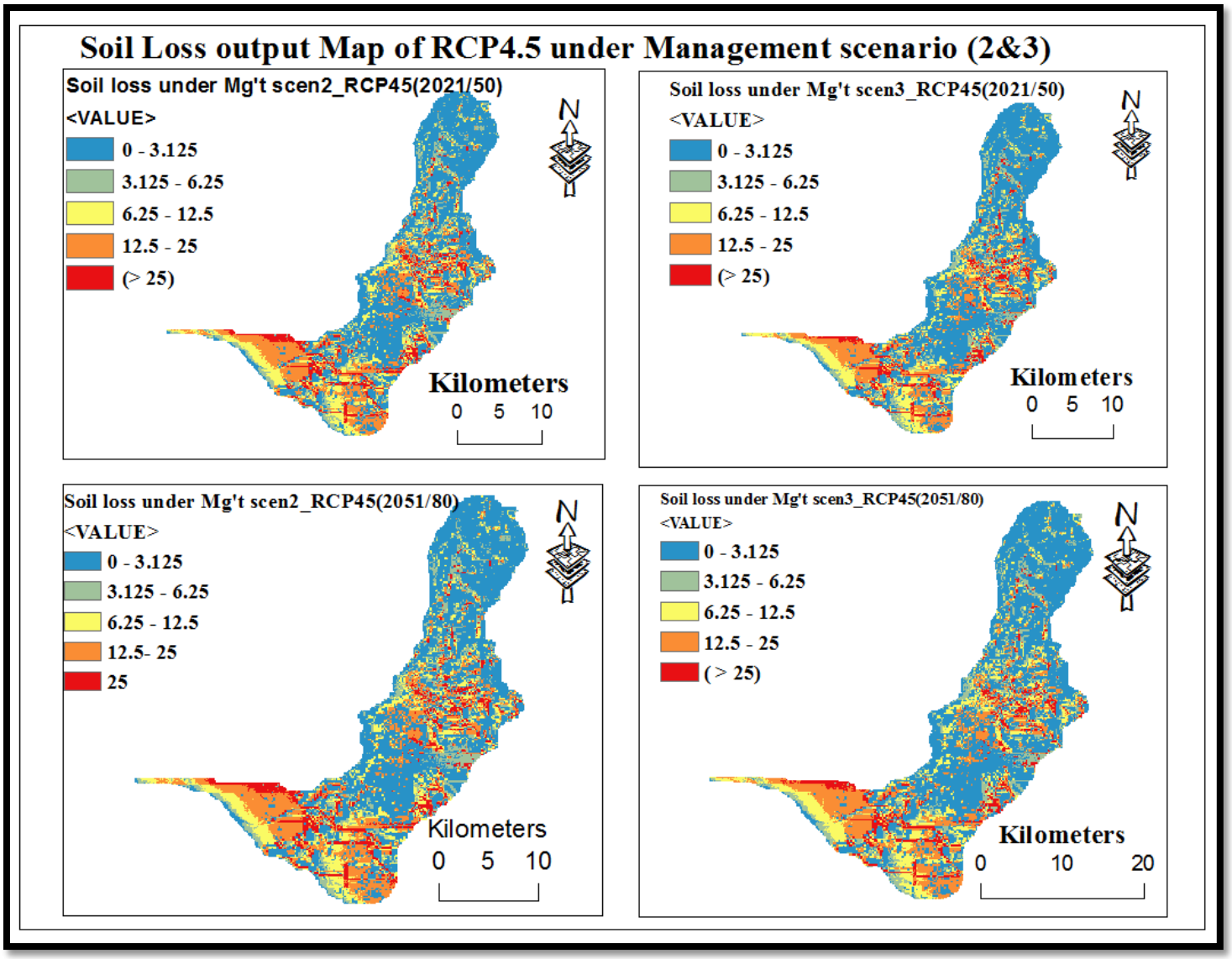
Soil Loss output Map of RCP4.5 under Management scenario (2&3)
Soil loss under Mg't scen2_RCP45(2021/50)
<VALUE>
0 - 3.125
3.125 - 6.25
6.25 - 12.5
12.5 - 25
(> 25)
N
Kilometers
0 5 10
Soil loss under Mg't scen3_RCP45(2021/50)
<VALUE>
0 - 3.125
3.125 - 6.25
6.25 - 12.5
12.5 - 25
(> 25)
N
Kilometers
0 5 10
Soil loss under Mg't scen2_RCP45(2051/80)
<VALUE>
0 - 3.125
3.125 - 6.25
6.25 - 12.5
12.5- 25
25
N
Kilometers
0 5 10
Soil loss under Mg't scen3_RCP45(2051/80)
<VALUE>
0 - 3.125
3.125 - 6.25
6.25 - 12.5
12.5 - 25
(> 25)
N
Kilometers
0 10 20

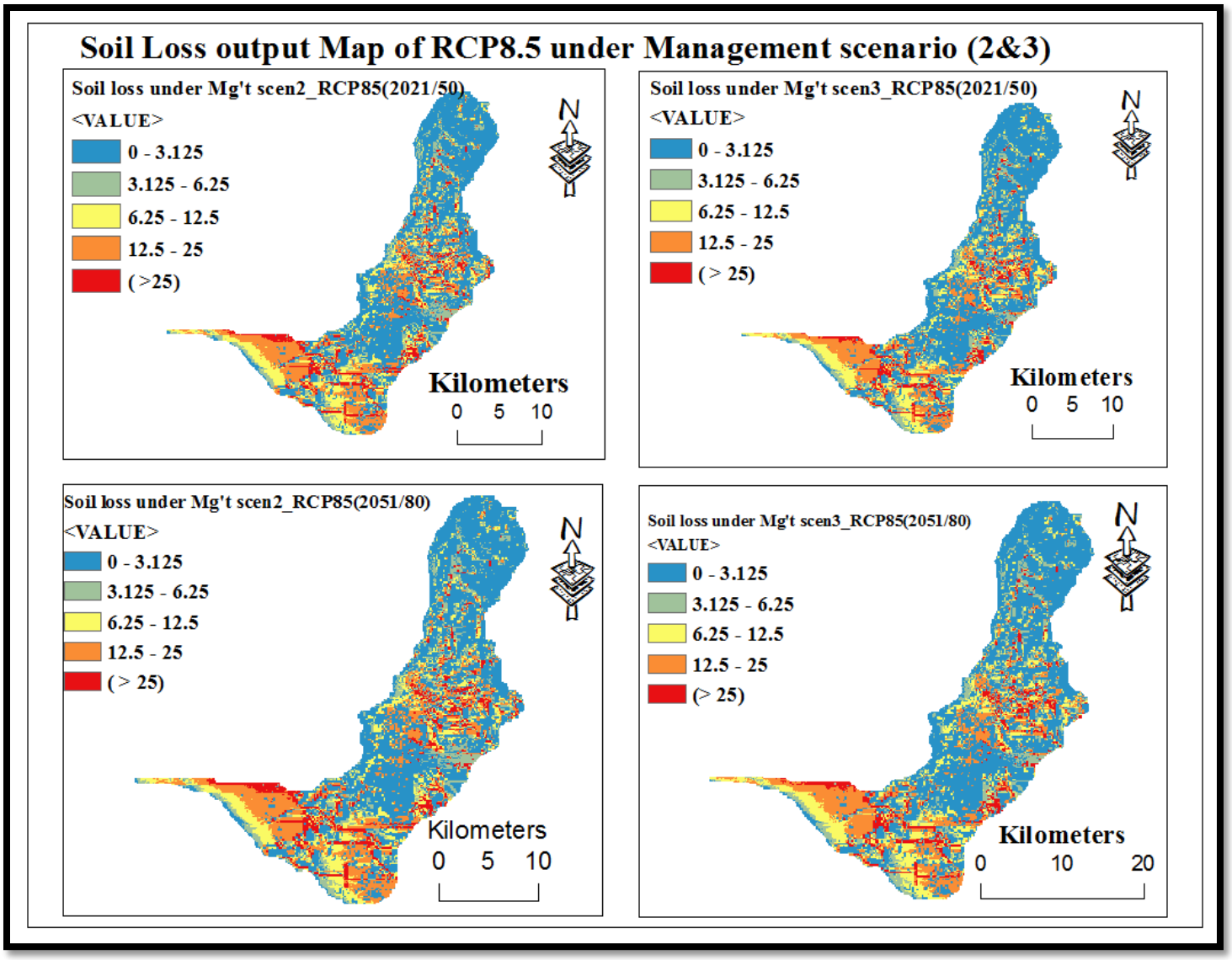
Soil Loss output Map of RCP8.5 under Management scenario (2&3)
Soil loss under Mg't scen2_RCP85(2021/50)
<VALUE>
0 - 3.125
3.125 - 6.25
6.25 - 12.5
12.5 - 25
(>25)
N
Kilometers
0 5 10
Soil loss under Mg't scen3_RCP85(2021/50)
<VALUE>
0 - 3.125
3.125 - 6.25
6.25 - 12.5
12.5 - 25
(> 25)
N
Kilometers
0 5 10
Soil loss under Mg't scen2_RCP85(2051/80)
<VALUE>
0 - 3.125
3.125 - 6.25
6.25 - 12.5
12.5 - 25
(> 25)
N
Kilometers
0 5 10
Soil loss under Mg't scen3_RCP85(2051/80)
<VALUE>
0 - 3.125
3.125 - 6.25
6.25 - 12.5
12.5 - 25
(> 25)
N
Kilometers
0 10 20